

UiT

NORGES
ARKTISKE
UNIVERSITET

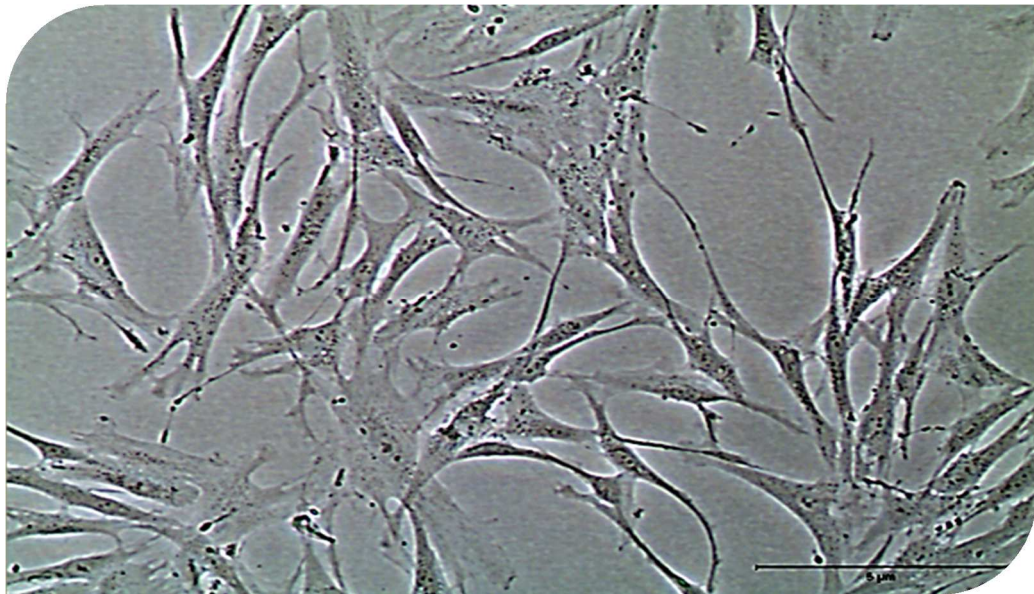
TRANSLATIONAL CANCER RESEARCH GROUP
DEPARTMENT OF CLINICAL MEDICINE
FACULTY OF HEALTH SCIENCES, UNIVERSITY OF TROMSØ

Immune-modulating properties of Carcinoma Associated Fibroblasts and their changes during radiotherapy

In vitro study of primary non-small cell lung carcinoma-associated fibroblasts

—
Laia Gorchs

Master thesis in Biomedicine __ May 2015



'...understanding how the parts relate to each other is a precondition to understanding process and understanding process is the precursor of uncovering principles.'

Bateson P., *Biol. Philos.* **21**, 553–558 (2006)

Acknowledgements

This thesis represents the work that I have carried out during my Master's Program in Biomedicine at the University of Tromsø, Norway, since January 2014.

First and foremost I would like to express my deepest gratitude to my supervisor, Professor **Iñigo Martínez-Zubiaurre**, from the Department of Clinical Medicine, who has guided me throughout my thesis with his patience and knowledge. I thank him for his continuous support, his stimulating discussions and for his optimism and encouraging words when results were unexpected but also for letting me the space to work independently and allowing me to make my own decisions which has helped me to grow professionally.

Special thanks to my co-supervisor, Professor **Tor Brynjar Stuge**, from the Department of Medical Biology, for introducing me to the exciting world of immunology and for his useful discussions from beginning to end.

Many thanks also to **Dr. Turid Hellevik**, for introducing me to radiation therapy research and for showing such a contagious enthusiasm for research.

Thanks to **Kirsten Nilsen Synnøve** for her help and guidance with ELISAs and to **Ketil André Camilio** for introducing me to new lab techniques and giving me the chance to learn new skills.

I would also like to express my gratitude to my parents for supporting every decision I have ever made and to my boyfriend, Anton for his love and encouragement.

Tromsø_May 2015

Summary

Background/aim of the study: Carcinoma-associated Fibroblasts (CAFs) comprise a heterogeneous population of cells and often represent the major cellular component of solid malignancies playing critical roles in tumor progression and metastasis. The purpose of this study was to gain more knowledge on the immunosuppressive traits of CAFs isolated from non-small cell lung carcinomas (NSCLC), and to explore whether high-dose radiotherapy (HD-RT), which has been proven to have highly favorable outcomes in patients with early-stage inoperable peripheral lung cancer, modify CAFs-mediated immune-regulating functions in one or another direction.

Methods: The study included primary cultures of CAFs isolated from freshly resected NSCLC (n = 7) and freshly isolated Peripheral Blood Mononuclear Cells (PBMCs) isolated from randomly selected healthy volunteers. A potential crosstalk between irradiated or non-irradiated CAFs and T-lymphocytes was examined using *in vitro* co-cultures and PBMCs exposed to CAF-conditioned medium (CM). Relevant cell functions were analyzed by a series of assays including lymphocyte proliferation assays, lymphocyte migration assays, Treg assays and T-cell cytokine production. In the search for mechanisms behind the observed effects, a series of molecular assays including multiplex protein arrays, ELISAs, LC-MS/MS proteomics and cytokines specific blocking assays were performed. Finally the induction of immunogenic cell death (ICD) of CAFs in response to HD-RT (1 x 18 Gy) was studied by examining the release of high motility group box 1 (HMGB1) and ATP into the extracellular space.

Results: All functional assays showed that CAF-derived soluble factors exhibit strong immunosuppressive effects on Phytohaemagglutinin-L (PHA-L) stimulated T-cells, affecting both their function ($P < 0.001$) and migration ($P < 0.05$) rates, and this effect was sustained after a single radiation dose of 18 Gy. Moreover, the 18 Gy irradiated CAF-secretome contained the same levels of the immunosuppressive cytokines, IL-6, TGF- β , PGE2, IL-10 and IDO as the non-irradiated CA-secretome. In addition, HD-RT did not induce the release of HMGB1 and ATP by CAFs. Finally, by specific blockade of well-

Summary

known factors it has been proven that IL-6, TGF- β , PGE2 and Galectin-3 do not play major roles in the immunosuppressive effects exerted by CAFs.

Conclusion: This study demonstrate that CAF-derived soluble factors mediate strong immunosuppressive effects over activated T-cells although the soluble factor responsible for these effects remains unknown. On the other hand, this study also demonstrates that HD-RT do not overcome the immunosuppressive effects exerted by non-irradiated CAFs and fails to induce substantial changes in the spectra of immune-regulatory molecules secreted by these cells. Moreover, CAFs do not switch on ICD responses after exposure to HD-RT.

Abbreviations

NSCLC: Non-Small Cell Lung Cancer/Carcinoma	M2: Alternatively activated Macrophage
HD-RT: High-Dose Radiotherapy	M-CSF: Macrophage-Colony Stimulating Factor
CAF: Carcinoma-Associated Fibroblast	TLR: Toll-Like Receptor
BMDC: Bone-Marrow-Derived Mesenchymal Cell	TSP: Thrombospondin
TAM: Tumor-Associated Macrophages	ICD: Immunogenic Cell Death
ECM: Extracellular Matrix	DAMP: Damage-Associated Molecular Pattern
EMT: Epithelial Mesenchymal Transdifferentiation	HMGB1: High-Mobility Group Box 1
α-SMA: α -Smooth Muscle Actin	CRT: Calreticulin
FAP: Fibroblast-Activation Protein	HSP: Heat Shock Proteins
FSP-1: Fibroblast-Specific Protein-1	DMEM: Dulbecco's Modified Eagle's Medium
PDGF: Platelet-Derived Growth Factor	IMDM: Iscove's Modified Dulbecco's Medium
MMP: Matrix degrading Metalloproteinase	FBS: Fetal Bovine Serum
SDF-1: Stromal-Derived Factor 1	DMSO: Dimethyl Sulfoxide
IL: Interleukin	PBS: Phosphate Buffered Saline
VEGF: Vascular Endothelial Growth Factor	PHA-L: Phytohemagglutinin-L
HGF: Hepatocyte Growth Factor	CFSE: CarboxyFluorescen Succinimidyl Ester
EGF: Epidermal Growth Factor	DTT: DiThioTreitol
TGF-β: Transforming Growth Factor- β	CM: Conditioned Medium
FGF2: Fibroblast Growth Factor 2	PBMCS: Peripheral Blood Mononuclear Cells
EPC: Epidermal Progenitor Cell	FACS: Fluorescent-Activated Cell Sorting
TN-C: Tenascin-C	GM-CSF: Granulocyte Macrophage-Colony-Stimulating Factor
MDSC: Myeloid-Derived Suppressor Cell	TNF: Tumor Necrosis Factor
NK: Natural Killer Cell	HRP: Horseradish Peroxidase
DC: Dendritic Cell	TMB: Tetramethylbenzidine
PGE2: Prostaglandin E2	SDS-PAGE: Sodium Dodecyl Sulfate–Polyacrylamide Gel Electrophoresis
IDO: Indoleamine 2,3-Dioxygenase	PVDF: Polyvinylidene Difluoride
PD: Programmed Death	MS: Mass Spectrometry
CTL: Cytotoxic T lymphocytes	LC: Liquid Chromatography
Th: T helper	MACS: Magnetic-Activated Cell Sorting
IFN-γ: Interferon- γ	
M1: Classically activated Macrophage	
Treg: T regulatory cell	

Table of contents

1. Introduction.....	1
1.1 Non-Small Cell Lung Cancer.....	1
1.2 The tumor microenvironment	2
1.3 Cancer-associated fibroblasts.....	3
1.4 Tumor Inflammation and Immunity	6
1.5 CAFs and tumor immune responses	7
1.6 Radiation Therapy.....	13
2. Aims of the study.....	17
3. Materials	18
3.1 Cell Culture Growth.....	18
3.2 Cell Culture Reagents	18
3.3 Supplies.....	19
3.4 Stains and Dyes.....	19
3.5 Antibodies	19
3.6 Drugs.....	20
3.7 Recombinant Proteins	20
3.8 Kit... ..	20
3.9 ELISAs Reagents	21
3.10 FACS Flow Products	21
3.11 Gel Electrophoresis and Western Blotting Products	21
3.12 In gel-reduction, Alkylation and Digestion Reagents.....	22
3.13 MACS Products	22
3.14 Instruments	22
3.15 Software.....	23
3.16 Mediums	24
4. Methods.....	25
4.1 Ethical Statement	26
4.2 Biological samples and Patients.....	26
4.3 Isolation and Culture of Primary NSCLC Fibroblasts.....	26
4.4 Irradiation and preparation of Fibroblast-Conditioned Medium	29
4.5 Isolation and Culture of human PBMCs.....	31
4.6 Lymphocyte proliferation assays	32
4.7 Transwell migration assays.....	34
4.8 Multiplex protein arrays (Luminex).....	35
4.9 Enzyme linked immunosorbent assays (ELISA)	37
4.10 Western Blotting of IDO expression	39
4.11 Identification of proteins by Mass Spectrometry.....	41
4.12 Regulatory T-cell proliferation assays.....	45
4.13 Specific Cytokines Targeted Drugs	48
4.14 ATP release assays	49
4.15 Measurement of HMGB1 protein by Western Blotting	50
4.16 Statistical analysis.....	51
5. Results	52
5.1 Irradiation promotes morphological changes of primary cultured CAFs	52

Table of Contents

5.2	PHA-stimulated T-lymphocytes exhibit decreased cell proliferation when co-cultured with irradiated and control CAFs.....	52
5.3	CD4 ⁺ and CD8 ⁺ T-cell subsets respond equally to irradiated and control CAF-mediated immunosuppression.....	54
5.4	Conditioned Medium harvested from irradiated and control CAFs decreases proliferation of activated T-lymphocytes.....	54
5.5	Conditioned Medium from irradiated and control CAFs inhibits effector cytokines expression by T-cells	56
5.6	PHA-stimulated T-lymphocytes showed reduced migration rate when cultured with conditioned medium from irradiated and control CAF cultures.....	58
5.7	Neither Tumor Cells nor Chondrocytes – conditioned medium exert immunosuppressive effects.....	59
5.8	T-regulatory cell proliferation assays	60
5.9	Control and irradiated CAFs supernatants contain equal levels of immunosuppressive cytokines	62
5.10	Undetected intracellular and extracellular expression of IDO in unstimulated CAFs	63
5.11	Identification of alternative paracrine factors released from irradiated and control CAFs	63
5.12	High-dose Irradiation does not induce Immunogenic Cell Death mechanisms.....	66
5.13	Blocking of IL-6, PGE2, TGF- β and Galectin-3 activity does not prevent the immunosuppressive effects of CAF-CM	67
6.	Discussion.....	69
	Additional files	79
	A Protocols	79
	B Solutions	83
	C Additional Results.....	84
	References	87

1. Introduction

1.1 Non-Small Cell Lung Cancer

Around 1.5 million new patients are diagnosed of lung cancer every year worldwide, and only 5 % will survive 10 or more years, making lung cancer the leading cause of cancer-related death in both men and women¹. Within lung cancer cases, about 80 % of tumors are defined as Non-Small Cell Lung Cancer (NSCLC). NSCLC develops from cells lining the respiratory tract (bronchi, bronchioles and alveoli) and it can be divided into three histological subtypes based on how cells appear under the microscope: Squamous Cell Carcinoma (30 %), Adenocarcinoma (30 %-40 %) and Large Cell Carcinoma (10 %-20 %)² (Figure 1.1).

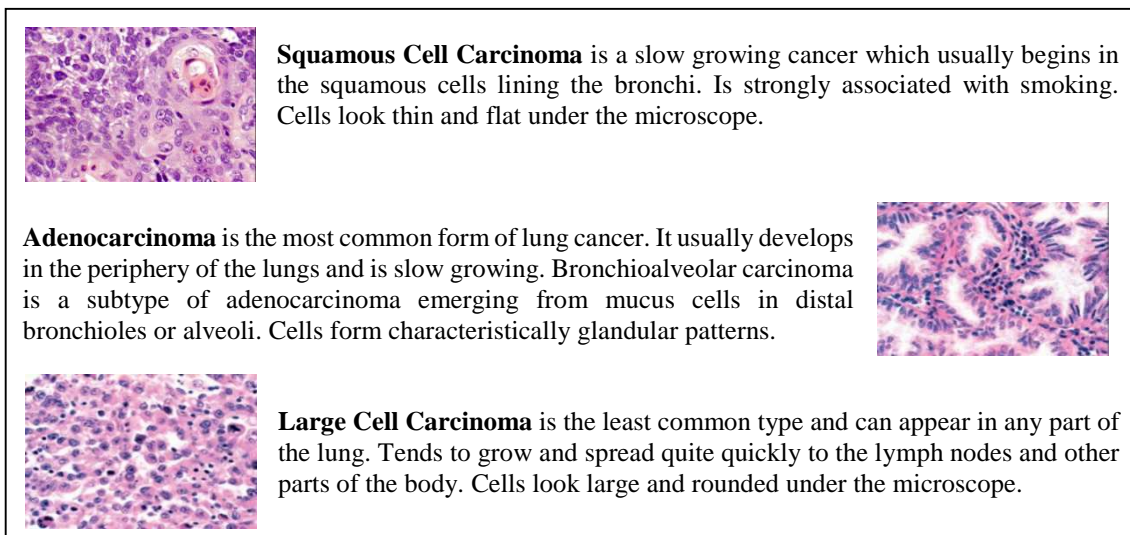


Figure 1.1 Non-small cell lung cancer sub-types. Histological abnormalities of Squamous cell carcinoma, Adenocarcinoma and Large cell carcinoma in the lung.

1.1.1 NSCLC diagnosis and treatment

When a lung tumor is detected usually by a chest X-ray test or by a computerized chromatography (CT) scan, biopsies specimens are normally obtained by bronchoscopy or by CT scan ultrasound-guided transthoracic fine needle aspiration to help to diagnose the tumor. In addition, to know whether the tumor has spread to other parts of the body or to the lymph nodes within the lungs, patients might also undergo a magnetic resonance imaging (MRI). Currently, a new generation of imaging test called positron emission tomography (PET) scan is becoming more and more popular³. Based on the uptake of a radiopharmaceutical tracer, typically fluor-18-labeled FDG, this imaging reveals areas of the body with high glucose metabolism usually associated with tumor tissues⁴.

1. Introduction

Even though surgery is the most effective treatment for patients with early stage lung cancer (stage I), the fact is that about 65 % of patients considered post-operative tumor free, will relapse within two years and subsequently die from metastatic cancer. Moreover, due to the lack of adequate screening and early detection measurements, most tumors at the time of diagnosis are in its advanced inoperable stages. For this reason, radiotherapy (RT) has become the most widely used treatment for NSCLC patients with more than half of all patients undergoing RT at some point during their disease. However, outcomes are far from being satisfactory⁵.

Fortunately, over the last decade, new hope with novel therapeutic strategies to treat NSCLC patients have raised. Unlike standard treatments, the new generation of treatments are more focused on the tumor and the microenvironment that supports its progression. Including cancer immunotherapy⁶, cancer targeted therapy⁷ and high-dose radiation regimens⁸ also referred as stereotactic ablative radiotherapy (SABR). As I will explain later, this last treatment has been proved to have highly favorable outcomes in patients with early-stage inoperable peripheral lung tumors⁹. In fact, due to the outstanding outcomes of high-dose radiotherapy (HD-RT), this treatment is being considered also for operable NSCLC⁸.

1.2 The tumor microenvironment

In the year 2000, a highly influential review article entitled the “Hallmarks of cancer” by Hanahan *et al.*, predicted how the cancer research community would turn their reductionist focus on cancer cells, which dominated the last two decades of the 20th century, to a heterotypic cell biology point of view¹⁰.

Today, as Hanahan anticipated, it is widely accepted that the stromal cells within the tumor microenvironment play an important role in all the stages of tumor growth and progression¹¹⁻¹³. Ever since we were in our mother’s womb, our cells have been communicating through a complex system of paracrine factors and cell-cell contact molecules in order to dictate whether a cell remains quiescent, proliferates, differentiates, or undergoes apoptosis. Processes aimed at maintaining homeostasis^{14,15}.

Based on this principle, as cancer cells gain and accumulate genetic mutations, the tissue homeostasis is altered and consequently, the tumor-associated stroma changes into an activated state called “reactive” stroma¹⁶ (**Figure 1.2**). In other words, the heterogeneous mixture of non-neoplastic cells in the reactive stroma are fundamentally being “educated”

1. Introduction

by neoplastic cells to reciprocate and promote growth, survival, invasion and metastasis¹⁷ through paracrine signaling.

1.2.1 Cell types of the tumor microenvironment

The stromal cell population surrounding the neoplastic cells consists of microvascular endothelial cells, pericytes, activated or reactive fibroblasts called cancer-associated fibroblasts (CAFs), bone-marrow-derived mesenchymal cells (BMDC) and infiltrated or resident inflammatory and immune cells such as specialized macrophages called tumor associated macrophages (TAM) and effector T-cells. All these cells are embedded in a network of fibrous and non-fibrous proteins called extracellular matrix (ECM)¹⁶ essential for the anchorage and migration of invasive cells (**Figure 1.2**).

In the following sections I will focus on the role of CAFs in tumor progression and the immune-modulating properties of CAFs.

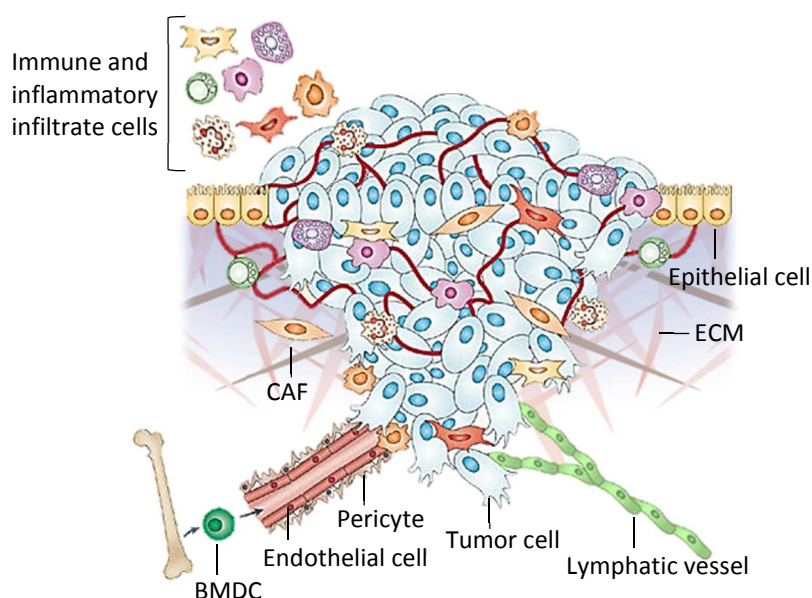


Figure 1.2 “Reactive” tumor stroma. Interactions between tumor cells and stromal cells promote both invasion and angiogenesis. *Abbreviations*; CAF, carcinoma-associated fibroblasts; ECM, extracellular matrix; BMDC, bone-marrow-derived cells. *Adapted from Johanna et al., Nature Reviews Cancer 9, 239-252 (2009).*

1.3 Cancer-associated fibroblasts

1.3.1 CAFs heterogeneity

CAFs represent the major cellular component of the tumor stroma in most solid malignances, and their presence in large numbers is often associated with poor prognosis¹⁸ (**Figure 1.4**). Different authors have reported evidence indicating that CAFs can derive from a wide variety of cell sources including tissue-resident fibroblasts, myofibroblasts¹⁹, endothelial cells²⁰, pericytes¹⁸, bone-marrow cells²¹, smooth muscle

1. Introduction

cells¹⁸, mesenchymal stem cells²² and normal epithelial cells²³ which acquire a CAF-like phenotype upon recruitment into the “reactive” tumor microenvironment. It has also been widely discussed whether CAFs derive from carcinoma cells via epithelial-mesenchymal trans-differentiation (EMT)²⁴. This possibility however, seems unlikely, since CAFs are not tumorigenic itself and it is still unclear whether CAFs carry genetic alterations or not^{25,26}.

The different CAF sources and subtypes may explain the heterogeneity in the expression of cellular markers within the entire CAF population including α -smooth muscle actin (α -SMA), fibroblast-activation protein (FAP), fibroblast-specific protein-1 (FSP-1) or platelet-derived growth factor (PDGF) receptor (PDGFR). This fact contributes to the difficulty for distinguishing among them and from other mesenchymal subpopulations expressing similar markers²⁴.

1.3.2 Normal Tissue Fibroblasts versus CAFs

Under normal conditions, fibroblasts maintain epithelial homeostasis²⁴ as well as the integrity of the connective tissue by continuously secreting ECM proteins like collagen and fibronectin²⁴. Fibroblasts also secrete matrix degrading proteases, such as matrix metalloproteinase (MMPs) essential for ECM remodeling²⁷. Moreover, during wound healing fibroblasts differentiate into activated myofibroblast which act as sentinel cells that initiate tissue repair and modulate the immune response²⁸.

In the cancer microenvironment, activated fibroblasts or CAFs acquire an increased contractile ability similar to the myofibroblast in wound healing, which promotes the expression of α -SMA as the major mesenchymal marker instead of vimentin expressed in quiescent fibroblasts²⁴. Unlike wound healing, fibroblasts in tumours remain activated. Therefore, cancer has been described as “a wound that never heals”, due to the permanently activated fibroblasts and its similarity with granulation tissue during wound healing¹⁸.

CAFs can secrete increased levels of numerous MMPs and their activators urokinase plasminogen activator (uPA)²⁷, immune-modulating cytokines and chemokines such as Stromal-derived Factor-1 (SDF-1)/CXCL12, Interleukin (IL)-1, IL-8 and IL-6, and growth factors including vascular endothelial growth factor (VEGF), hepatocyte growth factor (HGF), epidermal growth factor (EGF), transforming growth factor- β (TGF- β), PDGF and fibroblast growth factor 2 (FGF2). All these soluble factors are used as

1. Introduction

paracrine signaling to communicate with neoplastic and non-neoplastic cells in the tumor stroma to eventually promote tumor growth and metastasis^{29,30} (**Figure 1.4**) and as autocrine signaling to maintain their own phenotype³¹.

1.3.3 *CAF's role in angiogenesis*

The role of CAFs in supporting tumor angiogenesis is very well documented. Studies by Orimo *et al.*,³² showed that when MCF-7-ras human breast cancer cells were coinjected with CAFs isolated from an invasive mammary ductal carcinoma, into an immunodeficient nude mice, tumors grew faster than xenografts infused with normal control fibroblasts isolated from a non-cancerous area of the same patient. In the same study authors also demonstrated that SDF-1/CXCL12 released at high levels by CAFs was critical for the recruitment of endothelial progenitor cells (EPC) thereby promoting angiogenesis in the xenograft³². Noticeably increased vascularization was associated with the rapid growth of the tumor. A different study proved that PDGF, released by cancer cells, induced the release of the proangiogenic factor, FGF-2, by CAFs when binding to PDGFR on CAFs³³ (**Figure 1.4**).

1.3.4 *CAF's role in metastasis*

Metastasis is the process by which cancer cells gain the ability to colonize in distant organs and develop secondary tumors. In order for cancer cells to form a metastatic niche they first have to acquire motile properties through the EMT biological process. By this mechanism, cancer cells lose their cell-to-cell adhesions and acquire a mesenchymal phenotype with an aberrant motile and migratory capacity enabling the cells to invade the surrounding stroma and eventually intravasate into the vascular or lymphatic system. This process can be promoted by CAFs through the secretion of HGF and TGF- β ³⁴. CAFs can also promote cell invasion and progression through the secretion of ECM-degrading MMPs. ECM-degradation, in addition to provide the physical space for cancer cells expansion and motility, results in release of matrix-associated growth factors such as VEGF, which in turn stimulates tumor angiogenesis³⁵. Other factors released by CAFs have been shown to be important for the acquisition of metastatic phenotypes of tumor cells. For instance, recent studies have reported that one of the main matricellular proteins released by CAFs, Tenascin-C (TN-C)³⁶, plays a key role in forming a metastatic niche by enhancing NOTCH and WNT signaling pathways in cancer cells which triggers cell motility and colonization by inducing loss of focal adhesions and by providing at the same

1. Introduction

time a substratum that supports cell migration³⁷. TN-C is also associated with tumor angiogenesis³⁸ (**Figure 1.4**). Besides the established role of fibroblasts in promoting EMT, other evidence indicate that CAFs can also lead the breakout from the primary tumor together with the cancer cells and enter into the circulation (**Figure 1.3**). This way, CAFs not only protect metastatic cells in the blood circulation but they can also provide a favorable tumor microenvironment at the metastatic site^{39,40}.

In yet another study with *in vivo* xenograft models, it was demonstrated that FSP-1 positive CAFs enhance tumor metastasis by promoting an inflammatory environment⁴¹. All mentioned evidence put forward the pro-invasive and pro-metastatic roles of CAFs during cancer progression

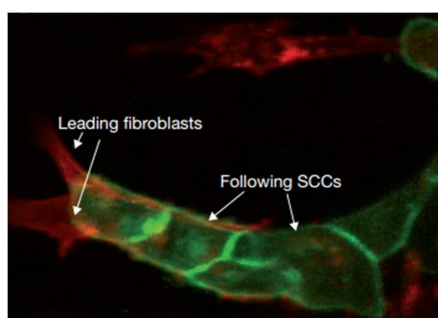


Figure 1.3 Fibroblasts followed by squamous cell carcinoma (SCC) cells in the process of invasion. Fibroblasts (in red) are clearing the path into naïve matrix for SCC (green) invasion. Adapted from Gaggioli *et al.*, *Nature Cell Biology* **9**, 1392-1400 (2007).

1.4 Tumor Inflammation and Immunity

1.4.1 Inflammation: a hallmark of cancer

The presence of cytokines and chemokines released at high levels by neoplastic and non-neoplastic cells, the activated angiogenic vasculature, the increased levels of tumor-infiltrating immune cells and the necrosis encountered in human solid tumors perfectly mirrors the chronic non-healing wound-mediated inflammation. Historically, this inflammation was considered as an attempt by the immune system to cure cancer. However, accumulating evidence from the beginning of this century indicate that inflammation indeed enhance tumor progression¹². Therefore, inflammation is now acknowledged as one of the hallmarks of cancer¹². In fact, chronic inflammatory disorders or wounded tissues have the potential to develop into a tumor⁴² due to the presence of reactive nitrogen and oxygen species released by the infiltrating immune cells which interacts with DNA in proliferating cells resulting in irreversible genomic alterations hence favoring the acquisition of a more invasive phenotype⁴³.

1. Introduction

1.4.2 Immune escape

The characteristics described above may explain why, despite expression of tumor antigens in large numbers, most malignant cells undergo a process of cancer immune-editing by which under the pressure of an efficient immune response, less immunogenic tumor cells are selected out of the immune attacks⁴⁴. Some of the mechanisms that have been described in the literature through which cancer cells escape immune-surveillance are summarized in **Table 1.1**^{44,45}.

Table 1.1 *Mechanisms of immune evasion*

Strategy	Mechanism
Hide identity	Mutation or down-regulation of tumor antigens
	Mutation or down-regulation of MHC- I
	Defects in MHC-I antigen-processing machinery (e.g., TAP, LMP deficiency)
Release of immunosuppressive factors	Cytokines (TGF- β , IL-10, VEGF, PGE2)
	Other Factors (soluble FAS, FASL and MICA)
Tolerance induction	Recruitment of Regulatory T-cells through CCL22 chemokine
	Recruitment of myeloid-derived suppressor cells through CCL2 chemokine
	Expression of ligands for T-cell inhibitory receptors (e.g. PD-L1)
Apoptosis resistance	Immune deviation (i.e., change from Th1 dominant immune response to a Th2 status)
	Expression of anti-apoptotic molecules in the cytoplasm
	Mutation and down-regulation of pro-apoptotic molecules

1.5 CAFs and tumor immune responses

Given the importance of tumor inflammation in the development of cancer, much effort has been put into understanding the reciprocal regulation of tumor cells and inflammatory cells within the tumor microenvironment including T-effector cells, TAMs, myeloid-derived suppressor cells (MDSC), Natural Killer (NK) cells and their secreted cytokines to establish immunoevasion⁴⁶. In spite of the increasing awareness on the role played by CAFs in tumor progression, data on the impact of CAFs on the overall tumor immunity is now just starting to emerge.

1.5.1 CAFs and lymphocytes

The complex cocktail of cytokines and chemokines found in the inflammatory milieu of tumors attracts a wide variety of different leukocytes including macrophages, granulocytes, NK cells, myeloid dendritic cells (DC) and lymphocytes. Although effector T-lymphocytes appear to constitute the majority of the tumor-infiltrating leukocytes⁴⁷, these cells seem to be incapable of destroying tumors.

1. Introduction

Growing evidences also show that different immunosuppressive mechanisms are behind this phenomenon^{48,49} and that CAFs may play a role (**Figure 1.4**) by releasing immune-regulating cytokines such as TGF- β ⁵⁰. TGF- β regulates many cellular processes including proliferation, differentiation and migration⁵¹ and in the context of tumor immunity this cytokine is known for its ability to suppress the cytotoxic function of CD8⁺ T-cells through the Smad2/3 pathway^{52,53} and for its ability to down-regulate mRNA levels of the activating immunoreceptor NKG2D on NK cells^{54,55} and CD8⁺ T-cells^{52,55}.

In metastatic melanoma, CAF-derived PGE2 (Prostaglandin E2) appears to be involved in the down-regulation of NK cells natural cytotoxicity receptors, NKp44 and NKp30, compromising the ability of NK cells to kill tumors⁵⁶. Consistent with these outcomes Li *et al.*,⁵⁷ demonstrated in *in vitro* experiments the inhibition of both indoleamine 2,3-dioxygenase (IDO) and PGE2 released by hepatocellular-CAFs, could partially recover NK cell functions.

In addition, lung-tumor derived CAFs are reported to suppress lymphocyte activation and proliferation through cell-cell contact via the co-inhibitory molecules, programmed death (PD)-ligand (L)1 and PD-L2⁵⁰.

1.5.2 CAFs and immune deviation

An effective systemic anti-tumor immunity involves the activation of both CD8⁺ cytotoxic T lymphocytes (CTL) and the CD4⁺ T helper subset T helper 1 (Th1). This type of response is also known as **Th1** immunity which is characterized by the release of (Interferon) (IFN)- γ into the extracellular space. IFN- γ stimulate DC-mediated Th1 differentiation, enhance classically activated (M1) macrophages and increase the surface expression of MHC class I and II molecules⁵⁸. Unfortunately in most cancers, as the tumor progress the “reactive” tumor stroma may drive a switch towards a **Th2** immunosuppressive cytokine profile, which includes IL-4, IL-5 and IL-13, promoting tumor growth and invasion⁵⁹. Cells involved in Th2 immunity includes T regulatory cells (Treg), MDSCs, alternatively activated macrophages (M2) and the T helper subsets Th2 and Th17 (**Figure 1.4**).

This shift from Th1 to Th2 immunity depends on the cytokine milieu and accumulating evidence show that CAF-derived soluble factors may play an important role. The prove of this theory is that elimination of CAFs with a pFAP vaccine in mice challenged with

1. Introduction

4T1 tumor cells (i.e., metastatic breast cancer model), has been shown to promote a shift towards Th1 cytokine expression which resulted in inhibition of tumor angiogenesis⁶⁰.

But which CAF-derived soluble factors promote immune deviation?

It has been suggested that CAF-derived IL-6 inhibit Th1 polarization by suppressing IFN- γ -mediated signaling through SOCS-1 (suppressor of cytokine signaling), and this up-regulation interferes with the JAK-STAT cytokine signaling pathway⁶¹. In yet another study, CAFs activated by IL-1 β and TNF- α has been shown to release a cytokine called Thymic Stromal Lymphopoietin which favors DC-mediated Th2 polarization⁶².

1.5.3 CAFs and Th17

Th-17 subsets have been named after their signature effector cytokine IL-17 which acts to recruit other immune cells, that in turn release other cytokines resulting in a pro-inflammatory cytokine cascade reaction that promote cancer progression⁶³. Thus, high levels of Th-17 is also associated with poor prognosis and cancer relapse⁶⁴. Since Th-17 differentiation requires cytokines such as TGF- β , IL-6 and IL-1⁶⁵ and CAFs are proven to release these cytokines in the tumor stroma it is suggested that CAFs may be favoring somehow the expansion of this T-cell subset⁶⁶. Moreover, in the same study authors demonstrated that CAF-released chemokine CCL5 (also known as RANTES) and CCL2 (or MCP-1) mediated migration of Th17 cells to the tumor microenvironment.

1.5.4 CAFs and Treg cells

Little information exists on the relation between Tregs and CAFs, but their differentiation and recruitment into the tumor stroma has been associated with cytokines and chemokines released by CAFs (**Figure 1.4**).

Treg cells are CD4⁺, CD25⁺, FOXP3⁺ positive T-cells that can inhibit T-cell effector functions in a direct cell-cell contact dependent manner or through the release of immunosuppressive cytokines such as TGF- β and IL-10⁶⁷. Based on the idea that TGF- β may affect the generation of Tregs by stimulating expression of the FOXP3⁺ transcription factor required for Treg differentiation and activation⁶⁸, it is thought that CAFs can induce Treg differentiation and recruitment by TGF- β secretion⁶⁹. In line with this theory Kinoshita *et al.*,⁶⁹ found a positive correlation between the presence of CAF-released soluble factors (TGF- β , VEGF) and the induction of positive FOXP3⁺ Tregs in NSCLC.

1. Introduction

1.5.5 CAFs and TAMs

Tumor-associated macrophages are derived from circulating blood monocytes attracted to the tumor microenvironment by the same chemokines that mediate Th17 migration, CCL2. Other chemokines also involved in TAM-infiltration are VEGF and Macrophage-Colony Stimulating Factor (M-CSF)⁷⁰. Accumulation of TAMs in tumors has been associated with tumor hypoxia, which together with other tumor microenvironmental conditions, promotes polarization of the infiltrated macrophages towards the M2 phenotype⁷¹. M2 macrophages, also known as alternatively activated macrophages differs in all aspects from the classically activated M1 phenotype: M1 polarization is dependent on IFN- γ and toll-like receptor (TLR) downstream signals and is involved in triggering an anti-tumor immune response, and thus Th1 immune response. M2 polarization on the other hand, is induced by Th2 cytokines IL-4 and IL-13, and other immune-regulatory cytokines such as IL-10 and TGF- β and is important for wound repair and to control inflammation. In addition, activated M2 macrophages can suppress T-cell activation and proliferation by releasing prostaglandins, IL-10 and TGF- β ⁷². Thus in analogy to Th1/Th2, polarization towards M2 phenotype is associated with tumor growth, invasion and metastasis.

CAFs from prostate cancer are reported to secrete increased levels of CCL2 and CXCL14 associated with macrophage infiltration, tumor growth and metastasis^{28,73}. Supporting this evidence, another study on oral squamous cell carcinoma, demonstrated a positive correlation between CAFs and M2 macrophages⁷⁴. CAF-derived IL-6 has also been reported to switch monocyte differentiation from antigen presenting DC to TAM by up-regulating the expression of M-CSF receptors on monocytes⁷⁵.

1.5.6 CAFs and MDSCs

Myeloid-derived suppressor cells are a heterogeneous population of immune cells which, like TAMs, can be generated in the bone marrow in response to cytokines released in the tumor microenvironment. Even though the relationship between CAFs and MDSC is not yet fully understood, it is thought that CAF-derived CCL2 can also recruit MDSC²⁸.

1.5.7 CAFs and ECM molecules

Another mechanism by which CAFs may mediate immune deviation away from Th1 signature is through the release of matricellular proteins like TN-C and thrombospondin-1 (TSP-1)³⁶. Besides promoting tumor cell migration and invasion, TN-C may also inhibit T-cell proliferation by binding to the T-cell receptor-CD3 complex and by down-

1. Introduction

regulating the expression of IL-2 receptors on T-lymphocytes³⁶. TSP-1 is another immune-modulating protein with increased expression in tumor tissues. Even though the role of TSP-1 in cancer progression remains controversial, it has been proposed that TSP-1 can interact with immune cells and suppress the surface expression of MHC class II and co-stimulatory molecules on DC, inhibiting DC-mediated Th1 differentiation³⁶.

1. Introduction

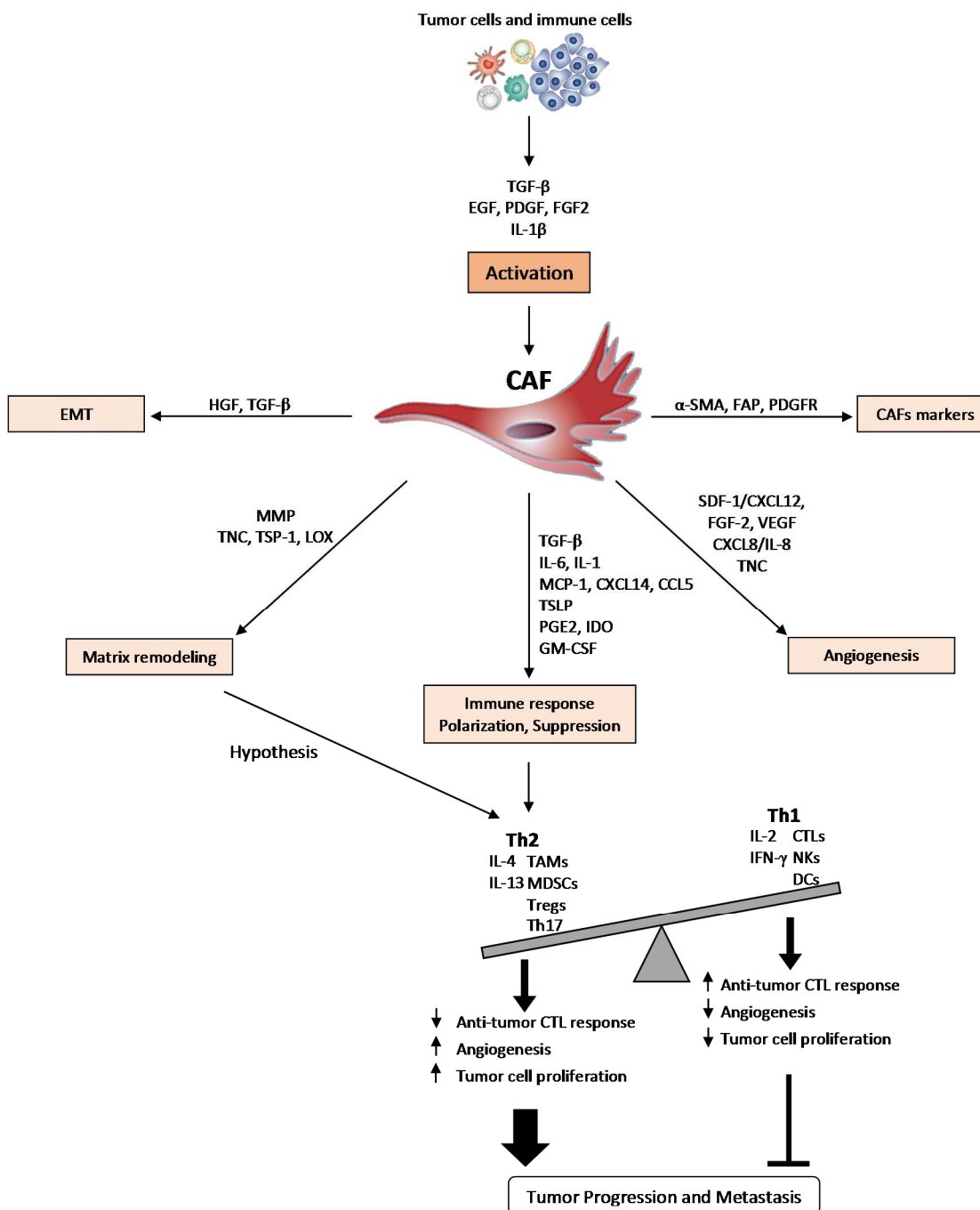


Figure 1.4 Carcinoma-associated fibroblasts (CAFs) as modulators of tumor progression and metastasis. CAFs are a heterogeneous population of cells with an activated phenotype that can promote tumor growth and progression through a variety of mechanisms including increased angiogenesis, immunosuppression, matrix remodeling and by facilitating epithelial-mesenchymal transdifferentiation (EMT) of cancer cells. These effects are mediated through paracrine signaling. CAFs can additionally affect tumor progression indirectly by releasing extracellular matrix proteins and recruiting tumor promoting cells such as Tumor-associated macrophages (TAMs), Myeloid derived suppressor cells (MDSCs), Tregs and Th17 promoting a shift to Th2 polarization.

Abbreviations: TGF- β , transforming growth factor- β ; EGF, epithelial growth factor; PDGF, platelet-derived growth factor; FGF2, fibroblast growth factor2; IL, interleukin; α -SMA, α -smooth muscle actin; FAP, fibroblasts activation protein; PDGFR, PDGF receptor; SDF-1, stromal cell- derived factor-1; CXCL, chemokine (C-X-C motif) ligand; VEGF, vascular endothelial growth factor; MCP-1, Human monocyte chemoattractant protein-1; CCL, chemokine (C-C motif) ligand; TSLP, thymic stromal lymphopoietin; PGE2, prostaglandin E2; IDO, indoleamine 2,3-dioxygenase; GM-CSF, granulocyte- macrophage-colony stimulating factor; MMP, matrix metalloproteinase; TNC, tenascin-c; TSP-1, thrombospondin-1; LOX, lysyl oxidase; CTLs, cytotoxic T-lymphocytes; NK, natural killer cells; DC, dendritic cells.

1. Introduction

1.6 Radiation Therapy

1.6.1 Radiotherapy in NSCLC

Even though projects like Early Lung Cancer Action Project (ELCAP) found that patients diagnosed at Stage I of lung cancer have an 88 % chance of living another full decade⁷⁶, annual screening for populations at risk for lung cancer is not yet available in most countries. Therefore, as stated previously, in most cases since early lung cancer is asymptomatic by the time of diagnosis is in its advanced or metastatic stages. Unfortunately for these cases, surgery, is unlikely to cure the cancer. In some other cases, although lung cancer is detected early, patients are not suitable for surgery resection due to advanced age or tobacco-related pulmonary illness.

Radiotherapy (RT) (**Figure 1.5**) is then used as an alternative approach to provide local treatment in these cases for its ability to inflict DNA damage and cell death. However, the response to conventional radiotherapy and survival rates has been proved to be very modest⁷⁷. A reason for this poor outcome could be because the dose per fraction in conventional RT (2 Gy) is too low to control the tumor. Fortunately, in the last decade, the advancement of imaging tools for planning RT, has been essential to accurately localize the tumor-bearing area⁷⁸ (**Figure 1.6**). Techniques like image-guided radiotherapy (IGRT) can monitor during the course of radiation treatment, the organ movement, the tumor shrinkage as well as the breathing of the patient^{79,80}. These revolutionary techniques have allowed delivery of higher radiation doses per fraction than the conventional 2 Gy with an acceptable toxicity^{79,81}. In inoperable early stage NSCLC, HD-RT delivered at 54 Gy in 3 fraction regimens (3 x 18 Gy) has been able to achieve outcomes comparable to that of surgery with 98 % tumor control and 56 % overall survival at 3 years⁸¹⁻⁸³.

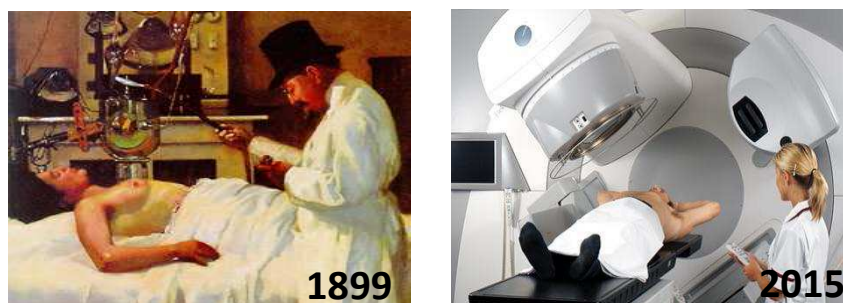


Figure 1.5 More than 100 years of experience in treating cancer patients with ionizing radiation. The progress in cancer imaging tools have allowed a more accurate radiotherapy planning, more precise radiation therapy dose delivery and a greater normal tissue sparing today than in 1899.

1. Introduction

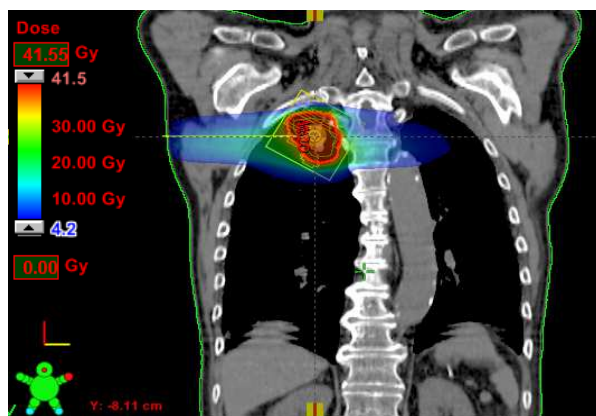


Figure 1.6 Coronal view of radiation treatment plan for a lung tumor in the right upper lobe. Planning target volumes is defined within the red line and will receive the prescribed dose (39 Gy) (3 times 13 Gy). Highest dose (39 Gy) delivered is shown in red while the blue areas are spared to less than 10 Gy. An optimal dose planning for each patient is essential to avoid delivery of high radiation doses to normal tissues and organs while securing maximal dose to the target volume.

Adapted from - http://www.wienkav.at/kav/kfj/91033454/physik/octavius/OD729_SBRT.htm -

1.6.2 Radiation therapy can modulate tumor immunogenicity

Recent evidences indicate that RT may induce anti-tumor immune responses by the generation of tumor antigens and the release of danger signals. During many years it has been believed that radiotherapy exerted exclusively immunosuppressive effects triggered by the collateral damage in the tumor tissue and to the tissue-resident antigen presenting cells causing lymphocytopenia⁸⁴⁻⁸⁷. However several recent *in vivo* experiments and clinical observations have reported a regression of distant metastatic tumors outside the radiated field⁸⁸⁻⁹⁰. Clearly, this systemic tumor response called abscopal response (i.e., away from the target) is more likely to be explained by a RT-induced pro-immunogenic effect than by a RT-induced immunosuppressive effect.

But how does radiation promote systemic immune response? Radiation can promote cross-priming of anti-tumor T-cells by causing immunogenic cell death (ICD) associated with the release of danger signals or alarmins from dying tumor cells. These alarmins, also known as damage-associated molecular patterns (DAMPs) trigger DC activation and maturation by binding to TLR among other cell surface receptors and enhance MHC class I and class II presentation of the tumor antigen-derived peptides to CD8⁺ and CD4⁺ tumor-specific T-cells respectively. In turn, primed CD8⁺ T-cells migrate to the tumor tissue and execute their effector functions (**Figure 1.7**). Danger signals that coordinate ICD includes the extracellular release of the high mobility group box 1 (HMGB1) which is a nuclear DNA binding protein, the surface translocation of the endoplasmic reticulum residing protein, calreticulin (CRT), the extracellular release of heat shock proteins (HSPs) 70 and 90 associated with stress cells, and the release of ATP into the extracellular space⁹¹.

1. Introduction

However, the effects of radiation depends on several factors including fraction numbers and dose per fraction, tumor microenvironment, types of mutations carried by the tumor cells as well as their position in the cell cycle at the time of radiation. Altogether, these issues dictate the cell death pathway induced and thus if the process culminate in ICD or not^{92,93}.

Radiation can induce various modes of cell death, but it can also modulate the expression of other cell surface molecules with immune-modulating functions making tumor cells visible to the immune system (**Figure 1.7**). Vascular endothelial cells, respond to RT by up-regulating the expression of adhesion molecules, vascular cell adhesion molecule-1 (VCAM-1), E-selectin and Intercellular Adhesion Molecule-1, facilitating T-cell arrest and adhesion⁹⁴. RT can also induce expression of T-cell chemokines, like CXCL16 that promote primed CD8⁺ T-cell adhesion and extravasation into the tumor microenvironment⁹⁵. Additionally, RT may increase the expression of MHC class I molecules⁹⁶ and NKG2D ligands⁹⁷ on the surface of tumor cells thereby increasing the chances of antigen-specific CD8⁺ T-cells and NK cells to recognize a tumor cell. Low dose radiotherapy but not high-dose radiotherapy presumably induces macrophages to shift towards M1 phenotype⁹⁸. Finally, RT can up-regulate expression of the FAS death receptor on tumor cells enhancing the ability of effector T-cells expressing FASL (Ligand) to bind to and kill the cancer cells⁹⁹.

Radiation can also modulate the cytokine production within the tumor microenvironment. For instance it can up-regulate the release of IFN- γ which can not only directly exert anti-tumor immune effects but it can also promote T-effector cells recruitment, enhance DC maturation and up-regulate MHC-I molecules on tumor cells among other effects¹⁰⁰.

1.6.3 Radiation induces a senescent-like phenotype in CAFs

Besides the impact of RT on immune cells and tumor cells, RT may induce phenotypic changes on tumor-resident fibroblasts that can affect tumor development. Many studies, reviewed elsewhere⁸, concur that CAFs can survive ablative doses above 50 Gy. However, CAFs exposed to single high-doses above 10 Gy entered into a state of permanent cell growth arrest called senescence by inducing irreversible DNA foci^{101,102}. Even though cells in senescent state do not divide, they are metabolically active which means that the cells can still release soluble factors. But how the irradiated senescent-secretory phenotype differ from the non-irradiated CAF-secretory phenotype and how

1. Introduction

these soluble factors affect tumor progression, remains controversial. While one study reported that senescent lung-CAFs have a reduced expression of the pro-angiogenic molecules SDF-1, angiogenin and TSP-2 and showed a moderate reduction in migration rates of Endothelial Cell lines¹⁰³. In another study senescent human lung-fibroblasts coinjected with cancer cells in nude mice enhanced cancer cells growth associated with an increased expression of MMPs¹⁰⁴. Supporting this last study, *Campisi* and colleagues have shown that senescent normal fibroblasts may stimulate pre-malignant and malignant epithelial skin cells to proliferate in culture and form tumors in mice^{105,106}. However, these two last studies that reported a senescent-fibroblast pro-malignant phenotype, were carried out with fibroblasts cell lines but not with reactive CAFs. It is important to keep in mind that CAFs are “activated” cells that release elevated levels of a wide array of tumor-promoting molecules such as matrix molecules, pro-angiogenic factors, immunosuppressive factors among other growth factors (**Figure 1.4**), while fibroblast residing in normal tissues are “resting” cells presenting a different secretory phenotype. In general, relatively little information exists on the role of irradiated CAFs in cancer progression. However, this area of knowledge represents the main interest of our research group.

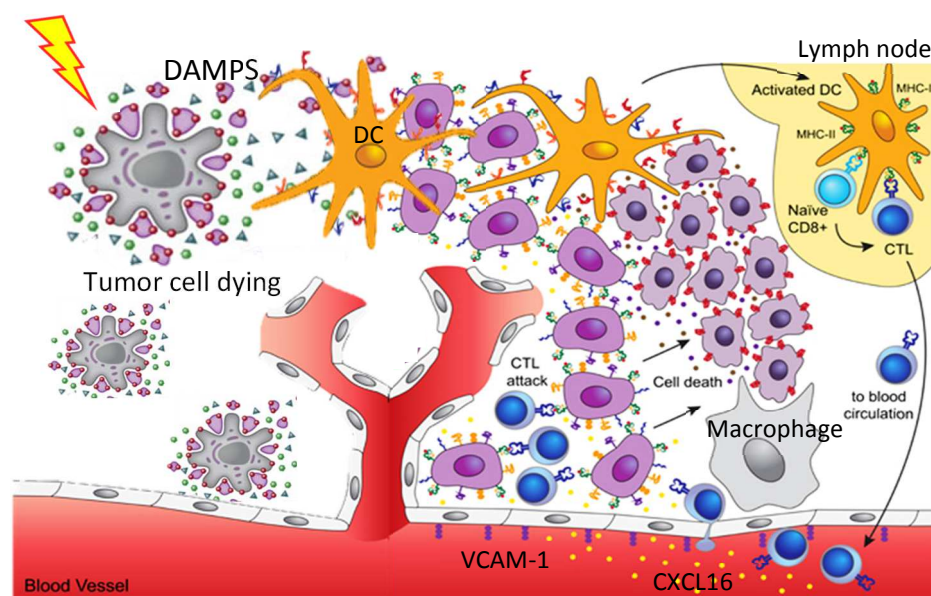


Figure 1.7 Effects of radiotherapy (RT) on the tumor microenvironment. RT can induce immunogenic tumor cell death which leads to the release of damage-associated molecular patterns (DAMPs), triggering DC activation and maturation. Mature DCs arrive to the draining lymph nodes and prime antigen specific CD8⁺ T-cells. In turn, primed CD8⁺ T-cells migrate to the tumor tissues and execute their effector functions against radiotherapy-resistant tumor cells. Other effects of RT on the tumor microenvironment includes the expression of VCAM-1, T-cell chemokines, CXCL16, the increase surface expression of MHC class I molecules on tumor cells and macrophages shift towards M1 phenotype. *Adapted from Demaria et al., Frontiers in Oncology, 2 1-7, 2012.*

2. Aims of the study

Previous studies have reported that CAFs significantly induce immunosuppression. However, it remains incompletely understood by which mechanisms CAFs exert their immunosuppressive role. Additionally, in the context of radiation, several studies agree that fibroblasts exposed to single high-dose radiotherapy undergo extensive and irreversible phenotypic alterations: however, not much attention has been paid yet to the potential consequences of irradiation on CAF-mediated immune-regulatory functions. Thus, in the present project we aimed at studying, immune-modulating properties of primary CAFs isolated from NSCLC tumors towards peripheral blood T-lymphocytes *in vitro*, and to ascertain whether these regulatory functions become changed after exposure to radiation. The main goal of this study has been subdivided into the following sub-goals:

1. To explore CAF-mediated immune-regulatory effects on activated T-cells during co-culture.
2. To ascertain whether the observed effects are induced by paracrine soluble factors or mediated by cell-cell contacts.
3. To study whether the same immune-regulatory effects are observed when fibroblasts are irradiated.
4. To ascertain if high-dose radiation induces immunogenic cell death signals on CAFs.
5. To search for potential CAF-produced effector molecules by analyzing expression of immune-suppressive molecules in CAFs supernatants.

3. Materials

3.1 Cell Culture Growth

	Catalog #	Supplier	Origin
Classical Media			
Dulbecco's Modified Eagle Medium (DMEM)	D6046	Sigma-Aldrich	USA
DMEM/F-12 (1:1)	31330-038	Gibco	UK
Iscove's Modified Dulbecco's Medium (IMDM)	BE12-722F	Lonza	Belgium
Supplements			
Fetal Bovine Serum (FBS)	S0115	Biochrom	Germany
Penicillin-Streptomycin	P0781	Sigma-Aldrich	USA
Insulin-Transferrin-Selenium (ITS)	354350	Corning	USA
Fortecortin (4mg/mL)	759423	Merck	SPAIN

3.2 Cell Culture Reagents

	Catalog #	Supplier	Origin
Cell Detachment			
Bacterial-Collagenase	C9407	Sigma-Aldrich	USA
Enzyme-Free detachment solution	S-014-B	EMDMillipore	Norway
Trypsin-EDTA	T4049	Sigma-Aldrich	USA
Cell Freezing			
Dimethyl Sulfoxide (DMSO)	WAK-DMSO-10	GMBH	Germany
PBMC Isolation			
Lymphoprep TM	1115754	Axis Shield	Norway
Cell Washing			
Phosphate Buffered Saline (PBS)	D8537	Sigma-Aldrich	USA
Bovine Serum Albumin (BSA)	4J013790	AppliChem Panreac	Germany
Mitogenic Reagents			
Phytohaemagglutinin-L (PHA-L)	1249738	Roche	Germany
Lysis Reagents			
Triton X-100	T8787	Sigma-Aldrich	USA

3. Materials

3.3 Supplies

	Catalog #	Supplier	Origin
Cell Culture Surfaces			
96-well-plate white sterile plates	655073	Greiner Bio-One	Germany
Costar® Low attachment 24-well-plates	CLS3473	Sigma-Aldrich	Netherlands
Falcon™ Tissue culture 24-well-plates	353047	BD Falcon	USA
Falcon™ Tissue culture 6-well plates	353046	BD Falcon	USA
Nunc PetriDishes	249964	ThermoScientific	USA
Nunc EasyFlask 25cm ²	156367	ThermoScientific	Denmark
Nunc EasyFlask 75cm ²	156499	ThermoScientific	Denmark
Nunc EasyFlask 175cm ²	159910	ThermoScientific	Denmark
Transwell cell culture inserts	CLS3464	Sigma-Aldrich	USA
Cell Freezing			
Nunc CryoTube Vials	363401	ThermoScientific	Denmark
Other Supplies			
Centrifugal Concentrator (VIVASPIN 6)	Vs0612	Startorius Stedim	Germany
Surgical blade	P308	PARAGON	UK
Syringe	300613	BD plastipal™	Spain
Syringe Filter Unit	SLHA033SB	EMD Millipore	Ireland
Nunc® inoculating loops	I7773	Sigma-Aldrich	USA

3.4 Stains and Dyes

Name	Catalog #	Supplier	Origin
Cell Trace™ CarboxyFluorescein Succinimidyl Ester (CFSE)	C34554	Molecular Probes	USA

3.5 Antibodies

	Conjugate	Catalog #	Supplier	Dilution	Origin
mAntibodies					
Mouse anti-human CD4	PE-Alexa Fluor® 610	MHCD0422	Molecular Probes	1:100	USA
Mouse anti-human CD8	PE	MHCD0804	Caltag Laboratories	1:50	USA
Mouse anti-human CD25	PE	341011	Becton Dickinson	1:10	USA
Primary antibodies					
IDO	mouse	NBP2-21672	Novus Biologicals	1:500	U.K
HMGB-1- ChIP grade	rabbit	Ab18256	abcam	1:500	U.K
Secondary antibodies					
Rabbit anti-mouse IgG	HRP	Ab97046	abcam	1:5000	U.K

3. Materials

Goat anti-rabbit IgG HRP Ab6721 abcam 1:5000 U.K

3.6 Drugs

	Catalog #	Supplier	Reconstitution	Origin
Anti-Inflammatory Drugs				
Tocilizumab (RoActemra 20 mg/ml)	375823-41-9	ROCHE	—————	U.K.
Diclofenac (FW = 318.1 g/mol)	15307-79-6	Cayman Chemical	50 mM in DMSO	USA
Anti-TGF- β 1,2,3 Antibody	MAB1835	R&D Systems	0.5 mg/mL in PBS	USA
Anti-hGalectin-3 Antibody	AF1154	R&D Systems	1 mg/mL in PBS	USA

3.7 Recombinant Proteins

	Catalog #	Supplier	Reconstitution	Origin
Chemokines				
Recombinant Human SDF-1- α	300-28A	PeProTech	10 μ g/mL in 1 % HSA	USA
Cytokines				
Recombinant Human TGF- β 1	100-21	PeProTech		UK
Recombinant Human IFN- γ	300-02	PeProTech	1 mg/mL in dH ₂ O with 0.1 % BSA	USA

3.8 Kits

	Catalog #	Supplier	Origin
ELISA Kits			
Human IFN- γ DuoSet® ELISA	DY285-05	R&D Systems	USA
Human TGF- β 1 DuoSet® ELISA	DY240-05	R&D Systems	USA
Human TNF- α DuoSet® ELISA	DY210-05	R&D Systems	USA
Indoleamine-2,3-Dioxygenase ELISA kit	SEB547Mu	ClouD-Clone Corp.	USA
Prostaglandin E ₂ Express EIA Kit	500141	Cayman Chemical	USA
Multiplex Protein Array (luminex) Kits			
Bio-Plex Calibration Kit	171-203060	BIO RAD	USA
Human Cytokine 10-Plex Panel	LHC001	Invitrogen	USA
Immunogenic Cell Death Signals Kits			
ATP Release Assay	FF2000	Promega	USA

3. Materials

3.9 ELISAs Reagents

	Catalog #	Supplier	Origin
DuoSet® ELISA Ancillary Products			
Reagent Diluent Concentrate 1	DY997	R&D Systems	USA
Color Reagent A and B	DY999	R&D Systems	USA
Tween 20	P416	Sigma-Aldrich	USA
Sulphuric Acid (H ₂ SO ₄) 95-95%	100731	Millipore	Germany
HEPES	H3784	Sigma-Aldrich	USA
Sodium Hydroxide (NaOH) (FW = 40)	71690	Sigma-Aldrich	USA
Wash Buffer (25x)	WA126	R&D Systems	USA
Reagent Diluent Concentrate 2	DY995	Sigma-Aldrich	USA
Normal Goat Serum	DY005	R&D Systems	USA
Tris (FW = 121.11)	72H5601	Sigma-Aldrich	USA
Sodium Chloride (FW = 58.44)	K26478104917	MERCK	Germany

3.10 FACS Flow Products

	Catalog #	supplier	Origin
Reagents			
FACSFlow	342003	BD Bioscience	Netherlands
FACSRinse	340346	BD Bioscience	Netherlands
Tubes			
Falcon™ Round-Bottom Polystyrene Tubes	352235	BD Bioscience	USA

3.11 Gel Electrophoresis and Western Blotting Products

	Catalog #	Supplier	Origin
Gels			
NuPAGE gel	NP0335BOX	Invitrogen	USA
Reagents & Buffers			
20x NuPAGE®MOPS SDS Running Buffer	NP0001	Invitrogen	USA
4x NuPAGE®LDS Sample Buffer	NP0007	Invitrogen	USA
10x NuPAGE® reducing agent	NP0009	Invitrogen	USA
Coomassie Staining Blue	LC6065	Invitrogen	USA
20x NUPAGE® Transfer Buffer	NP0006	Invitrogen	USA
Antioxidant	NP0005	Invitrogen	USA
MagicMark™ Xp Western Protein Standard	LC5602	Invitrogen	USA
PVDF transfer membrane, 0.45 µm	88518	Invitrogen	USA
Super signal West Pico Chemiluminescent Substrate	SC-2048	ImmunoCruz™	USA

3. Materials

3.12 In gel-reduction, Alkylation and Digestion Reagents

Reagents	Catalog #	Supplier	Origin
LC-MS grade Acetonitrile (ACN)	PI85188	VWR	USA
DiThioTreitol (DTT)	43815	Sigma-Aldrich	USA
Iodacetamide (IAA)	I6125	Sigma-Aldrich	USA
LC-MS grade Formic Acid (FA)	85174	Thermo Scientific	USA
Trypsin Porcine	V5111	Promega	USA

3.13 MACS Products

	Catalog #	Supplier	Origin
Accessories			
MACS MultiStand	130-042-303	Miltenyl Biotec	USA
Separator			
MidiMACS Separator	130-042-302	Miltenyl Biotec	USA
Reagents			
CD4 MicroBeads	130-045-101	Miltenyl Biotec	USA
Columns			
LS Columns	130-042-401	Miltenyl Biotec	USA

3.14 Instruments

	Supplier	Origin
Bioluminescent image analyzer		
Image Quant LAS 4000	GE HealthCare	Germany
Centrifuges		
Heraeus Sepatech Biofuge 13	Heraeus Sepatech GmbH	Germany
Multifuge X3R	ThermoScientific	Germany
Rotina 420R	Hettich	Germany
Centrifugal Vacuum Concentrator (Rotavapor)	Eppendorf /lifescience	Germany
Flow Cytometry		
FACSAria™	BD Bioscience	USA
FACSCalibur™	BD Bioscience	USA
Incubators		
37°C Incubator	Termaks AS	Norway
HERAcell 150i (CO ₂ cell culture incubator)	ThermoScientific	Germany
HERAcell 240i (CO ₂ cell culture incubator)	ThermoScientific	Germany

3. Materials

Microplate Readers		
Bio-Plex® 200 systems	BIO-RAD	USA
EMax®	Molecular Devices	USA
Luminometer	Labsystems Luminoskan	USA
Multiskan Ascent	ThermoElectronCorporation	USA
Microplate Washer		
WellWash 4 MK 2	ThermoElectronCorporation	USA
Filtration Vacuum manifold for bead washing	Pall® Life Sciences	USA
Microscope		
Inverted Microscope ECLIPSE TS100-F	NIKON	Japan
Protein measurements		
NanoDrop® Spectrophotometer	Saveen Werner life science	USA
Sonicator		
Bioruptor® Sonication System version 1.1	Diagenode	Belgium

3.15 Software

	Supplier	Origin
Flow Cytometer		
CellQuest™ Pro Software	BD Bioscience	USA
Flow Jo Office V7/8	Tree star	USA
FACSDiva Software	BD Bioscience	USA
Microplate Readers		
Ascent Software®	ThermoElectronCorporation	USA
Bio-Plex Manager™ 6.0 Software	BIO-RAD	USA
SoftMax® Pro Software	Molecular Devices	USA
Statistics Software		
Excel® 2013	Microsoft	USA
GraphPad Prism 5	GraphPad	USA
Image Software		
Spot Software 4.7	Diagnostic Instruments Inc.	USA

3. Materials

3.16 Mediums

Complete DMEM growth medium

DMEM with 10 % FBS and 1 % Penicillin-Streptomycin

Serum-Free DMEM medium

DMEM with 1 % Penicillin-Streptomycin, 0.1% ITS and Fortecortin (1 µg/mL)

CAFs Freezing medium

DMEM with 10 % DMSO and 20 % FBS

Complete IMDM medium

IMDM with 10 % FBS and 1 % Penicillin-Streptomycin

PBMCs Freezing medium

FBS with 10 % DMSO

4. Methods

A detailed description of the methods used in the current study is given in the following sections. The flowchart from **Figure 4.1** gives an overview of the pathways and methods used and followed in the present project.

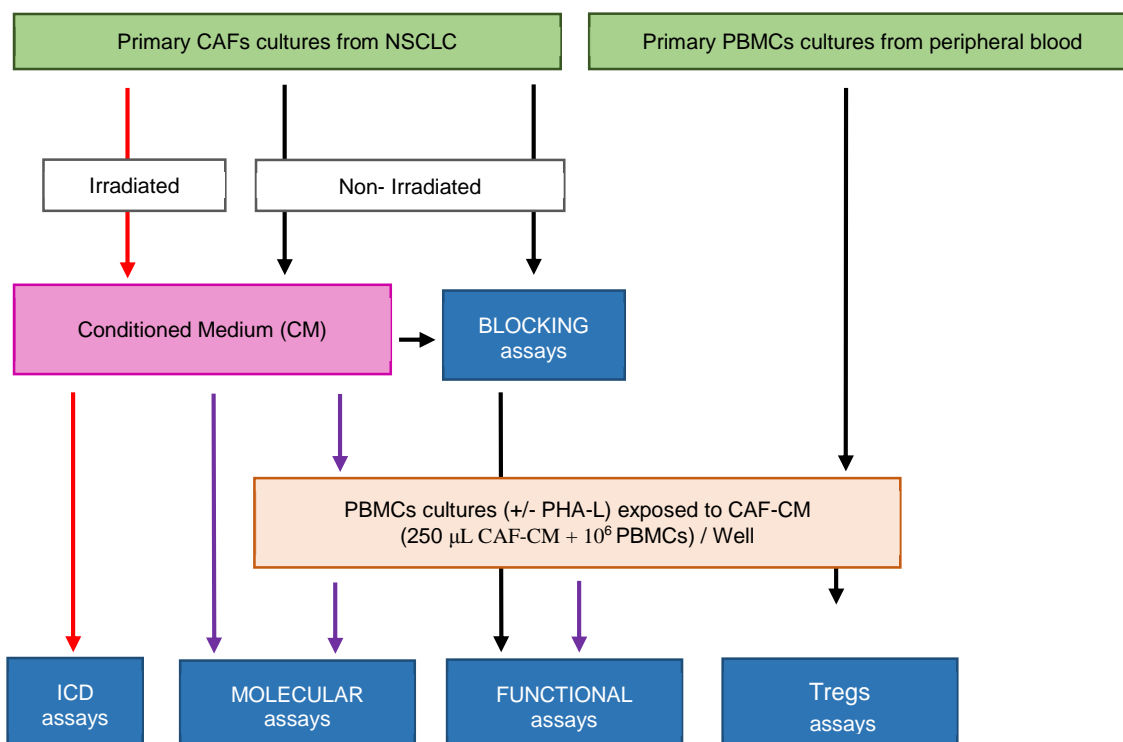


Figure 4.1 Flowchart of pathways followed in the present study. Starting with the isolation and cultures of primary CAFs from non-small cell lung carcinoma (NSCLC) and Peripheral Blood Mononuclear Cells (PBMCs), T-cell cultures from PBMCs containing Conditioned Medium (CM) from irradiated or non-irradiated CAFs were carried out with or without the mitogenic reagent PHA-L. Afterwards, Molecular, Functional, Tregs and Blocking assays were performed aiming at studying the immune-modulating properties of CAFs and the possible changes induced by radiation. At the same time Immunogenic Cell Death (ICD) assays were performed to ascertain whether CAFs switch on ICD responses after exposure to irradiation. **Red arrows** show assays performed with irradiated CAFs. **Black arrows** show assays performed with non-irradiated CAFs. **Purple arrows** show assays performed with both irradiated and non-irradiated CAFs cultures.

4. Methods

4.1 Ethical Statement

Human blood samples and human lung tumor specimens were anonymously coded and a written informed consent was obtained from all patients and healthy volunteers in accordance with the Declaration of Helsinki. The study is approved by the Regional Ethical Committee (REK-Nord).

4.2 Biological samples and Patients

Lung tumour specimens were obtained from randomly selected patients diagnosed with NSCLC with different stages and operated at the University Hospital of Northern Norway, with an average age of 61 years (range 58-67) (**Table 4.1**). Patients included in this study were not undergoing additional therapy when their samples were collected.

Peripheral blood samples were obtained from healthy, volunteer blood donors attending the University Hospital of Northern-Norway Blood Bank.

Table 4.1 Donor features corresponding to the source of CAFs used for experimentation in this study

Number	Age	Sex	Tumor Type	T-size (mm)	T-stage and N-stage
Donor 1	60	F	MD-SCC	35 mm	pT2aN0
Donor 2	67	F	MD-SCC	30 mm	pT1bN0
Donor 3	62	F	BAA	12 mm	pT1aN0
Donor 4	57	F	MD-AC	30 mm	pT2aN1
Donor 5	64	F	LD-AC	30 mm	pT1bN0
Donor 6	58	M	MD-AC	60 mm	pT2bN0
Donor 7	60	F	BAA	6 mm	pT1aN0

F: Female; M: Male

MD: Middle differentiated; LD: Low differentiated

SCC: Squamous Cell Carcinoma; BAA: Bronchioalveolar Adenocarcinoma; AC: Adenocarcinoma

pT1a: Tumor is 2 cm or less; pT1b: Tumor is larger than 2 cm but not larger than 3 cm; pT2a: Tumor is 5 cm or less, pT2b: Tumor is larger than 5 cm but not larger than 7 cm

N0: There is no spread to nearby lymph nodes; N1: The cancer has spread to lymph nodes within the lung and/or around the area.

4.3 Isolation and Culture of Primary NSCLC Fibroblasts

4.3.1 Selection of cell source: Primary cells

Our laboratory has chosen to work with human primary cell cultures (i.e., cells directly isolated from a tissue and expanded *in vitro*) over cell lines (i.e., immortalized cells) for the simple reason that primary cells display closer phenotypic characteristics of the original tissue¹⁰⁷. Even though fibroblasts obtained from primary cell cultures have a limited proliferative capacity and may reach the state of replicative senescence (i.e., permanent growth arrest), during culturing, they closely mimic *in vivo* fibroblasts traits. Thus, the extrapolation of *in vitro* data to *in vivo* effects in humans can be done more

4. Methods

accurately. In contrast, fibroblasts obtained from cell lines show transformed phenotypes where chromosomal aberrations are frequently found leading to an abnormal, unlimited proliferative capacity¹⁰⁸.

A limitation that can be encountered when working with human primary cell cultures is that the original features of the primary cultures can change in every passage (i.e., subculture). Thus, to ensure consistent results, isolated cells were expanded enough at one time and cryopreserved to guarantee that the cells were at the same passage in all the experiments.

4.3.2 General procedure

Human CAFs were harvested from freshly resected lung tumor tissues from patients diagnosed with NSCLC and operated at our hospital. Tumor specimens of about 1 cm³, were delivered by pathologists to the laboratory within 24 hrs after surgical resection in sterile DMEM (section 3.1). Samples were then processed quickly to avoid cell death in an aseptic environment using a biological safety cabinet.

Four steps for isolating and culturing primary NSCLC fibroblasts were followed:

- a) Enzymatic digestion
- b) Selective detachment by enzyme-free cell detachment solution
- c) Fibroblasts cell passage
- d) Cryopreservation of primary fibroblasts

a) Enzymatic digestion

Tumor tissues were minced into small pieces (1-1.5 mm³) in a Petri dish with the help of two surgical blades. Tissue pieces were then collected in a T-25 cell culture flask and subjected to enzymatic digestion for 1.5 hrs with 0.8 mg/mL bacterial-collagenase (section 3.2) in a final volume of 10 mL DMEM/F-12 (section 3.1) placing the T-25 flask on an orbital shaker in a standard incubator at 37°C. Subsequently, the digested tissue solution was vigorously shaken in order to liberate possible cells trapped in the small pieces of tissue, collected in a 50 mL sterile tube and spun down at 400 x g for 5 min to eliminate collagenase. The supernatant was discarded and the pellet was resuspended in 24 mL of fresh complete growth medium consisting of DMEM supplemented with 1 % penicillin-streptomycin and 10 % FBS (section 3.1). The cell suspension was then added into 6-well tissue culture plates (2 mL/well) and placed in a cell culture incubator at 37°C with low oxygen (3 % O₂) overnight, letting the cells attach to the solid substrate.

4. Methods

b) Selective detachment by enzyme-free cell detachment solution

The next day, in order to obtain pure fibroblasts cultures, the medium was removed from the wells and the primary culture mixture was washed with 2 mL PBS (section 3.2) (per well) for 1-2 min. The PBS was then removed, and 2 mL of Enzyme-Free cell detachment solution (section 3.2) was added to the wells. After incubating for 5 min at 37°C with 3 % O₂, the 6-well plate was examined under a microscope to confirm fibroblasts detachment. In case of poor detachment 500 µL of pre-warmed Trypsin-EDTA (0.25 %) solution (section 3.2) was added to the wells for 1 min. –While enzyme-free solution detaches cells while maintaining the structural integrity of cell surface proteins, Trypsin-EDTA cuts away the focal adhesions that are anchoring the cells to the flasks –. The detached fibroblasts were then collected in a 15 mL tube, spun down at 400 x g for 5 min and resuspended in 10 mL of complete growth medium. Cell suspension was then split in two T-75 flasks and brought to a final volume of 10 mL complete medium. Flasks were then placed for further propagation in a cell culture incubator at 37°C in a 5 % CO₂ humidified atmosphere.

c) Fibroblasts cell passage

Cells were observed under a microscope every 24 hrs, and the growth medium was replaced with fresh medium every 2-3 days until they reached 80 % - 90 % confluence. Fibroblasts have elongated shapes and are anchorage-dependent, which means that they grow in monolayers while attached to a solid or semi-solid substrate (**Figure 4.2**).

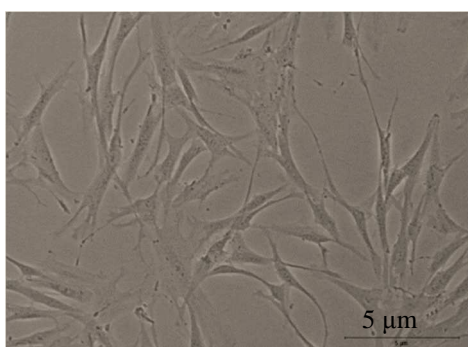


Figure 4.2 CAFs in culture. Image shows isolated NSCLC primary fibroblasts in culture growing in monolayers attached to the surface. Characterized by their cytoplasmic extensions.

Once confluent, the medium was discarded and cells were detached using 5 mL Enzyme-Free cell detachment solution for 5 min at 3 % O₂. To prevent cell aggregation, 1 mL of Trypsin-EDTA (0.25 %) solution was added during the last min of incubation. When cells became round and detached, the cell solution was collected in a 15 mL tube, spun down,

4. Methods

resuspended with 10 mL of complete growth medium, split in two T-175 flasks with 15 mL final volume of complete DMEM medium and incubated at 37°C, 5 % CO₂.

d) Cryopreservation of primary fibroblasts

After reaching confluence, CAFs (from passage 2) were directly used for analysis or cryopreserved and used in later experiments. For cryopreservation, cells were detached as previously described, counted in a counting chamber, spun down and cryopreserved at – 80°C in CAFs freezing medium consisting of DMEM with 10 % DMSO and 20 % FBS at 5 x 10⁵ cells per mL per CryoTube.

DMSO is the most commonly used cryoprotectant, due to its ability to prevent formation of ice crystals during the cooling process which can easily rupture the cell membrane. However, a limitation of working with DMSO is that it can be toxic for the cells at high concentration (> 10 %) or if the cells are exposed to DMSO for prolonged periods.

Therefore, to obtain the best survival as possible, thawing of the cryopreserved cells was carried out as quickly as possible. Once the CryoTube was removed from the freezer it was placed into a 37°C water bath until it was completely thawed. The cell suspension was then slowly added (drop by drop) in 10 mL pre-warmed complete medium. Cells were then seeded in a T-75 flask at 37°C, 5 % CO₂ and incubated for 24 hrs for attachment. The next day the incubation medium was replaced with fresh medium to completely remove the DMSO.

4.4 Irradiation and preparation of Fibroblast-Conditioned Medium

Conditioned Medium (CM) was collected from irradiated and non-irradiated cultured CAFs to examine fibroblasts' paracrine effects on lymphocytes. CM is the used medium collected from cultured cells which contains many mediator substances such as growth factors and cytokines secreted into the medium by the cells.

4.4.1 General procedure

At the 3rd passage CAFs were seeded at 4 x 10⁵ cells per T-75 flask and incubated for 24 hrs for attachment at 37°C, 5 % CO₂. After the initial cell attachment and spreading until 60 % - 70 % confluence (ca. 2-3 days after seeding), the medium was removed and 6 mL of complete DMEM medium was added followed by irradiation.

CAFs were irradiated with high-energy photons resulting from 15 megavoltage (MV) beams produced by a Varian clinical linear-accelerator, and a single dose of 18 Gy (1 x

4. Methods

18 Gy) was typically applied. For a beam produced by an energy of 15 MV, the dose from photons to tissue is at its maximum (18 Gy) at about 30 mm depth within the body. Therefore T-75 flasks were placed in the center of a 20 x 20 cm field, and a depth of 30 mm was constructed by letting the beam pass through three (10 mm thick) tissue-equivalent Perspex-plates, and positioning the gantry, which transports the beam from the linear-accelerator to the target, at 180 degrees (i.e. below the plates) (**Figure 4.3**).

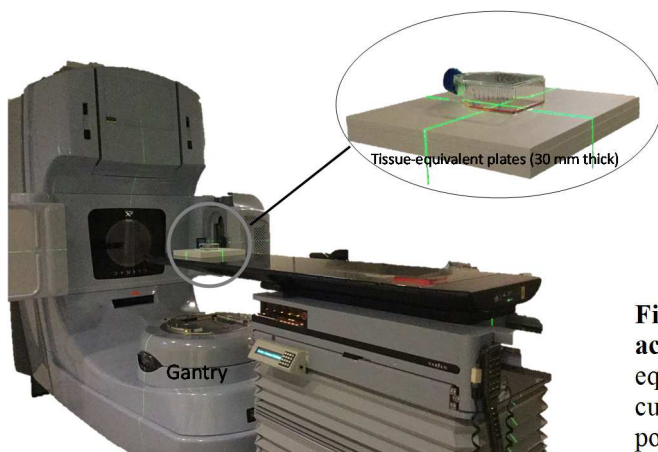


Figure 4.3 Varian clinical linear-accelerator. Image shows the tissue-equivalent plates where the flask with cultured cells was placed. The gantry was positioned below the flask.

CM was replaced with 6 mL of fresh complete medium 3 days post-irradiation and collected 6 days post-irradiation in 15 mL tubes, centrifuged (2.200 x g, 5 min) and passed through a 0.22 μ m filter for elimination of potential contaminant cell bodies. CM was either used immediately for experimental analysis or frozen at -80°C for further analysis in Eppendorf Protein LoBind tubes (1 mL/tube). The cell density from the CM was about 350.000 cells/mL.

Before analysis, CAF-CM was thawed and vortexed for 30 seconds to ensure adequate mixing of the protein suspension.

Supernatants from non-irradiated CAFs were similarly collected after 3-days conditioning at a density of ~ 350.000 cells/mL. Of importance, non-treated cells were not allowed to reach overconfluence before harvesting since cells could enter a senescence state.

Of note, some CAF cultures ($n = 3$) received a total dose of 8 Gy in 4 fractions of 2 Gy each (4 x 2 Gy). Fractions were delivered every 24 hrs via linear accelerator and the CM of all samples was collected following the same procedure as for the 1 x 18 Gy CAF-CM.

4. Methods

4.5 Isolation and Culture of human PBMCs

Peripheral Blood Mononuclear Cells (PBMCs) from healthy volunteers were isolated using a density gradient media called Lymphoprep™ (section 3.2).

4.5.1 General principles

Lymphoprep™ is a density barrier method by which cells with higher densities than this medium (1.077 g/mL) such as red blood cells and polymorphonuclear leukocytes sediment through the medium while cells with densities below 1.077 g/mL, such as mononuclear cells, are retained at the interface by centrifugation.

4.5.2 General procedure

Peripheral blood obtained in bags and with a volume of approximately 50 mL was diluted 1:1 in PBS in 2 x 50 mL tubes. Approximately 24 mL of Blood – PBS was then slowly layered over 12 mL Lymphoprep™ in 4 x 50 mL tubes, followed by 30 min of centrifugation at 700 x g at room temperature without breaks. The PBMCs from the interface were then carefully collected using a Pasteur pipette in 4 x 50 mL tubes, and washed 3 times (3x) with 40 mL of 0.2 % PBSA (section 3.2) (0.2 % bovine serum albumin in PBS) by centrifugation at 350 x g for 10 min at room temperature to eliminate platelets. Of note, when PBMCs are washed, it is important to add a protein, in this case albumin, in the PBS to avoid cell aggregations.

After the last washing-step, supernatants were discarded and the cells from all the tubes were mixed in one tube and added in 10 mL freezing medium consisting of 90 % FBS with 10 % DMSO. Cells were then rapidly added in CryoTubes (1 mL/tube) and cryopreserved at – 80°C until analysis. The cell density was approximately of 5×10^7 cells per CryoTube.

Before analysis, PBMCs were quickly thawed in 10 mL complete medium consisting of IMDM (section 3.1) supplemented with 10 % FBS and 1 % penicillin-streptomycin and cultured overnight in T-75 flasks at 37°C in a 7.5 % CO₂ humidified atmosphere. Unlike fibroblasts, PBMCs are cultured in cell suspension, thus they do not attach on the surface of the flask.

It is important to culture PBMCs in 7.5 % CO₂ because the buffering capacity of IMDM media is optimal at this CO₂ concentration so the pH is maintained stable.

4. Methods

4.6 Lymphocyte proliferation assays

T-cell proliferation assays comprising PHA-L (section 3.2) -activated lymphocytes in (a) co-culture with irradiated or non-irradiated CAFs or in (b) culture with irradiated or non-irradiated CAF-CM were carried out.

PHA-L are lectins found in plants and are carbohydrate-binding proteins that bind to T-cell surface receptors triggering T-lymphocytes activation and proliferation in an antigen independent manner.

Rates of T-cell proliferation were assessed by Flow-cytometry using the CFSE (section 3.4) dye dilution assay, also known as CFSE assay.

4.6.1 General principles

CFSE assay is an effective mean to monitor lymphocyte proliferation. CFSE is a membrane-permanent dye with high capacity to label lymphocytes by covalently coupling to long-lived intracellular molecules. Thus, when a CFSE-labeled cell divides, the CFSE dye is divided equally between the two daughter cells. This progressive halving of fluorescence intensity within daughter cells can be clearly visualized by Flow cytometry, Fluorescent-Activated Cell Sorting (FACS) Calibur™ (section 3.14).

The basic principle of FACSCalibur™ is to count and identify single cells by their physical characteristics as they pass one by one through a light source. Besides identifying single cells by their size and density (i.e., number of cytoplasmic granules, membrane size), this flow cytometer can also identify single cells by their cell-surface molecules or their intrinsic molecules bound to either fluorescent-labeled antibodies or fluorescent dyes like CFSE. Thus, the light source which is a laser beam excite the fluorescent molecules to a higher energy state and emit light at varying wavelengths. In the case of CFSE labeled-intracellular molecules, green light is emitted when exposed to blue (488 nm) laser light in the flow cytometer. The intensity of light emitted is proportional to the amount of dye present in the cells.

When the laser hit the cells, the light is also dispersed and the combination of scattered and fluorescent light is detected and analyzed by detectors placed around the stream of fluid that carries the cells. Fluorescent light is detected by fluorescent detectors while scattered light is detected by a Forward Scatter (FSC) which corresponds to the cell size, and a Side Scatter (SSC) which corresponds to the cell density¹⁰⁹. Data is then analyzed by a computer connected to the flow cytometry using a CellQuest™ ProSoftware (section 3.15).

4. Methods

4.6.2 General procedure

Proliferation assays were divided into three parts:

- a) CFSE-labeled PBMCs
- b) Proliferation assays
- c) Analysis via FACSCalibur

a) CFSE-labeled PBMCs

Cultured PBMCs were resuspended and collected in a 15 mL tube (leaving some cells in the flask, for FACSCalibur™ calibration), spun down (400 x g, 4 min) and washed once in 10 mL PBSA (0.2 %) by centrifugation (400 x g, 4 min). After washing, cells were resuspended in 1 mL of PBSA (0.2 %) and CellTrace™CFSE was added at a final concentration of 2.5 µg/mL. The mixed was then incubated into a 37°C water bath for 15 min. Following incubation, the labeled-cells were cooled on wet ice and resuspended in 10 mL cold complete IMDM medium and washed 3x with PBSA (0.2 %).

b) Proliferation assays

In co-culture experiments, irradiated and non-irradiated CAF (n = 5) cultures were seeded in duplicates in 24-well tissue culture plates at a concentration of 10.000 cells/well and CFSE-labeled PBMCs were added at a density of 1×10^6 cells per well in 0.5 mL complete IMDM medium (CAFs-PBMC ratio: 1:100).

For proliferation assays with CAF-CM, instead of CAFs, 72 hrs CM from irradiated or non-irradiated CAF cultures was diluted (1:1) with fresh pre-warmed complete IMDM medium and cultured with 1×10^6 PBMCs.

Immediately after initiation of co-cultures and mono-cultures, cells were exposed to the mitogenic reagent, PHA-L at a final concentration of 1 µg/mL. A negative and a positive control were prepared in duplicates by adding PBMCs alone in suspension. PHA-L was added in all the wells with exception of the negative control. Mixed cultures were then incubated for 5 days at 37°C, at 7.5 % CO₂ changing half of the medium (250 µL) with fresh complete IMDM medium with PHA-L (1 µg/mL) on day three.

c) Analysis via FACSCalibur

Following incubations, PBMCs were harvested in Falcon™ Round-Bottom Polystyrene Tubes, centrifuged (400 x g, 4 min) and resuspended in 0.5 mL of PBSA (0.2 %). CFSE fluorescence was analyzed by FACSCalibur™ flow cytometer after gating the lymphocyte population on the forward and side scatter. The Flow cytometry data was then analyzed by FlowJo Office V7/8 software (section 3.15).

4. Methods

Of note, T-cell proliferative responses of CD8⁺ and CD4⁺ subsets in co-culture with irradiated and non-irradiated CAFs (n = 5) were also determined by FACSCalibur™ flow cytometry in duplicates. For this purpose, cells were stained with CD4- PE-Alexa 610 or CD8-PE conjugated monoclonal antibodies (section 3.5) for 30 min on ice and washed with PBSA (0.2 %). Frequencies of CD4⁺ or CD8⁺ T-cells with CFSE dye dilution was determined by flow cytometry, and by plotting fluorescence intensity for CD8 or CD4 against CFSE dye dilution.

PE-Alexa 610-conjugated emit red light (610 nm) when exposed to blue (488 nm); R-PE-conjugated emit red/orange light (575 nm) when exposed to blue, whereas the CFSE dye (FITC-conjugated) emit green light (525 nm) when exposed to blue.

4.7 Transwell migration assays

Migration of PHA-L activated lymphocytes towards conditioned medium from fibroblasts in the presence or absence of the chemo-attractant SDF-1 (section 3.7), was assessed in Transwell migration chambers and analysed by Flow cytometer, FACSCalibur™.

4.7.1 General principles

Transwell migration assays, also known as Boyden chamber assays are commonly used to measure the motile and invasive capacity of live cells towards a chemo-attractant gradient. Boyden chambers consist of lower and upper wells separated by a membrane filter with pores. The chemo-attractant solution is placed in the bottom wells, while cells are added in the upper wells and after a period of time, cells that have migrated through the pores to the bottom wells are collected and counted¹¹⁰. Membrane pore size used in the assays should be smaller than the diameter of the cells to avoid passive migration through the pores. Thus, choosing the right pore size is a key factor for success. In the present assay, bare polystyrene transwell membrane with 8 µm pore size was used, since human lymphocytes are 10 µm in diameter (**Figure 4.4**).

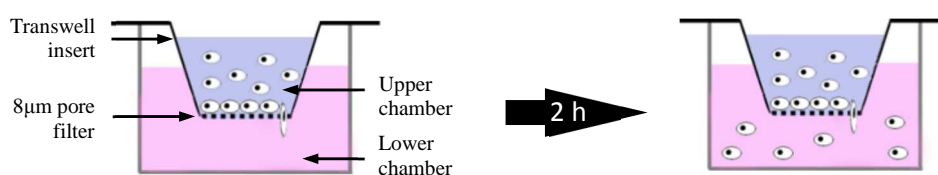


Figure 4.4 Lymphocytes migration assays. Experimental setup for lymphocyte migration assays using polycarbonate filter chambers with 8µm pore size.

4. Methods

Cultured PBMCs in 10 mL complete IMDM medium (section 4.5.1) were activated with PHA-L (1 µg/mL) 24 hrs prior to the assay and incubated in a T-75 flask at 37°C, 7.5 % CO₂. After 24 hrs, cells were collected in a 15 mL tube, counted, spun down (400 x g, 4 min) and suspended at density of 1 x 10⁶ cells/100 µL in complete IMDM medium. Then, 100 µL of PBMCs solution were cultured in the top chamber of 6.5 mm diameter 8 µm pore transwell culture insert (section 3.3), and incubated in triplicates with 600 µL of CAF-CM from irradiated and non-irradiated cultures (n = 4) (section 4.4.1) with or without the chemo-attractant SDF-1 at a final concentration of 50 ng/mL in the bottom chamber. Cultures were incubated for 2 hrs at 37°C, 7.5 % CO₂. Following this incubation period, transmigrated cells into the lower chamber were harvested in Falcon™ Round-Bottom Polystyrene Tubes, centrifuged (400 x g, 4 min), resuspended in 0.5 mL of PBSA (0.2 %) and counted by FACSCalibur™ flow cytometer for 60 seconds at high flow rate, gating on the forward and side scatter the lymphocytes population.

The optimal incubation time (2 hrs) and the minimal effective concentration of the chemo-attractant SDF-1 (50 ng/mL) was determined by two pilot experiments. In the time-course pilot experiment, non-activated PBMCs were cultured in the upper chamber and incubated with complete IMDM medium with or without SDF-1 (100 ng/mL) in the lower chamber for 3, 6 and 12 hrs. In the second pilot experiment, non-activated PBMCs cultured in the upper chamber were incubated with complete IMDM medium with 50, 10 and 2 ng/mL SDF-1 in the lower chamber for 2 hrs (*additional files C.1*).

4.8 Multiplex protein arrays (Luminex)

Quantitative measurements of cytokines and inflammatory factors released into the culture medium were performed using a suspension array technique. Supernatants from (a) irradiated and non-irradiated CAF cultures (n = 5) (section 4.4.1); (b) PBMCs, obtained from the negative and positive controls in section 4.6.2, and (c) CAF-CM – PBMCs cultures (n = 5), also obtained from the lymphocyte proliferation assay (section 4.6.2) were thawed and analyzed in duplicates using a human cytokine 10-Plex panel kit (section 3.8).

4. Methods

4.8.1 General principles

Multiplex protein arrays use color-coded beads that permit a quantitative measure of many proteins (up to 100 cytokines) precisely and simultaneously in experimental samples. The present multiplex bead immunoassay is designed to measure a total of 10 human cytokines: Granulocyte-macrophage colony-stimulating factor (GM-CSF), IFN- γ , IL-1 β , IL-2, IL-4, IL-5, IL-6, IL-8, IL-10 and Tumor Necrosis Factor (TNF)- α in serum, plasma or tissue culture supernatants. In this kit, capture antibodies against the cytokines of interest are covalently coupled to beads with defined spectral properties. The capture antibody-coupled beads are added to the sample and allowed to react. After the incubation time and appropriate washing steps with a filtration vacuum manifold (section 3.14), biotinylated detector antibodies are added and allowed to bind to the specific immobilized proteins resulting in a sandwich of antibodies around the cytokine. The immune complexes are then detected by the addition of streptavidin conjugated to the fluorescent protein, R-Phycoerythrin (RPE) which bind to the biotin of the detector antibodies¹¹¹. The spectral properties of the beads and the amount of associated RPE fluorescence is then analyzed with a Luminex detection system which is based on the principles of flow cytometry. This analyzer has two lasers, one laser recognizes the beads and determines the cytokine that is bound to it and the second laser determines the magnitude of fluorescent intensity which is proportional to the amount of bound cytokine¹¹¹. Data is then examined by a Bio-Plex Manager™ software (section 3.15).

When performing multiplex bead immunoassays, a standard solution containing a known amount of cytokines needs to be included in duplicates.

4.8.2 General procedure

All samples were analyzed in duplicates and in dilutions of 1:4 in the same complete DMEM medium according to the manufacturer protocol (*additional files A.1*). A seven point standard curve using 3-fold serial dilutions was prepared.

Levels of proteins included in the array were detected using the Luminex Bio-Plex® 200 system (section 3.14), according to instructions from the manufacturer. Results were analyzed using the Bio-Plex Manager™ 6.0 Software which determines the absolute concentrations of the samples by building a standard curve for each specific cytokine upon a five parameter algorithm equation with a weighted function ($1/y^2$), this function minimizes residuals (i.e., errors) at the high end of the standard curve (residuals increases as concentration increases). Residuals = (Calculated Concentration – Expected

4. Methods

Concentration). Standards outliers analyzed by the percent recovery ((Calculated Concentration / Expected Concentration)*100), calculated by the software were invalidated (i.e., standard points below 70 % recovery or above 130 % recovery were considered as outliers).

4.9 Enzyme linked immunosorbent assays (ELISA)

Further quantitative protein measurements in cell-culture supernatants were performed by “sandwich” ELISAs unless otherwise indicated.

4.9.1 General principles

The principle of a sandwich ELISA method is very similar to the multiplex protein arrays previously explained (section 4.8), with several substantial differences. Capture antibodies of the ELISAs are not coupled to beads, but they are attached to the flat surface of a 96-well-plate. Another difference is that the streptavidin that detects and binds to biotinylated detection antibodies is not conjugated with a fluorescent protein but an enzyme (Horseradish Peroxidase (HRP)) which is detected by a substrate (Tetramethylbenzidine (TMB)). The enzyme – substrate complex converts the substrate to a colored reaction product. Thus, ELISAs use a colorimetric substrate as a reporter instead of a fluorogenic substrate. Most importantly, ELISAs can only quantify one specific protein in a sample.

4.9.2 General procedure

A total of five ELISAs were carried out in the present study to measure and quantify the levels of: PGE₂, IDO, TGF- β 1, IFN- γ and TNF- α .

Concentrations of PGE₂, IDO, TGF- β 1, IFN- γ and TNF- α in 72 hrs CM from irradiated or non-irradiated CAFs cultures were determined using, PGE₂ Express EIA Kit, Indoleamine-2,3-Dioxygenase ELISA kit, Human TGF- β 1 DuoSet® ELISA kit, Human IFN- γ DuoSet® ELISA kit and Human TNF- α DuoSet® ELISA kit respectively (section 3.8) in triplicates according to the manufacturer’s instructions (*additional files A.2-A.4*). Unless otherwise indicated, plates were read in a Multiskan Ascent microplate reader (section 3.14) at wavelength 450 nm. Ascent Software® (section 3.15) was used for construction of standard curves and determination of protein concentration in unknown

4. Methods

samples. Curve fitting was done with a four – parameter logistic algorithm according to the manufacturer’s instructions,

Solutions and reagents were provided in the kits or purchased separately (section 3.9) and reconstitute as indicated in the protocol manual.

Standard reagents were diluted by a two-fold serial dilutions and run in duplicates for all the ELISAs. Complete DMEM medium was used as a negative control for all the Kits unless indicated otherwise.

a) Specific features for PGE2 ELISA kit

This assay is a “competitive” ELISA where PGE2 from the sample and PGE2-acetylcholinesterase (AChE) conjugate from the kit compete for a limited amount of PGE2 specific monoclonal antibody. At the end of the assay Ellman’s reagent, which contain the substrate to AChE, is added to the wells, the product of the enzymatic reaction is a yellow color and is inversely proportional to the amount of PGE2 in the sample. Thus, the higher the sample PGE2 concentration, the weaker the eventual signal.

PGE2 enzyme-substrate reaction was read in an EMax[®] microplate reader (section 3.14) at a wavelength of 405 nm and SoftMax[®] Pro Software (section 3.15) was used for construction of standard curves.

b) Specific features for IDO ELISA kit

CM from CAFs cultures treated with recombinant IFN- γ (100 ng/mL) (section 3.7) for 48 hrs were included as positive controls.

The standard curve fitting for IDO was done with a linear regression graph according to the manufacturer’s instructions.

c) Specific features for TGF- β 1 ELISA kit

In the present ELISA, CAF-CM were prepared as in section 4.4.1 with the exception that at the time of irradiation instead of 6 mL of complete DMEM medium, 6 mL of serum-free DMEM medium (section 3.16) was added. The reason for these adjustments in the cell culture medium is that in this assay latent TGF- β 1 in the samples was acid-activated by addition of 1 M hydrochloric acid (HCl) for 10 min, followed by neutralization with 1.2 M NaOH / 0.5 M HEPES. In view of the high levels of latent TGF- β 1 in serum, CM containing 10 % FBS would give a false positive result. Thus, serum-free DMEM medium was included as a negative control.

4. Methods

d) Specific features for IFN- γ and TNF- α ELISA kits

Concentration of IFN- γ and TNF- α were in addition, measured in the supernatants of **(a)** irradiated and non-irradiated CAF-CM – PBMCs cultures (n = 2) and **(b)** control PBMCs cultures obtained from the proliferation assays (section 4.6.2). Samples were diluted 1:2 and 1:4 respectively in reagent diluent.

Supernatants of PHA-L – activated PBMCs were used as a positive control.

4.10 Western Blotting of IDO expression

Western Blot analysis of IDO expression in non-irradiated CAF-CM and of CAF intracellular IDO expression from cell lysates were carried out as described below.

4.10.1 General principles

Western blot is a technique used to analyse protein expression in a defined sample. First, the proteins are separated by a 1D sodium dodecyl sulfate–polyacrylamide gel electrophoresis (SDS-PAGE) according to size. In a SDS-PAGE, the proteins are first boiled together with the detergent Lithium dodecyl sulfate (LDS) and the reducing reagent, DTT. The heat disrupts quaternary and non-covalent bonds in the tertiary structures of a protein, DTT reduces the covalent disulfide bonds in the tertiary structure in order to have an optimal secondary structure and LDS helps the DTT to be more efficient by avoiding protein refolding. Moreover LDS coats the protein with uniform negative charges in proportion to its relative molecular weight, masking the intrinsic charges of the protein, thus when an electric field is applied into the PAGE the negatively charged proteins migrate towards the positive pole in different rates depending on its molecular weight (polypeptide length). The proteins are then transferred to a polyvinylidene difluoride (PVDF) membrane where the protein of interest is detected by specific antibodies. For a successful Western blot, it is important to use an antibody that specifically reacts with the protein of interest and has little or non-cross-reactivity with other proteins.

4.10.2 General procedure

Western Blotting can be divided in five steps:

- a) Sample preparation
- b) Run SDS-PAGE
- c) Transfer of proteins PVDF membrane
- d) Protein identification with IDO-specific antibodies
- e) Develop the membrane using Bioluminescent Image Analyzer

4. Methods

CAF cultures treated with recombinant IFN- γ (100 ng/mL) (section 3.7) for 48 hrs were prepared in parallel and included as positive controls.

a) Sample preparation

CM from irradiated and non-irradiated cells ($n = 2$) cultured in a serum-free DMEM medium were collected, filtered (section 4.4.1) and ultra-concentrated in VIVASPIN centrifuge tubes (section 3.3) by spinning at 2.200 x g for 30 min. The VIVASPIN sample concentrator is a tube divided into an upper compartment and a lower compartment separated by a semipermeable membrane with a molecular weight cut-off of 5.000 Da. Six mL of CAF-CM were added in the upper compartment. After centrifugation, the more concentrated sample (~150 μ L) was left in the upper chamber while the less concentrated sample passed through the membrane to the lower chamber.

Next, to concentrated supernatant samples 1:2 final volume of 4x NuPAGE LDS Sample buffer (section 3.11) and 1:10 final volume of 10x NUPAGE sample Reducing Agent (section 3.11) were added (the principles of Lithium dodecyl sulfate (LDS) sample buffer and reducing agent are explained in section 4.11).

At the same time, a fixed amount of CAFs corresponding to 5×10^5 cells were lysed with 250 μ L of a Mastermix containing 1:2 final volume of 4x NuPAGE LDS Sample buffer and 1:10 final volume of 10x NuPAGE Sample Reducing Agent in Milli-Q water and sonicated with a sonicator (section 3.14) (for cell disruption) for six 20 seconds cycles.

b) Run SDS-PAGE

All samples were heated for 10 min at 70°C. Denatured samples (30 μ L) were then loaded on a 1D SDS-PAGE gel (NuPAGE[®]Novex 4-12% Bis-Tris Gel 1.5 mm 10 well) (section 3.11) and proteins were separated by electrophoresis at 200 V for 45 min in 1x NuPAGE[®]MOPS SDS Running Buffer (section 3.11), containing 0.1 % antioxidant (section 3.11) which prevent reoxidizing of the proteins. Additionally, 3 μ L of protein ladder (section 3.11) for detection of molecular weight (kDa) was loaded on the gel.

c) Transfer of proteins onto PVDF membrane

The negatively charged proteins from the SDS-PAGE were transferred by electrophoresis onto a positively charged PVDF membrane (section 3.11). Prior to transfer, the PVDF

4. Methods

membrane was exposed to 100 % methanol for some seconds in order to hydrate the membrane and improve transfer and protein binding.

The polyacrylamide gel was placed on the PVDF membrane in between two filter papers and four sponges. All the material was soaked in 1x NUPAGE transfer buffer (section 3.11) containing 10 % methanol and 0.1 % antioxidant and placed in the blotting chamber in 1x transfer buffer. Cold water was added to the outer chamber to cool the system during running. Blotting was performed at 30 V for 1 hr and 15 min.

d) Protein identification with IDO-specific antibodies

Next, the membrane was placed in 50 mL tube and blocked with 5 mL blocking buffer consisting of 1x TBS (Tris Buffered Saline pH 7.4) containing 0.1 % Tween20 and 5 % non-fat dry milk for 1 hr rotating at room temperature. This step is crucial to prevent non-specific binding of antibody to the membrane. The membrane was then incubated rotating overnight at 4°C with the primary antibody, IDO mouse-monoclonal IgG₃ antibody (section 3.5) diluted 1:500 in blocking buffer. Following incubation period, the membrane was washed 4x for 5 min at room temperature in TBS with 0.1 % Tween20 and incubated for 2 hrs with the secondary antibody, HRP-conjugated rabbit polyclonal anti-mouse IgG (section 3.5), diluted 1:5000 in blocking buffer.

e) Develop the membrane using Bioluminescent Image Analyzer

The membrane was washed, incubated with SuperSignal West Pico Chemiluminescent Substrate kit (section 3.11) and immediately imaged with a Bioluminescent Image Analyzer (section 3.14).

4.11 Identification of proteins by Mass Spectrometry

Possible proteins in CAF supernatants from irradiated and non-irradiated cultures (n = 4), were identified by mass spectrometric assays.

The identity of individual proteins within a heterogeneous mixture, as well as its structure, function, post-translational modifications and size can be determined by Mass spectrometry (MS).

4. Methods

4.11.1 General principles

The first step for the identification of proteins by MS (**Figure 4.5**) is to separate the different proteins by a 1D SDS-PAGE (section 4.10.1). The second fundamental step is the reduction and alkylation of cysteines residues in proteins. By this process, the remaining covalent disulfide bonds are irreversible broken. Finally, the denatured proteins are further digested by trypsin and the resulting peptide mixture is analyzed by MS.

The tool of MS is a Mass spectrometer and it consists of three major components: an Ion Source which forms ions, a Mass Analyzer which determines the mass-to-charge ratio (m/z) of the ions and a Detector. The three main components, are in vacuum, since the ions should move freely without hitting air molecules.

Since the analyzed samples in the present assay contained a complex mixture of proteins, a Liquid Chromatography (LC) coupled to a MS supplemented by tandem MS (MS/MS) was used (**Figure 4.5**). In a LC-MS method, peptides are first physically separated (i.e., eluted) in a liquid chromatography and concentrated in a very fine capillary. As the analytes leave the tip of the capillary (hydrophilic peptides come before hydrophobic) they are ionized (i.e., charged) into an electrospray ion source by gaining or losing protons. Then an electric field guide the ions to the mass analyzer where the ions are sorted according to their m/z ratio. The LC-MS in tandem (MS/MS) means that the generated ions are further fragmented by energetic collision with a gas (e.g., nitrogen (N_2)) and a second Analyzer (MS2) measures the m/z values of these “daughter ions”. Finally the detector records the m/z value of the ions and measures its abundance, the results are then sent to a computer connected to the Detector which plots in a chart the m/z values (on the x axis) against its relative abundance (on the y axis)^{112,113}.

Data from these fragmented peptides from LC- MS/MS is then compared with the peptide masses on a public database.

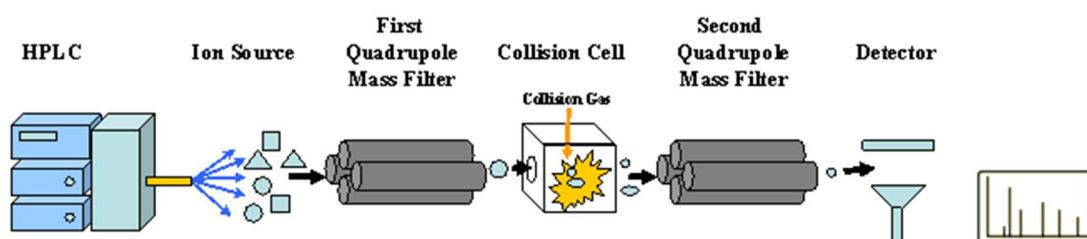


Figure 4.5 Schematic of tandem mass spectrometry. Major components of a LC-MS/MS.

4. Methods

4.11.2 General procedure

Mass spectrometry assay can be divided in five parts:

- a) Sample preparation
- b) Measure protein concentration by NanoDrop® Spectrophotometer
- c) Run SDS-PAGE (to clean the samples)
- d) In-gel reduction, alkylation and digestion
- e) Proteins identification by LC-MS/MS

a) Sample preparation

CM from irradiated and non-irradiated CAFs (n = 4) cultured in a serum-free DMEM medium were ultra-concentrated in VIVASPIN centrifuge tubes (*section 4.10.2*)

b) Measure protein concentration by NanoDrop® Spectrophotometer

Protein concentration (mg/mL) of the samples was determined by UV absorbance measurement at a wavelength 280 nm (A₂₈₀) using a NanoDrop® Spectrophotometer machine (*section 3.14*). Thoroughly mixed samples were pipetted carefully onto the lower measurement pedestal to not introduce air bubbles. Only a drop of 2 µL of sample was needed for the measurements. Between each measurement the sample pedals were cleaned with a dry laboratory wipe. An absorbance of 1 at 280 nm equals a concentration of protein of 1 mg/mL.

c) Run SDS-PAGE

A fixed amount corresponding to 0.50 mg/mL in 30 µL of sample was boiled together with 10 µL of 4x NuPAGE® LDS sample buffer and 4 µL of 10 x NuPAGE® sample reducing agent at 70°C for 10 min. Denatured samples (30 µL) were then loaded on a SDS-PAGE (NuPAGE® Novex 4-12% Bis-Tris Gel 1.5 mm 10 well) and separated by electrophoresis at 200 V for 10-15 min in 1x NuPAGE® MOPS SDS Running Buffer, containing antioxidant. A protein ladder was not added because the goal of this SDS-PAGE was not to identify the molecular weight (kDa) of the proteins but to clean the samples from salts and other non-protein solutes. Between loaded samples an empty well was left to avoid overflow.

Next, the proteins within the gels were fixed with a gel fixing solution (*additional files B.1*) for 1 hr on orbital shaker and washed 3x with Milli-Q Water for 5 min. To analyze the bands, the gel was stained with Coomassie staining Blue (~ 20 mL) (*section 3.11*) and incubated on orbital shaker for one hr. To destain, gels were washed 3x for 5 min with Milli-Q Water.

4. Methods

Next, the entire band spectrum of each sample was excised into 3 gel fractions with the help of two surgical blades. During this process is very important to work in the hood and use powder-free nitrile gloves to prevent or minimize keratin contamination (the biggest contaminant in protein ID). Each band was then transferred to a LoBind Eppendorf tube.

d) In-gel reduction, alkylation and digestion

The gel bands were crushed in pieces by a sterile disposable inoculation loop (~1mm² pieces) and washed twice in 100 µL of wash solution (*additional files B.1*) for 20 min at room temperature. The excess of solution was removed and the gel pieces were dried by adding 50 µL of LC-MS grade ACN (section 3.12), after 2 min on a shaker excess of ACN was removed.

The dried gel bands were then subjected to an in-gel reduction and alkylation. Cysteines were reduced by adding 50 µL of 10 mM DTT (section 3.12) (*additional files B.1*) at 56°C for 45 min. Samples were then cooled down on wet ice and DTT solution was removed. Immediately after, 50 µL of 55 mM IAA (section 3.12) (*additional files B.1*) was added for cysteine alkylation at room temperature for 30 min in the dark. IAA binds covalently to the Thiol groups of the cysteine preventing the proteins to form disulfide bonds again. Immediately after, IAA was removed and the gel pieces were washed for 20 min with wash solution as previously described and dried with ACN. Proteins were then digested using 6 ng/µL of Trypsin Porcine (from porcine pancreas) (section 3.12) (*additional files B.1*) and rehydrated on wet ice for 30 min. Samples were incubated overnight at 37°C.

The next day, in order to extract the peptides from the gel, samples were cooled down on wet ice, the excess solution was saved in an Eppendorf tube and gel pieces were reconstituted with 40 µL of LC-MS grade FA (section 3.12) to stop the digestion activity. After incubating at room temperature for 20 min in the Eppendorf mixer, excess solution was saved with the previous solution and the gel pieces were reconstituted with 60 % ACN / 0.1 % FA for 20 min in the Eppendorf mixer. For the last time excess solution was saved with the previous ones. Finally, the combined solutions were vacuum by dry solution in a Rotavapor (section 3.14) until it remained 10 - 15 µL of sample containing the peptides mixture.

4. Methods

e) Proteins identification by LC-MS/MS

Peptides mixtures containing 0.1 % FA were loaded onto the LC-MS/MS by Jack-Ansgar Bruun from the department of medical Biology at UiT.

Proteins were identified by MASCOT software against the Swiss-Prot database. Then the results of “all entries” were compared with those with “homo sapiens” taxonomy filter. A list of proteins with a significant MASCOT Score was presented. Identified proteins were then classified by functionality using Protein Discoverer and Perseus software.

4.12 Regulatory T-cell proliferation assays

Proliferation rates were compared between three different populations of T-cells in culture with non-irradiated CAF-CM (n = 2): **(a)** a population enriched with Tregs (CD4⁺ CD25^{high} T-cells); **(b)** a CD4⁺ T-cells population without Tregs (CD4⁺ CD25^{low/int} T-cells) and **(c)** a control group with all the T-cell subsets. For this purpose CD4⁺ CD25^{high} T-cells and CD4⁺ CD25^{low/int} T-cells were sorted from freshly isolated human PBMCs using magnetic-activated cell sorting (MACS) (section 3.13) and FACS Aria flow cytometer (section 3.14).

4.12.1 General principles

The principle of the MACS separation is to isolate specific cell populations by their surface antigens (CD molecules). When isolating cells with a MACS, samples are incubated with magnetic microbeads coated with monoclonal antibodies against a particular CD molecule. Then, the cell solution is loaded onto a MACS column which is placed in a strong magnetic field. Labeled cells with the magnetic microbeads are retained within the column while the unlabeled cells flow through. When the column is removed from the magnetic field, the magnetic retained cells are eluted as the positively selected cell population.

On the other hand, FACS Aria Flow cytometry is based on FACSCalibur principles but FACS Aria enables subpopulation of cells gated and visualized by fluorochrom-conjugated monoclonal antibodies to be separated from the sample suspension with a high degree of purity. When sorting cells, as the samples flow through the fluid stream a vibrating nozzle vibrates the fluid stream and breaks the fluid into droplets containing single cells. Droplets will then receive an electric charge (+,-) depending on the cell population that are carrying, then the stream of droplets passes through a pair of electric plates (+,-) so charged droplets can be sorted into 15 mL centrifuge tubes. Data is

4. Methods

analyzed by a computer connected to the flow cytometry using a FACSDiva Software (section 3.15).

4.12.2 General procedure

Tregs assays were divided into three parts:

- a) CFSE-labeled PBMCs
- b) Cell sorting
- c) Proliferation assays

A parallel group or control group was also prepared in order to validate our results.

a) CFSE-labeled PBMCs

30×10^7 cultured PBMCs were labeled with CFSE ($2.5 \mu\text{g/mL}$ per 20×10^6 total cells) as explained in section 4.6.2. In order to stain cells uniformly the volume of CFSE was scaled up accordingly. Labeled-CFSE PBMCs were then cultured overnight.

b) Cell sorting

The next day, PBMCs were collected, and sorted.

First separation (MACS): CD4^+ T-cells were isolated from the total PBMCs by positive selection using CD4^+ magnetic microbeads and a LS MACS column (section 3.13) according to the manufacturer's instructions (*additional files A.5*). Positive selected CD4^+ T-cells were then analyzed by flow cytometry for purity using CD4-PE-Alexa 610 conjugated antibody (section 3.5) and compared with the negatively selected cells CD4^{neg} found in the flow through and with the lymphocytes before separation (**Figure 5.9**).

Second separation (FACS Aria): The enriched population of $\text{CD4}^+ \text{CD25}^{\text{high}}$ Tregs and the $\text{CD4}^+ \text{CD25}^{\text{low/int}}$ T-cells population were then sorted by FACS Aria from the pure fraction of CD4^+ T-cells in two 15 mL centrifuge tubes. Briefly, the pure fraction of CD4^+ T-cells (40×10^6 cells) were labeled with CD25-PE conjugated antibody (section 3.5) for 30 min on ice in the dark. Immediately after, cells were washed with 10 mL PBSA and resuspended in 500 μL of IMDM supplemented with 40 % of FBS. When sorting cells by flow cytometry, lots of cells die in the process. Therefore additional FBS is added to the growth media to help the cells to survive the process. Cells were then transferred to Falcon™ Round-Bottom Polystyrene Tubes for FACS Aria analysis.

In order to sort the two populations of interest by FACS Aria, lymphocytes were first identified by forward and side scatter, and sorting gates around the enriched population

4. Methods

of CD4⁺ CD25^{high} Tregs and around the CD4⁺ CD25^{low/int} T-cells population were placed so that the cytometer knew which cells to sort (**Figure 4.6**).

For cell sorting, besides the sorted cells, a group of cells labeled with appropriate monoclonal antibodies for FACSARIA calibration is also required. Conjugated antibodies (section 3.5) were added for each group as shown in **Table 4.2**.

Table 4.2 Group of cells with the appropriate Monoclonal Antibodies or dyes

Group of cells	mAbs/dyes	Amount
Cells for sorting 40 x 10⁶ cells		In 500 μL complete IMDM
	CFSE dye	
	CD4-PE-Alexa 610 conjugated	5 μL
	CD25-PE conjugated	50 μL
Cells for calibration 1x 10⁶ cells		In 100 μL complete IMDM
1 st tube	Cells alone	
2 nd tube	CFSE dye	
3 rd tube	CD4-Alexa 610 conjugated	1 μL
4 th tube	CD8-PE conjugated	2 μL

c) Proliferation assays

Immediately after sorting, cells were spun down (400 x g, 4 min) and resuspended in complete IMDM medium. Proliferation assays for the sorted populations, CD4⁺ CD25^{high} Tregs, CD4⁺ CD25^{low/int} T-cells and for the control group in culture with CAF-CM (n = 2) were carried out as explained in section 4.6.2, with the exception that instead of 24-well-plates, 96-well-plates were used. Thus, the amount of cells and CAF-CM was scaled down accordingly. Briefly, lymphocytes were plated at 6 x 10⁴ cells/well and cultured with CAF-CM (n = 2) diluted 1:1 with complete IMDM medium to a final volume of 200μL.

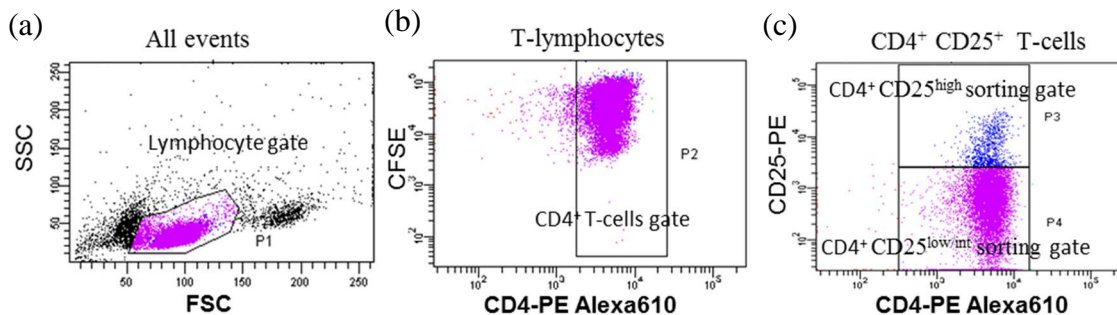


Figure 4.6 Gating specific T-cell populations for sorting in FACSARIA. (a) Lymphocytes were identified with the forward (FSC) and side scatter (SSC), from this gate (b) CD4⁺ T-lymphocytes population was gated and from this gate (c) increase population of CD4⁺ CD25^{high} Tregs and CD4⁺ CD25^{low/int} T-cells were gated for sorting in two different 15 mL tubes.

4. Methods

4.13 Specific Cytokines Targeted Drugs

Next, proliferation assays with targeted cytokines were carried out. A total of four cytokines activities (IL-6, PGE2, TGF- β and Galectin-3) were targeted (one by one) with appropriate drugs or monoclonal antibodies.

4.13.1 General principles

Cytokine targeted Drugs can have different mechanism of action; some drugs target the cytokines while others target a specific cytokine receptor or the enzyme that synthesizes it.

4.13.2 General procedure

Targeted drugs used in the present assay were:

- a) Tocilizumab
- b) Diclofenac
- c) Anti-TGF- β 1,2,3 antibody
- d) Anti-hGalectin-3 antibody

a) Tocilizumab

Tocilizumab (section 3.6) is a humanized monoclonal antibody against the IL-6 receptor. When doing proliferation assays (section 4.6.2), tocilizumab was added at a final concentration of 1 μ g/mL or 10 μ g/mL to the cultured CFSE-labeled PBMCs in 250 μ L of complete IMDM medium and incubated for 30 min at 37°C prior to adding CAF-CM (n = 2) to the 24-well-plates.

A control group of PBMCs cultured alone with 10 μ g/mL of Tocilizumab was prepared in duplicates.

b) Diclofenac

Diclofenac's (section 3.6) mechanism of action is to inhibit the enzyme that catalyzes the PGE2 synthesis, the Cyclooxygenase-2 (COX2). Therefore, in order to do proliferation assays with this targeted cytokine, isolated CAFs (n = 2) (section 4.3.2) at a density of about 350,000 cells/mL were cultured with or without Diclofenac at 5 μ M or 20 μ M in complete DMEM medium (6 mL). After an incubation of 24 hrs CAF-CM of all the flasks were collected and proliferation assays were carried out.

In order to confirm the PGE2 inhibition an ELISA with the collected CAF-CM was run as described in section 4.9.2.

4. Methods

c) Anti-TGF- β 1,2,3 Antibody

Anti-TGF- β 1,2,3 antibody (section 3.6) is a monoclonal mouse IgG₁ antibody that directly neutralizes the TGF- β in CAF-CM. Therefore, in order to proceed with the proliferation assay, CAF-CM from non-irradiated cultures ($n = 2$) were first incubated with the anti-TGF- β Antibody (5 $\mu\text{g}/\text{mL}$) for 1 hr at 37°C. Immediately after incubation-period, proliferation assays were carried out. A control group of PBMCs cultured alone with TGF- β Antibody (5 $\mu\text{g}/\text{mL}$) was prepared in duplicates.

An ELISA was run to confirm TGF- β inhibition in CAF-CM as described in section 4.9.2.

d) Anti-hGalectin-3 Antibody

Anti-hGalectin-3, (section 3.6) is a purified polyclonal goat IgG antibody that directly neutralizes the Galectin-3 in CAF-CM. Therefore, same procedures as for anti-TGF- β 1,2,3 antibody were followed. The working concentration for Anti-hGalectin-3 was 10 $\mu\text{g}/\text{mL}$.

4.14 ATP release assays

To study ICD responses, the extracellular release of ATP by irradiated CAFs at different time points (1 hr, 6 hrs and 24 hrs) after irradiation was measured by means of a modified luciferin-based ENLITEN ATP assay (section 3.8).

4.14.1 General principles

ENLITEN ATP assay is based on a light reaction yielded by the ATP-dependent oxidation of luciferin by luciferase. Oxyluciferin which is the luminescence product of the luciferase reaction, is proportional to the amount of ATP in the cell culture samples (Figure 4.7). In ATP assays it is important to use gloves and work in an aseptic environment to avoid ATP contamination from our hands.

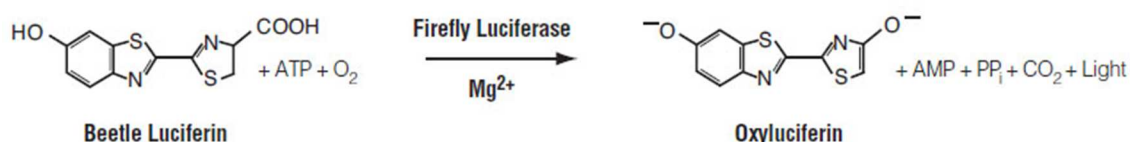


Figure 4.7 ENLITEN ATP assay based reaction. In the presence of ATP, Luciferin, Mg²⁺ and molecular Oxygen, the firefly luciferase catalyzes the oxidation of Luciferin and synthesizes the luminescence product, Oxyluciferin.

4. Methods

4.14.2 General procedure

At the 3rd passage, CAFs (n = 2) were seeded in duplicates per each time point and controls at a density of 40,000 cells per well in 24-well tissue culture plates (x5) with 500 μ L of complete DMEM medium and incubated at 37°C, 5 % CO₂ for 24 hrs for attachment. After attachment, cultures were washed with PBS and new Serum-Free DMEM medium (500 μ L) was replaced, followed by irradiation of cultures. Supernatants were collected at 1 hr, 6 hrs and 24 hrs post-irradiation and centrifuged (2,200 x g, 5 min) for ATP analysis using a modified luciferin-based ENLITEN ATP assay. Briefly, 100 μ L of supernatant was mixed with 100 μ L of rLuciferase/Luciferin (rL/L) reagent provided in the kit in 96-well white sterile plates. ATP-driven bioluminescence was then assessed on a luminometer microplate reader (section 3.14). The ATP measurement were expressed in Relative Light Units since no standard curve was used.

Non-irradiated CAFs were treated in parallel with the irradiated CAFs and their CM was used as a negative control. Lysed CAFs with 0.1 % triton X-100 for 10 min (to permeabilize the cell membrane) was used as a positive control.

4.15 Measurement of HMGB1 protein by Western Blotting

The secretion of HMGB1 protein into the extracellular space is also used as a ICD biomarker¹⁴.

4.15.1 General procedure

CAF supernatant HMGB1 levels from irradiated and non-irradiated cultures, prepared in 24-well-plates as previously described (section 4.14.2), were measured by western blotting at different time points following the same protocol shown in section 4.10.2.

Briefly, CAF conditioned medium was collected 1 hr, 6 hrs, 24 hrs and 120 hrs after irradiation and ultra-concentrated using a VIVASPIN centrifuge tubes. Samples were boiled in a reducing NuPAGE LDS sample buffer, resolved on NuPAGE Novex 4–12 % Bis–Tris gels and electrotransferred onto a PVDF membrane. Membranes were hybridized with rabbit polyclonal to HMGB1-ChIP grade primary antibody (section 3.5) diluted 1:500, followed by HRP-conjugated goat polyclonal anti-rabbit IgG secondary antibody (section 3.5) diluted 1:5000 and developed by Western blot luminol reagent.

CAF lysates prepared as in section 4.10.2 was used as a positive control.

4. Methods

4.16 Statistical analysis

The values are expressed as means with standard error of means (SEM) or standard deviations (SD) as indicated. In Multiplex protein arrays and ELISAs only readings above the detection limit of the assay are represented in figures. Data were analysed using paired Student's t-test. *P* values <0.05 denoted the presence of statistically significant differences. All statistics were determined with Graph pad prism version 5.00 for windows (Graphpad). Graphs were made using Microsoft Excel 2013 and GraphPad Prism 5 (section 3.15).

5. Results

5.1 Irradiation promotes morphological changes of primary cultured CAFs

In a previous work from our laboratory¹¹⁵ the purity from isolated CAFs obtained by methods described in section 4.3.2, was determined with the specific marker α -SMA. On the same work, authors also showed by means of β -galactosidase assays that irradiation (1 x 18 Gy) activates premature cell senescence. In the present study we did not perform these assays but we could observe under an inverted microscope that fibroblasts adopt a flat and an enlarged morphology after irradiation indicative of cell growth arrest (**Figure 5.1**).

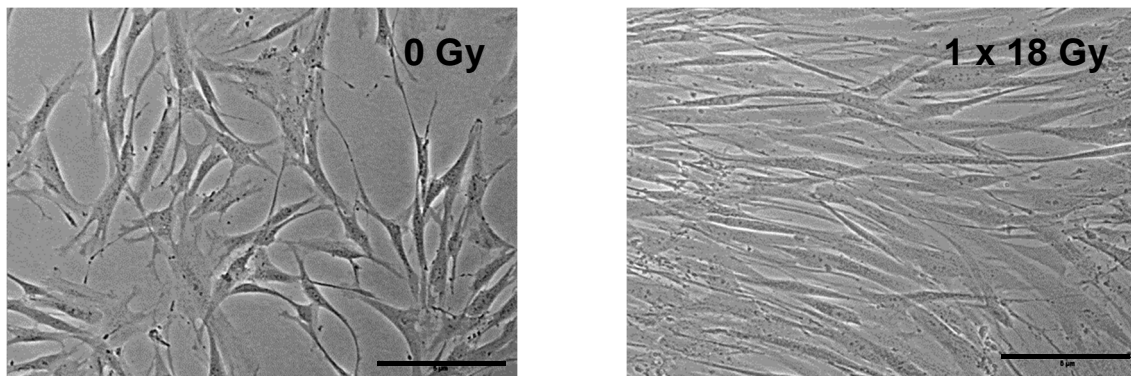


Figure 5.1 CAFs morphological changes after 1 x 18Gy irradiation. Irradiated CAFs (1x18Gy) adopts a senescent morphology, becoming flat and enlarged. Scale 5 μ m. Picture was taken with an inverted microscope connected to SPOT 4.7 image software.

5.2 PHA-stimulated T-lymphocytes exhibit decreased cell proliferation when co-cultured with irradiated and control CAFs

It has been previously shown in *in vivo* experiments that CAFs-targeting strategies enhance cancer immune surveillance, which suggests that fibroblasts may play an immunosuppressive role^{60,116-118}. Based on these observations, we performed *in vitro* functional assays to investigate whether cultures of CAFs in contact with PHA-L activated T-lymphocytes showed immune-regulatory capabilities and whether HD-RT modifies the potential outcomes. Results in **Figure 5.2** show indeed a significant immunosuppressive effect of CAFs as compared to the positive control where PHA-stimulated T-lymphocytes were cultured alone. Interestingly, irradiation (1 x 18 Gy) does not alter the immunosuppressive effects.

5. Results

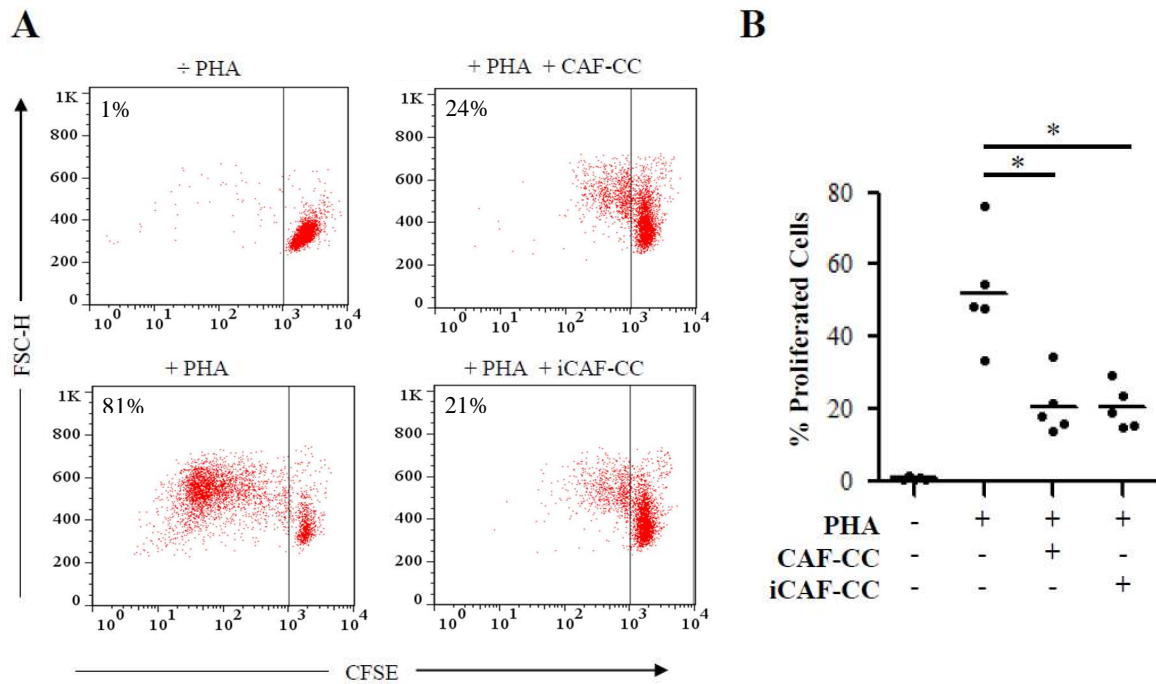


Figure 5.2 T-cell proliferation assays: immune-suppressive effects elicited by irradiated and control CAFs during co-culture. T-cell proliferation assays were performed using CellTrace™ CFSE-labeled human PBMCs activated with 1µg/mL PHA. PBMCs were co-cultured with irradiated (iCAF-CC) or non-irradiated CAFs (CAF-CC), and allowed to proliferate for 5 days. T-cell proliferation was determined by decrease in CFSE fluorescence intensity after gating the lymphocytes population on the forward (FSC-H) and side scatter. **(A)** Representative flow cytometry dot plots showing the percentage of low CFSE-labeled T-cells. **(B)** Quantitative analysis of T-cells proliferation rates, where outcomes using CAFs from five different donors are represented. Values (dots) represent average of duplicate determinations. Student's T-test value (* $P < 0.05$).

5. Results

5.3 CD4⁺ and CD8⁺ T-cell subsets respond equally to irradiated and control CAF-mediated immunosuppression

Similar co-culture assays were carried out to investigate whether the T-cell proliferative response of PHA-activated CD8⁺ and CD4⁺ T-cell subsets were similar. Results in **Figure 5.3** show that the proliferation rates of both subsets, CD4⁺ **Figure 5.3 (A)** and CD8⁺ **Figure 5.3 (B)** are equally inhibited (by more than 50%) by control and irradiated CAF-cultures.

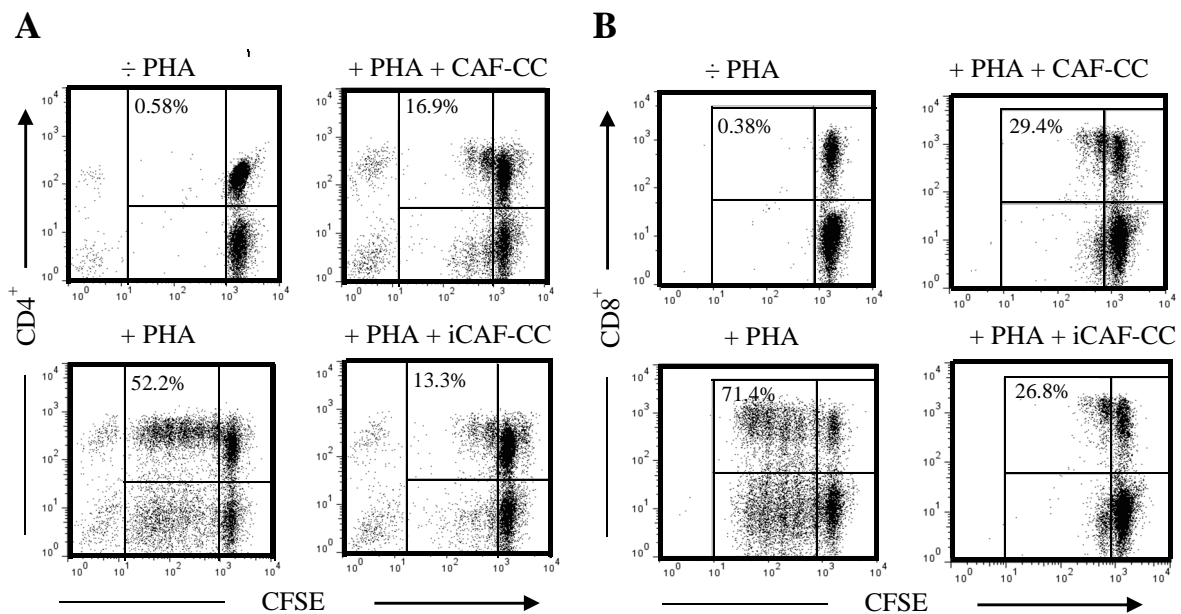


Figure 5.3 Proliferative response of CD4⁺ and CD8⁺ T-cell subsets are equally inhibited by irradiated and control CAFs during co-culture. T-cell proliferation assays were performed using CellTrace™ CFSE-labeled human PBMCs activated with 1 µg/mL PHA. PBMCs were co-cultured with irradiated (iCAF-CC) or non-irradiated CAFs (CAF-CC), and allowed to proliferate for 5 days. PBMCs were then stained with anti-CD4-PE Alex610 or anti-CD8-PE fluorochrome-conjugated monoclonal antibodies. Lymphocytes were identified by forward and side scatter, and the frequencies of CD4⁺ or CD8⁺ T-cells with CFSE dye dilution was determined by plotting fluorescence intensity for CD4⁺ or CD8⁺ against CFSE dye dilution. *Representative flow cytometry dot plots showing the percentage of low CFSE-labeled (A) CD4⁺ T-cells and (B) CD8⁺ T-cells.*

5.4 Conditioned Medium harvested from irradiated and control CAFs decreases proliferation of activated T-lymphocytes

To determine if the immunosuppressive effects of CAFs were dependent on cell-cell contact or on paracrine signalling, we harvested conditioned media from CAFs cultivated for 72 hrs-irradiated and non-irradiated cultured CAFs and then, proliferation assays comprising PHA-L activated T-lymphocytes with CAF-CM were carried out. As shown

5. Results

in **Figure 5.4** the effects of both irradiated and non-irradiated CAF-CM on T-lymphocytes proliferation are in the same line than the results shown in Figure 5.2.

Of importance, we also evaluated differential effects of low-dose fractionated radiotherapy (to mimic standard low-dose regimens typically given in the clinic) vs. single high-dose radiotherapy on T-lymphocytes. For this purpose T-lymphocytes proliferation assays were carried with CM from CAFs cultures (n = 3) treated with fractionated radiotherapy (4 x 2 Gy), single high-dose radiotherapy (1 x 18 Gy), or non-treated (control group). Immune-suppressive effects remained unperturbed under both radiation regimens (*additional files C.2*). ,

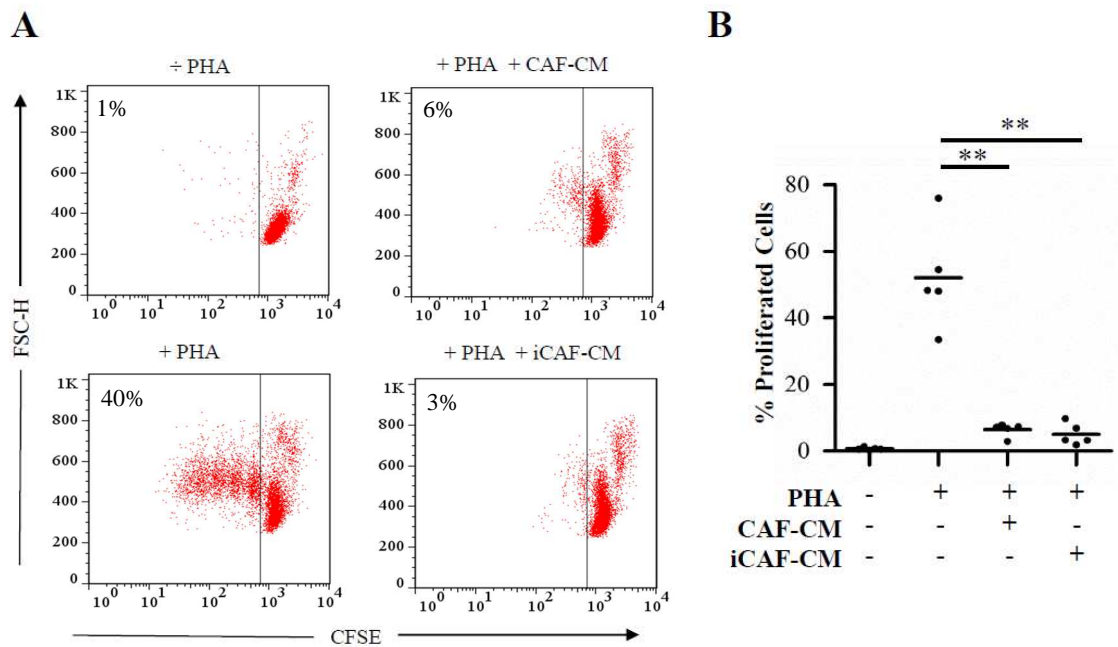


Figure 5.4 T-cell proliferation assays: immune-suppressive effects elicited by irradiated and control CAFs conditioned medium. T-cell proliferation assays were performed using CellTrace™ CFSE-labeled human peripheral blood mononuclear cells (PBMCs) activated with 1µg/mL PHA, and incubated with conditioned medium and fresh medium at 1:1 ratio for 5 days. Assays were performed with 72 hrs CM harvested from irradiated (iCAF-CM) or non-irradiated (CAF-CM) CAFs cultures. T-cell proliferation was determined by decrease in CFSE fluorescence intensity after gating the lymphocytes population on the forward (FSC-H) and side scatter. **(A)** Representative flow cytometry dot plots showing the percentage of low CFSE-labeled T-cells. **(B)** Quantitative analysis of T-cell proliferation rates, where outcomes using conditioned medium from five different donors are represented. Values (dots) represent average of duplicate determinations. Student's T-test value (** $P < 0.001$).

5. Results

5.5 Conditioned Medium from irradiated and control CAFs inhibits effector cytokines expression by T-cells

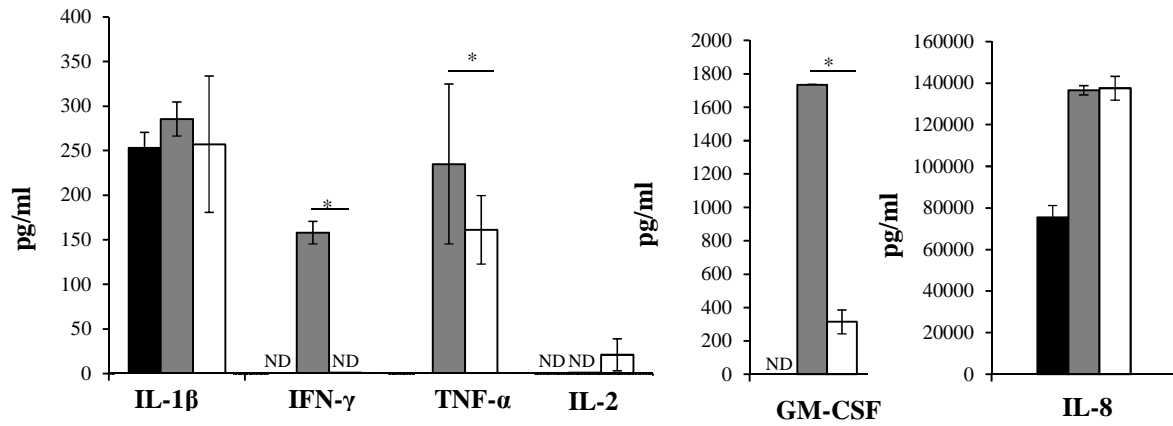
Under the hypothesis that CAF-CM – derived immunosuppressive effects shown in Figure 5.4 are accompanied by alterations in cytokine production of PHA-L activated T-lymphocytes, we proceeded by quantifying by multiplex protein arrays, anti-inflammatory (**Figure 5.5 (A)**) and pro-inflammatory (**Figure 5.5 (B)**) cytokines expressed in the supernatants of activated T-lymphocytes in the presence or absence of CM from non-irradiated CAFs cultures.

Consistent with the previous outcomes, two key T-cell immune-modulating cytokines, IFN- γ and TNF- α , significantly released by activated T-lymphocytes were strongly blocked when cultured with control CAF-CM (**Figure 5.5**). These results were confirmed by human IFN- γ and TNF- α – specific ELISA kits (**Figure 5.6**). Conditioned medium from irradiated CAFs showed very similar outcomes (**Figure 5.6**)

Interestingly, IL-10 was detected in T-cells/CAF-CM cultures supernatants but not in PHA-L stimulated T-cells cultures (**Figure 5.5 (B)**).

5. Results

A



B



Figure 5.5 Effects of CAF-CM on T-cell-derived immunogenic cytokines. (A) Expression of pro-inflammatory cytokines (IL-1 β , IFN- γ , TNF- α , IL-2, Granulocyte-macrophage colony-stimulating factor (GM-CSF) and IL-8) and (B) anti-inflammatory cytokines (IL-10) were measured by Luminex® multiplex cytokine assays in the supernatants of PHA-activated PBMC cultures in the presence or absence of conditioned medium from non-irradiated (CAF-CM) CAFs cultures. Data represent the mean \pm SEM values of five different CAFs donors from duplicate determinations. Student's T-test value (* P < 0.05). ND, Non-detected.

5. Results

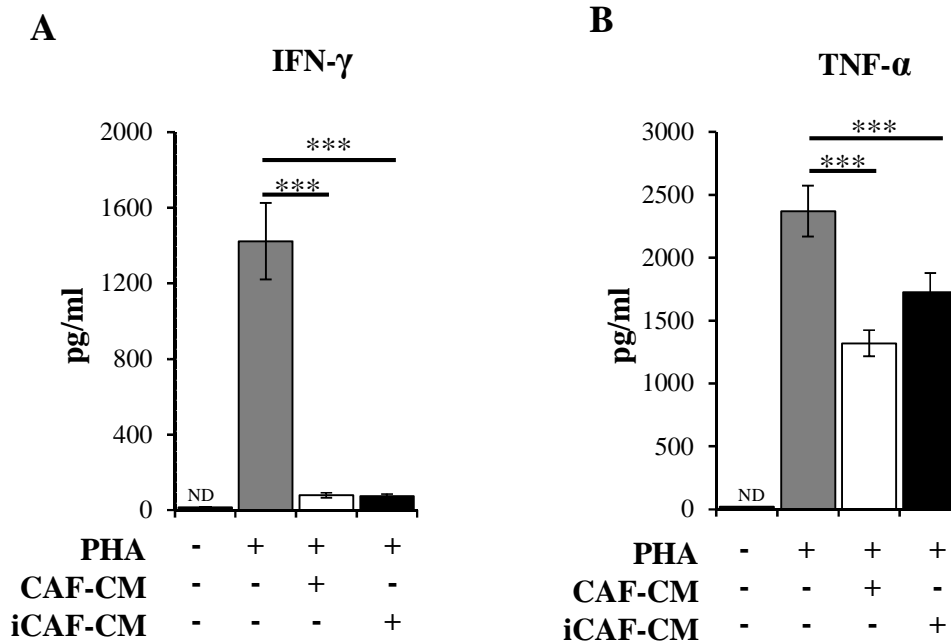


Figure 5.6 Inhibition of T-cells-derived immunogenic cytokines secretion by conditioned medium from irradiated and control CAFs. Expression of (A) IFN- γ and (B) TNF- α were measured by ELISA assays in the supernatants of PHA-activated PBMC cultures in the absence or presence of conditioned medium from irradiated (iCAF-CM) and non-irradiated (CAF-CM) CAFs cultures. Data represent the mean \pm SD values from four independent experiments measured in duplicates. Student's T-test value (***) $P < 0.0001$. ND, Non-detected.

5.6 PHA-stimulated T-lymphocytes showed reduced migration rate when cultured with conditioned medium from irradiated and control CAF cultures

To further investigate CAF-mediated immunosuppressive effects we performed migration assays by means of a Boyden Chamber. Pre-activated lymphocytes with PHA were seeded in the upper chamber while CAF-CM with or without 50 ng/mL recombinant SDF-1 protein was added in the lower chamber. Data in **Figure 5.7** represented by the negative control show that addition of DMEM/FBS with SDF-1 in the lower chamber is inducing strong migratory forces. However, addition of SDF-1 containing supernatants from irradiated or non-irradiated CAF cultures, significantly decreases the migrating effects (up to 50%). When CAF-CM is not containing SDF-1, migration is not observed. Once more, irradiated CAFs show similar outcomes as control CAFs. Of note, the same

5. Results

experiment was carried out with non-activated T-lymphocytes, but curiously, CAF-CM did not modify cell migration compare to that in controls (*additional files C.3*).

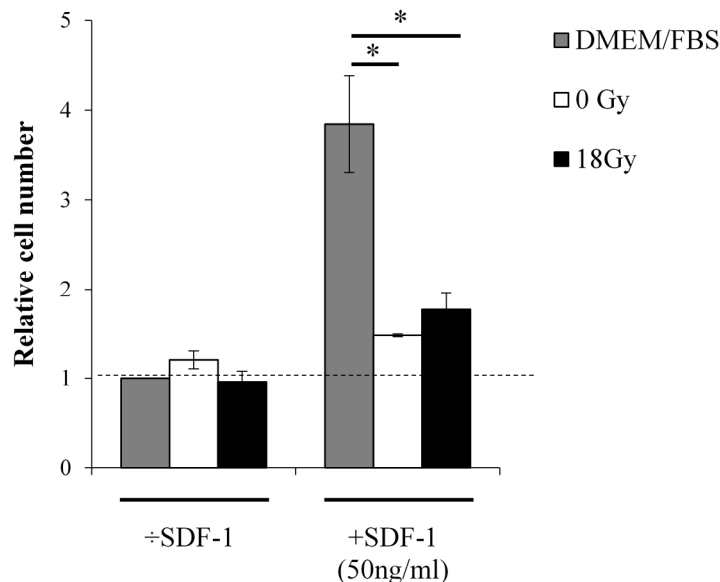


Figure 5.7 Lymphocytes migration assays: Conditioned medium from both irradiated and non-irradiated CAFs influence the migratory abilities of PHA-activated lymphocytes. Relative number of migrating lymphocytes (recovered from lower chambers). Lower chambers contained conditioned medium from irradiated (iCAF-CM) and non-irradiated (CAF-CM) cultures with or without SDF-1 (50 ng/mL) as chemo-attractant. Cell migration activity towards the lower chamber was significantly reduced in wells containing CAF-CM or iCAF-CM compared to the wells where the lower chamber contained DMEM/FBS. Histograms represent the mean \pm SEM of four different CAFs donors measured in triplicates. Student's T-test value (* P <0.05).

5.7 Neither Tumor Cells nor Chondrocytes – conditioned medium exert immunosuppressive effects

To prove whether the preceding immunosuppressive effects are specific for CAFs or can also be exerted by factors released by other cell types, like tumor cells or other mesenchymal cell-types like Chondrocytes, similar T-lymphocytes proliferation assays were carried out with CM from Tumor cells isolated from NSCLC and chondrocytes provided by Iñigo Martínez-Zubiaurre. Representative data in **Figure 5.8** show that neither tumor cells nor chondrocytes-derived factors exert the same immunosuppressive effects as CAF-released factor (figure 5.4).

5. Results

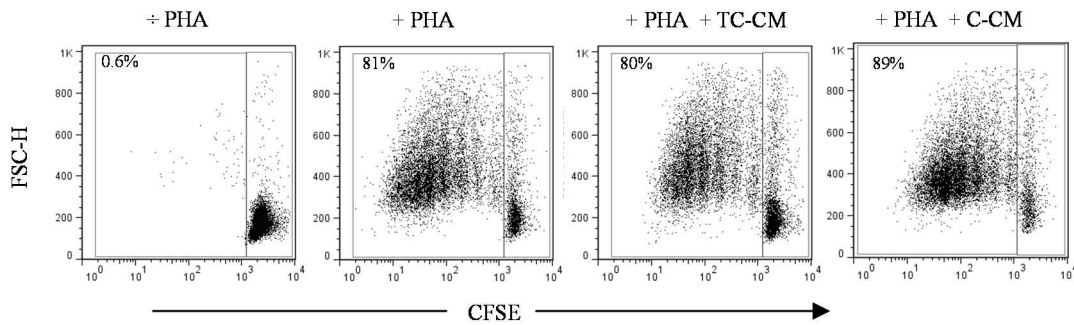


Figure 5.8 T-cell proliferation assays: Tumor cells and chondrocytes conditioned medium do not elicit immune-suppressive effects. T-cell proliferation assays were performed using CellTrace™ CFSE-labeled human PBMCs activated with 1 μ g/mL PHA, and incubated with conditioned medium (CM) and fresh medium at 1:1 ratio for 5 days. Assays were performed with CM harvested from Tumor Cells (TC) and Chondrocytes (C) cultures three days post-seeding. T-cell proliferation was determined by decrease in CFSE fluorescence intensity after gating the lymphocytes population on the forward (FSC-H) and side scatter. *Representative* flow cytometry dot plots showing the percentage of low CFSE labeled T-cells.

5.8 T-regulatory cell proliferation assays

T-regulatory cells have been the topic of many scientific articles for their capability to inhibit other T-cell subsets functions capable of inducing immunological tolerance^{67,119,120}. The present study aimed to investigate whether Tregs play any role in the immunosuppressive effects exerted by CAFs. For this purpose, an enriched population of CD4⁺ CD25^{high} Tregs and a population of CD4⁺ CD25^{low/int} T-cells from isolated human PBMCs were sorted by MACS CD4-positive selection and FACS Aria and conventional proliferation assays with CAF-CM were then carried out. By using MACS CD4-positive selection, highly pure CD4⁺ T-cells were obtained (**Figure 5.9**). Results in **Figure 5.10** show a comparison in proliferation rates between the enriched populations of CD4⁺ CD25^{high} Tregs, the CD4⁺ CD25^{low/int} T-cells population and a control group. As expected, CD4⁺ CD25^{high} Tregs did not proliferate in any of the groups. Surprisingly, the positive control for the PHA-stimulated CD4⁺ CD25^{low/int} T-cells (+PHA) failed to proliferate. This phenomenon will be further discussed in a later section.

5. Results

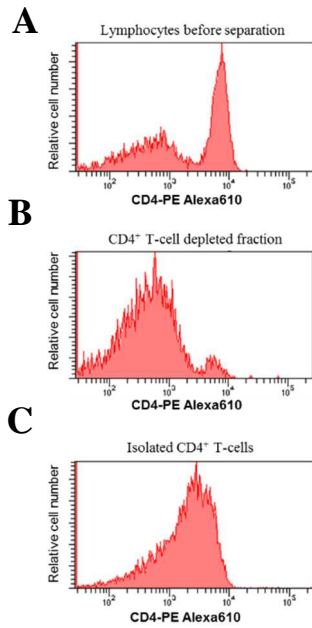


Figure 5.9 Separation of CD4⁺ cells using MACS CD4 positive selection. CD4⁺ T-cells were isolated from human PBMCs using CD4 Microbeads, an LS column and a MidiMACS separator. PBMCs were fluorescently stained with CD4-PE Alexa610 antibody. Lymphocytes were identified by forward and side scatter. Histograms show CD4-PE Alexa610 fluorescence for (A) the T-lymphocytes before separation (B) CD4^{neg} depleted T-cells and (C) CD4⁺ isolated T-cells.

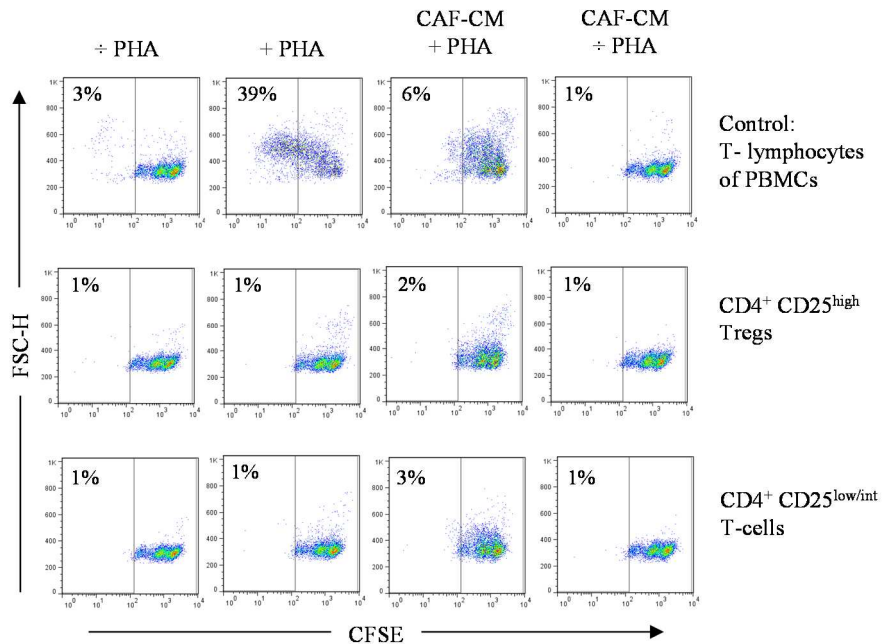


Figure 5.10 Comparison of proliferation rates between three T-cell populations. CFSE-labeled CD4⁺ CD25^{high} Tregs and CD4⁺ CD25^{low/int} T-cells were isolated from PBMCs and set up for proliferation assays. Sixty thousand T-lymphocytes stimulated with PHA (1µg/mL) or unstimulated (÷PHA), were placed in culture with or without 72 hrs CAF-CM. Proliferation assays were harvested five days later and T-cell proliferation was determined by decrease in CFSE fluorescence intensity after gating the lymphocytes population on the forward (FSC-H) and side scatter. The representative flow cytometry dot plots show the percentage of low CFSE-labeled T-cells.

5. Results

5.9 Control and irradiated CAFs supernatants contain equal levels of immunosuppressive cytokines

The next step in our investigation was to perform molecular assays to gain a deeper knowledge of CAF-driven paracrine effects. While functional assays are generally aimed at characterizing a function of a cell, molecular assays are aimed at characterizing a particular molecule by qualitative or quantitative techniques.

First, we quantified the expression of acknowledged immunosuppressive molecules in the conditioned medium from CAFs and irradiated CAFs by immune-based assays. As shown in **Figure 5.11** the immunosuppressive molecules, IL-10 or IDO were not detected in CAF-supernatants, however, other important immune-regulators such as IL-4, TGF- β or PGE2 were detected, in the culture medium of five different CAFs donors. Once more, results show approximately the same amounts of all three factors in supernatants from both irradiated and non-irradiated cells.

The immunosuppressive cytokine IL-6 was also detected in both supernatants, but data are not included since levels were above the detection limit of the assay (5000 pg/mL). The concentration of this protein in CAFs supernatants (22 ng/mL) however, has been already determined by our laboratory and is published in Hellevik *et al.*,¹⁰³.

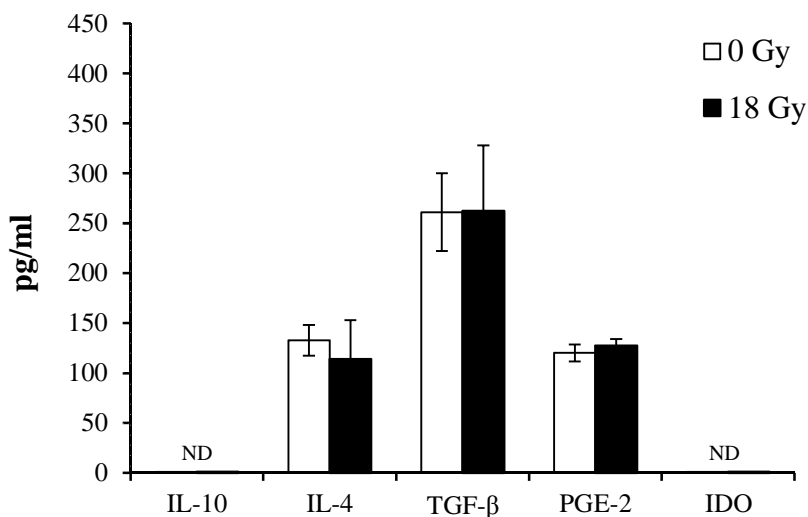


Figure 5.11 Even expression of immunosuppressive factors measured in conditioned medium from irradiated and non-irradiated CAFs. Levels of different immunosuppressive factors were measured by specific Enzyme linked Immunosorbent assays (ELISA) and by Luminex® multiplex cytokine assays in conditioned medium (CM) obtained from irradiated (18 Gy) or non-irradiated (0 Gy) CAFs cultures. Each bar represents mean \pm SEM of five different CAFs donors from duplicate determinations. ND. Non- detected.

5. Results

5.10 Undetected intracellular and extracellular expression of IDO in unstimulated CAFs

To confirm that IDO is not expressed by CAFs, Western Blot analysis of total cell lysates (5×10^5 CAFs) and of concentrated proteins from 6 mL of 48-hrs old non-irradiated CAF-cultures supernatants were carried out. Since IDO is an intracellular enzyme that can be triggered by IFN- γ or other inflammatory stimuli¹²¹, lysates of CAF-cultures (5×10^5 cells) stimulated with recombinant IFN- γ (100 ng/mL) for 48 hrs were included as positive controls. Results in **Figure 5.12** clearly show that stimulated CAFs express intracellular IDO (42 kDa). However, neither CAF-supernatants nor non-activated CAF-lysates express IDO. Despite that the growth medium was changed to a serum-free media, a background of the secondary antibody in the CM was found due to the presence of serum proteins.

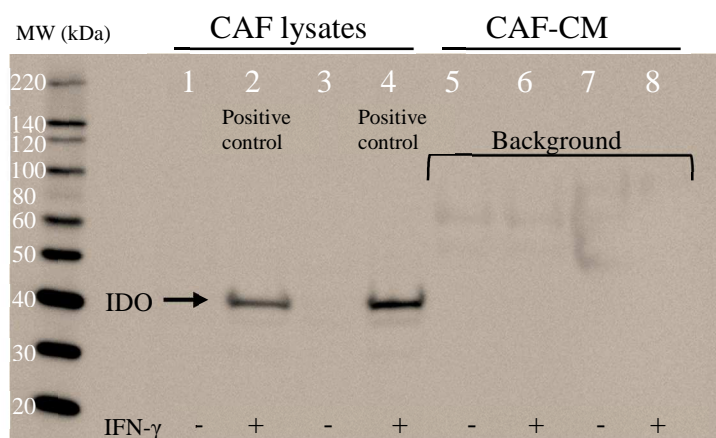


Figure 5.12 Neither CAFs supernatants nor non-activated CAFs lysates express IDO. Western blot analysis of CAF cells lysates, untreated (-) (lanes 1 and 3) or treated (+) with recombinant Interferon- γ (IFN- γ) (100 ng/ml) for 48 hrs (lanes 2 and 4 (positive control)), and of CAF culture supernatants (CAF-CM) untreated (lanes 5 and 7) or treated (lanes 6 and 8) with IFN- γ using IDO Antibody. Data from two CAFs donors is shown; Donor 1, lanes 1, 2, 5 and 6; Donor 2, lanes 3, 4, 7 and 8.

5.11 Identification of alternative paracrine factors released from irradiated and control CAFs

New or alternative immunosuppressive paracrine factors, other than those suggested in the literature, released from CAFs and iCAF of 4 different donors, were identified by proteomics. Approximately 15 μ g of extracellular proteins concentrated from 3 mL of 72-hrs old-culture supernatants were loaded onto a SDS-PAGE, run for 10 min, and then the entire spectrum was cut from the gel, excised in three bands and analysed by LC-MS/MS.

5. Results

Proteins were identified by MASCOT software against the Swiss-Prot database and a list of 978 proteins with a significant MASCOT Score was shown. The Mascot Score is the total score for the individual peptide ion masses matching a given protein. For a positive protein identification, the mascot score has to be above the 95 % confidence level ($P < 0.05$). Proteins were then classified by functionality using Protein Discoverer and Perseus software. A total of 261 proteins were selected for its relevance in the context of defense responses, cell communication and inflammation. Finally, from this selection, 28 proteins, listed in **Table 5.1**, had immune-modulating effects and could be identified in supernatants from both irradiated and control CAFs of at least 2 donors.

5. Results

Table 5.1 List of selected immunosuppressive factors identified in common by LC-MS/MS in irradiated (18 Gy) and control (0 Gy) CAF-supernatants

<i>Protein Name</i>	<i>Gene Name</i> *	<i>0 Gy</i>	<i>18 Gy</i>	<i>Mascot Score</i>	<i>Seq. coverage</i>	<i>Function</i>
Plasminogen activator inhibitor-1	SERPINE1	<i>n</i> = 4	<i>n</i> = 4	11343	72.1 %	Serine protease inhibitor
Pentraxin-related protein	PTX3	<i>n</i> = 4	<i>n</i> = 4	3595	60.6 %	Inflammatory reactions
Thrombospondin-1	THBS1	<i>n</i> = 4	<i>n</i> = 4	3325	46.5 %	Adhesive glycoprotein
Complement C1r	C1R	<i>n</i> = 4	<i>n</i> = 4	3271	59.4 %	Catalytic activity
Growth arrest-specific protein-6	GAS6	<i>n</i> = 4	<i>n</i> = 4	2852	50.2 %	Ligand for tyrosine-protein kinase receptors (AXL, TYRO3)
Metalloproteinase inhibitor-1	TIMP1	<i>n</i> = 4	<i>n</i> = 4	2705	68.6 %	Metalloproteinase inhibitor
Complement C1s	C1S	<i>n</i> = 4	<i>n</i> = 4	2649	57.4 %	Catalytic activity
Complement C3	C3	<i>n</i> = 3	<i>n</i> = 4	2561	65.0 %	Activation of the complement system
Complement factor H	CFH	<i>n</i> = 4	<i>n</i> = 4	1724	55.6 %	Cofactor for factor I-mediated inactivation of C3b
Metalloproteinase inhibitor-2	TIMP2	<i>n</i> = 4	<i>n</i> = 4	1594	68.2 %	Metalloproteinase inhibitor
Thrombospondin-2	THBS2	<i>n</i> = 4	<i>n</i> = 4	1016	39.8 %	Adhesive glycoprotein
Prostaglandin-H2 D-isomerase	PTGDS	<i>n</i> = 4	<i>n</i> = 4	897	64.2 %	Catalytic activity
Complement component C7	C7	<i>n</i> = 3	<i>n</i> = 3	628	50.7 %	Constituent of the membrane attack complex
Complement factor D	CFD	<i>n</i> = 4	<i>n</i> = 4	453	47.8 %	Catalytic activity
Plasminogen activator inhibitor-2	SERPINE2	<i>n</i> = 3	<i>n</i> = 3	418	45.3 %	Inhibits urokinase-type plasminogen activator
Complement factor I	CFI	<i>n</i> = 4	<i>n</i> = 4	395	37.1 %	Catalytic activity
Complement C4-A	C4A	<i>n</i> = 3	<i>n</i> = 4	387	21.6 %	Inflammatory process
Heat shock protein HSP 90-beta	HSP90AB1	<i>n</i> = 2	<i>n</i> = 3	366	30.0 %	Molecular chaperone
Galectin-1	LGALS1	<i>n</i> = 4	<i>n</i> = 4	308	73.3 %	Regulates apoptosis, cell proliferation and differentiation
Heat shock protein HSP 90-alpha	HSP90AA1	<i>n</i> = 3	<i>n</i> = 3	305	33.5 %	Molecular chaperone
Complement factor B	CFB	<i>n</i> = 3	<i>n</i> = 3	301	27.9 %	Component of the alternative pathway of complement system
Bone morphogenetic protein-1	BMP1	<i>n</i> = 2	<i>n</i> = 3	237	22.4 %	Catalytic activity
Heat shock cognate 71 kDa protein	HSPA8	<i>n</i> = 3	<i>n</i> = 4	212	31.0 %	Repressor of transcriptional activation
Interleukin-6	IL6	<i>n</i> = 4	<i>n</i> = 4	205	43.9 %	Cytokine activity
Calreticulin	CALR	<i>n</i> = 3	<i>n</i> = 4	199	22.5 %	Calcium-binding chaperone
Connective tissue growth factor	CTGF	<i>n</i> = 3	<i>n</i> = 4	131	31.0 %	Mediates cell adhesion, differentiation and proliferation
Galectin-3	LGALS3	<i>n</i> = 4	<i>n</i> = 4	125	28.4 %	Inflammatory responses
Transforming growth factor beta receptor 3	TGFB3	<i>n</i> = 2	<i>n</i> = 3	91	12.2 %	Binds to TGF-beta

n Number of donors in which the protein was identified from a total of four analyzed

* Human

5. Results

5.12 High-dose Irradiation does not induce Immunogenic Cell Death mechanisms

Accumulating evidences indicate that radiotherapy has the potential to boost the patients' immune system by triggering ICD¹²². This immune-driven effect of radiotherapy is thought to occur as a result of released danger signals, such as ATP and HMGB1, to the extracellular space by necrotic cells. Based on this notion we explored by means of an ENLITEN ATP assays and Western Blotting assays whether irradiated CAFs at different time points, post treatment, release ATP or HMGB1 into the extracellular environment. Results clearly show that CAFs do not turn on ICD mechanisms at any time point after exposure to 1 x 18 Gy (**Figure 5.13**).

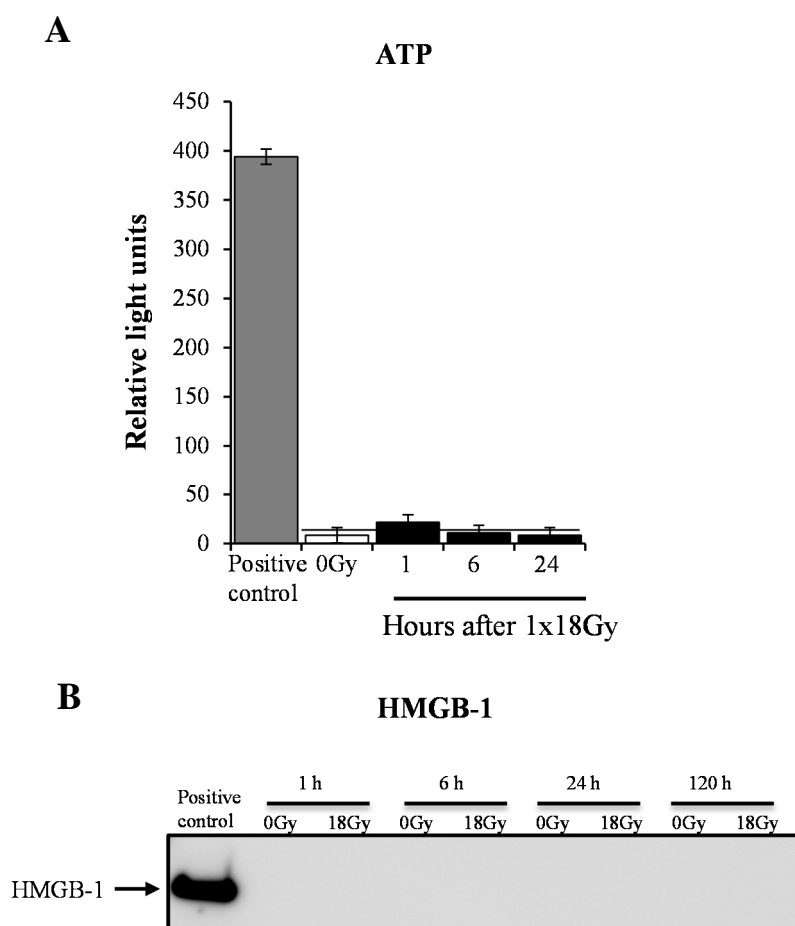


Figure 5.13 Irradiated CAFs do not release immunogenic cell death signals. (A) Levels of extracellular ATP measured on CAFs supernatants at 1 hr, 6 hrs and 24 hrs post 1 x 18Gy irradiation and non-irradiated cells. Positive controls were obtained by lysing the cells with 0.1 % triton X-100 for 10 min. Each bar represent mean \pm SD from two different CAFs donors measured in triplicates. (B) Expression of high-mobility group box 1 (HMGB1) (30kDa) in CAFs supernatants analyzed 1 hr, 6 hrs, 24 hrs and 120 hrs after irradiation (18Gy) or in non-irradiated cells (0Gy) by western blot. Positive control represents intracellular HMGB1 levels from non-irradiated CAFs cultures. Data from one representative CAF donor is shown. Identical results were obtained with 2 different CAF donors.

5. Results

5.13 Blocking of IL-6, PGE2, TGF- β and Galectin-3 activity does not prevent the immunosuppressive effects of CAF-CM

In the previous studies we found that CAF-derived factors inhibit T-cell proliferative responses (Figure 5.4). In the following study we focus on the mechanism of how CAFs modulate T-cell inactivation. Evidence has shown that IL-6, PGE2, TGF- β and Galectin-3 release by non-neoplastic cells into the tumor microenvironment, may induce a state of immunosuppression. To investigate whether these CAF-derived anti-inflammatory factors represent relevant mediators in the observed T-cell inactivation, we used specific neutralizing antibodies or inhibitors to suppress the effects of IL-6, PGE2, TGF- β and Galectin-3 (**Figure 5.14 (A-D)**) with the goal to overcome the immunosuppressive effects of CAF-CM in proliferative assays. The pink histograms in **Figure 5.14** show that by blocking these specific proteins with Tocilizumab, Diclofenac, anti-TGF- β 1,2,3 antibody and anti-hGalectin-3 antibody respectively, we did not abolish the immunosuppressive effects of CAF-CM shown in brown histograms. ELISA's tests were used to determine the blocking of PGE2 and TGF- β levels in CAF-CM (*additional files C.4*).

5. Results

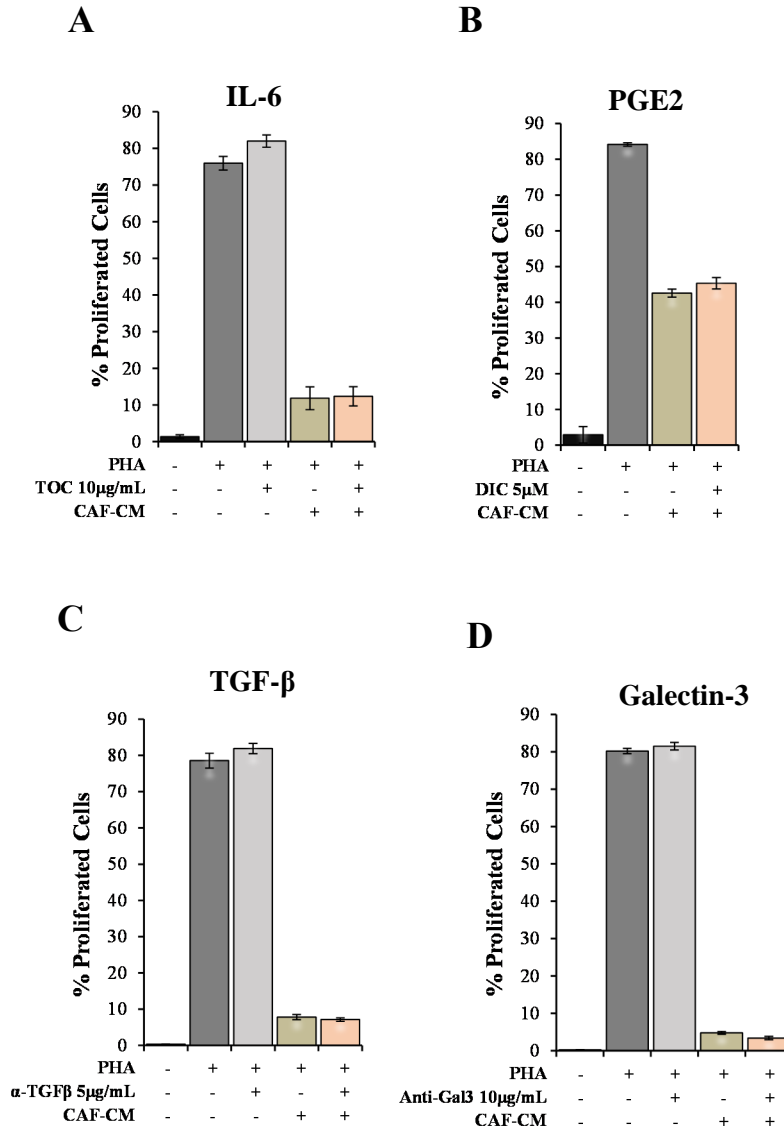


Figure 5.14 Neutralization of IL-6, PGE2, TGF- β and Galectin-3 do not overcome CAF-CM-mediated immunosuppressive effects. Proliferation assays were carried out after blocking specific cytokines with specific drugs (A) 10 μ g/mL of Tocilizumab (TOC) was used to block IL-6 receptor on T-lymphocytes (B) 5 μ M of Diclofenac (DIC) was used to block the enzyme (COX2) produced by CAFs that directly synthesizes PGE2, (C) 5 μ g/mL of TGF- β monoclonal antibody (α -TGF- β) and (D) 10 μ g/mL of anti-Galectin3 polyclonal antibody (anti-Gal3) was used to neutralize the soluble TGF- β and Galectin-3 in CAF-CM respectively. DATA show quantitative analysis of T-cell proliferation rates from one representative CAF donor. Identical results were obtained with 2 different CAF donors. Each bar represents mean \pm SD values of duplicate determinations.

6. Discussion

Cancer-associated fibroblast is a key stromal cell type that plays a pivotal role in cancer progression through a) stimulation of tumor cell proliferation; b) activation of angiogenesis; c) promotion of epithelial-mesenchymal transdifferentiation; d) regulation of the extracellular matrix deposition and e) formation of a metastatic-niche. Moreover, accumulating evidence show that CAFs promote tumor growth and metastasis by inducing f) polarization towards a Th2 immunity and by suppressing immune responses.

The function of CAFs in regulating the immune system has been previously characterized, but the reported effects of CAFs on T-cells are still divergent. Various studies *in vivo* have demonstrated that systemic CAF-targeted therapies are correlated with an increase in Th1 cytokine expression and CD8⁺ T-cell responses^{60,117}. Contrary to this assumption, other studies have shown that local depletion of CAFs in pancreatic ductal adenocarcinomas is associated with poor immunosurveillance responses¹²³. In yet another study, co-cultures of CAFs from lung tumors with autologous tumor associated T-cells showed donor-specific immune responses in both directions, enhancing and inhibiting T-cell functions⁵⁰. Here, in an attempt to further investigate CAF-mediated immune-modulating functions, CAF/T-cell co-cultures were carried out. Our results indicate that CAFs isolated from freshly resected non-small cell lung carcinoma from seven different donors exhibit consistent inhibitory effects ($P < 0.05$) on human PHA-L activated T-cells isolated from peripheral blood of healthy volunteers. It has been proposed in previous studies that the expression by CAFs of the co-regulatory membrane molecules, programmed cell death-ligands (PD-L1 and PD-L2) could be involved in immunosuppressive functions^{41,50,124}. Here, however, we have determined that the inhibitory effects of CAFs is mediated by paracrine signals and not by contact-dependent signals, since CAF-mediated suppressive response on T-lymphocytes could be reproduced by culturing activated T-cells with CAF-cultures supernatants.

The reason why CAF-CM-mediated immunosuppression is more significant ($P < 0.001$) than the one demonstrated in co-cultures ($P < 0.05$) is that the cell density of the collected CM was much higher (~ 350.000 CAFs/mL) than in co-cultures, where cells were seeded at a density of 10.000 cells per well on a 24-well-plate.

6. Discussion

In this study we also demonstrate that the immunosuppressive effects observed are specific for CAFs since the same effects could not be reproduced by other mesenchymal cell types like, chondrocytes, or by freshly isolated NSCLC tumor cells.

Freshly isolated immature myeloid derived suppressor cells from tumor-bearing mice was originally shown to suppress CD8⁺ T-cell responses but not CD4⁺ T-cell responses via direct cell-cell contact, and was presumably dependent on MHC class I molecules^{125,126}. Even though this view has later on been challenged by other studies, which demonstrated that activated MDSCs can suppress the functional activity of both T-cell subsets in a MHC-I-independent manner¹²⁷, it is accepted that activated CD8⁺ and CD4⁺ T-cells may respond differently to distinct regulatory influences, including membrane co-stimulatory molecules and/or released factors^{128,129}. However, the way by which immune-modulating factors released by immune and non-immune cells in the tumor microenvironment shape the immune profile is still poorly understood. In the present study we evaluated the effect of CAFs on the proliferative responses of two T-cell subsets individually and we show that CAFs suppress both CD4⁺ and CD8⁺ T-cell responses similarly.

The movement of lymphocytes from the blood into the tissues is believed to be promoted by the combined action of chemokines and cell adhesion molecules¹³⁰. Orimo *et al.*, demonstrated that CAFs in tumor-bearing-mice release elevated levels of the chemokine SDF-1/CXCL12, which results in recruitment of endothelial progenitor cells and therefore tumor angiogenesis³². Moreover, it is well characterized that SDF-1 can promote chemotaxis of T-lymphocyte via their constitutively expressed receptors CXCR4^{131,132}. Based on this understanding we hypothesized that CAF-CM would enhance lymphocyte migration by generating a SDF-1 gradient. However, contrary of what we expected, we establish here, for the first time, that NSCLC fibroblast-released factors strongly diminish the migratory capacity of PHA-L stimulated T-lymphocytes towards the chemoattractant SDF-1 ($P < 0.05$). Of importance, levels of SDF-1 released by CAFs in *in vitro* assays have been detected, but at relative low levels (3 ng/mg of total protein) in previous studies in our laboratory¹⁰³. Considering that the minimum amount of SDF-1 to induce migration is 10 ng/mL (***additional files C.1***) it is not surprising that CAF-CM alone do not induce migration.

Curiously, the same migration assay repeated with non-activated lymphocytes did not show any alterations of the migratory capacity of T-lymphocytes compared to the control

6. Discussion

groups (*additional files C.3*). This may suggest that PHA-L induces expression of receptor/s on T-lymphocytes which interacts with CAF-derived soluble factors leading to suppression of the SDF-1 receptor (CXCR-4) function. Based on these findings we hypothesize that the soluble factor affecting T-cell functions is also affecting T-cell migratory responses.

On the bases of these observations, it is clear that there is a continual cross-talk between CAFs and the diverse population of immune cells through the secretion of soluble factors that results in immunosuppression. Supporting this awareness we observed that the immunosuppressive response induced by CAF-CM is accompanied by a decrease in the amount of two key immune-modulating cytokines, IFN- γ and TNF- α ($P < 0.0001$) that are typically produced by activated T-lymphocytes at high levels. The pro-inflammatory cytokine, IFN- γ has been described in several articles for its importance towards anti-tumor responses (i.e., recruitment of immune cells, enhanced maturation of dendritic cells, activation of macrophages and natural killer cells among other effects). In fact, one of the mechanisms by which tumor cells escape immunosurveillance is through the development of IFN- γ insensitivity¹³³. On the other hand, TNF- α is also a pro-inflammatory cytokine involved in T-cell activation and proliferation¹³⁴. It could be that CAF-released factors decrease the levels of TNF- α indirectly by modulating T-lymphocyte IFN- γ production, since IFN- γ synergizes with TNF- α through the NF- κ B pathway¹³⁵.

Another fact that supports the observed CAF-immunosuppressive effects is the detection of IL-10 in the supernatants of T-cells/CAF-CM cultures. IL-10 is an immunosuppressive cytokine with the ability to reduce the production of IL-2 and IFN- γ by T helper type 1 cells¹³⁶. But, which cell type is actually producing this cytokine in our cultures? Neither T-cells nor CAF-culture-supernatants tested positive for IL-10 when cultured alone. Literature-based-research indicates that this cytokine is primarily produced by Treg cells and M2 macrophages in the tumor microenvironment^{137,138}. Thus, our finding that T-cells in culture with CAF-CM produce IL-10 raises the question of whether CAFs immunosuppressive activity on T-cells is exerted indirectly through the release of cytokines that promote the differentiation of other immunosuppressive cell types such as Treg cells.

In an attempt to address the possibility that Tregs could be involved in CAF-CM mediated immunosuppression, we wanted to compare the proliferation rates between an enriched

6. Discussion

population of CD4⁺ CD25^{high} Tregs and CD4⁺ CD25^{low/int} T-cells when cultured with CAF-CM. It is expected that the enriched population in Tregs would proliferate less than the population without Tregs in the PHA-stimulated cells since Tregs are anergic (nonproliferative) to mitogenic stimulations but at the same time in the presence of the mitogen they become suppressive and inhibit the proliferation of the other activated T-cell subsets^{119,120,139}. The fact that purified CD4⁺ CD25^{high} and especially CD4⁺ CD25^{low/int} T-cells failed to proliferate at all upon activation by PHA at concentrations that induced autologous non-purified lymphocytes of PBMCs to proliferate, might suggest that the purified CD4⁺ T-cell cultures lacked a cellular component present in PBMCs cultures that is necessary for PHA-mediated activation. An alternative hypothesis is that the CD25^{int} T-cells present in the purified CD4⁺ CD25^{low/int} T-cell population also exert immunosuppressive effects. Previous studies by other authors have reported that immunomagnetic isolated CD4⁺ CD25⁺ Tregs, can block the proliferation of whole CD4⁺ T-cell population, cultured at a 1:1 ratio¹³⁹. Thus, based on this study, a simple pilot experiment could be done in order to study this last hypothesis: We could isolate CD4⁺ CD25⁻ T-cells on one hand and CD4⁺ CD25⁺ T-cells on the other hand and proceed with the same experimental set-up. If the CD4⁺ CD25⁻ T-cell population is able to proliferate and CD4⁺ CD25⁺ T-cells are hyporesponsive, it would reflect that the isolated CD25^{int} T-cells in our experiment exert immunosuppressive effects on CD4⁺ CD25^{low} T-cells. All in all, our initial hypothesis suggesting that a CM factor/s produced by CAFs have the ability to directly promote T-cell inhibition cannot be answered by this experimental set-up.

Granulocyte-macrophage colony-stimulating factor is strongly released by activated T-cells, and is significantly blocked when cultured with CAF-CM. But it is still undefined whether this cytokine has direct effects on T-cells¹⁴⁰ and whether it exerts immunosuppressive or pro-inflammatory roles. It seems that GM-CSF can promote traditional pro-inflammatory reactions by recruiting circulating monocytes, neutrophils and lymphocytes and by enhancing DC maturation^{141,142}. However, in the tumor microenvironment this cytokine can also promote an indirect immunosuppressive effect on anti-tumor T-cell immunity through the recruitment of immunosuppressive cells, like MDSCs^{143,144}. Due to its puzzling role, this cytokine was not further investigated.

6. Discussion

Given the increasing evidences showing that fibroblasts are able to modulate T-cell responses, it is of great interest to understand which paracrine signal released by CAFs induces the observed immunosuppressive effects. But to determine the role of CAF-released cytokines can be challenging. Despite the many efforts made for gaining a more complete understanding of the cytokine networks and targets in cancer development and pathogenesis, the attempt to characterize a single cytokine as anti-inflammatory/pro-inflammatory or as anti-tumorigenic/pro-tumorigenic may be challenging due to the inherent cytokine pleiotropy and redundancy behavior. Hence, some cytokines can signal through multiple receptor complexes and one receptor complex can be the target of multiple cytokines^{145,146}.

A great quantity of cytokines in the tumor milieu can have both negative and positive effects on tumor growth, and examples of well documented cytokines produced by CAFs that have this pleiotropic effect are IL-4¹⁴⁷, TGF- β ¹⁴⁸, IL-6¹⁴⁹ and IL-1 β ^{150,151}. The last two pro-inflammatory cytokines are examples of the concept that inflammation can lead to pro-tumorigenic activities by promoting a shift differentiation and recruitment of tumor promoting effector cells (Treg, Th17, Th2 and MDSC). Here, we study acknowledged cytokines produced by CAFs, including TGF- β , PGE2, IDO and IL-6 that affects T-cell functions directly or indirectly via other cells such as Treg or Th17 cells. In addition, we also analyze other recognized immunosuppressive molecules, including IL-10 and IL-4. All the investigated cytokines were detected with quantitative approaches in CAF cell culture supernatants with the exception of IDO and IL-10.

IL-6 concentrations were above the detection limit of the assay (5000 pg/mL) and PGE2, IL-4, and TGF- β concentrations ranged from 120 pg/mL to 261 pg/mL.

On the other hand, IDO, a tryptophan-degrading enzyme, has the potential to suppress immunoresponses. Even though its mechanisms of action are not yet fully understood, it has been suggested that the tryptophan metabolites accumulated downstream upon tryptophan degradation may induce somehow T-cell tolerance to tumors¹⁵²⁻¹⁵⁴. Although it is widely accepted that CAFs stimulated with IFN- γ are an important source of IDO and/or the tryptophan metabolite kynurenine^{57,155}, we did not detect IDO expression within unstimulated CAF lysates or CAF supernatants by western blotting or ELISA. Since the immunosuppressive effects observed on T-lymphocytes are mediated by supernatants obtained from unstimulated CAFs cultures, we concluded that IDO is not our molecule of interest.

6. Discussion

In further attempts to define which CAF-derived factor is responsible for the inhibitory effects observed, we removed the expression or the effect of CAF-produced IL-6, PGE2, TGF- β and Galectin-3 in individual proliferative assays. Despite the high IL-6 levels found in CAF supernatants, its inhibition did not overcome the CAF immunosuppressive effect. Additionally, the blocking of TGF- β or PGE2 could not revert the immunosuppressive effects by CAFs. TGF- β has dominated the field of cancer progression since its discovery in the early 1980s, for its ability to suppress T-cell responses to IL-2¹⁵⁶ and its role as an immune modulator in general^{157,158}. In fact, previous studies by Nazareth *et al.*,⁵⁰ have shown that in the presence of function blocking TGF- β antibodies, T-cell response was increased. Therefore, our finding that TGF- β neutralization did not promote T-cell proliferation was unexpected. An explanation to this observation could be that detected levels of TGF- β (261 pg/mL) in CAF supernatants are not high enough to trigger T-cell tolerance. Another hypothesis is that CAF-released TGF- β has a higher impact on self-stimulation of cell proliferation (autocrine effects) than on T-cells (paracrine effects).

Interestingly, in an effort to identify new and relevant immunomodulators in the CAFs secretome by means of an unbiased mass spectrometry analysis, we identified, among a list of 28 immune-modulating factors, a well-known immunosuppressive molecule called Galectin-3. In adults, galectin-3 is expressed on a wide variety of normal cell types and tissues. It is a cytosolic protein but it may translocate into the nucleus or be secreted from the cytosol into the extracellular space via the non-classical pathway¹⁵⁹. Even though this molecule is involved in a variety of biological processes (cell adhesion, cell activation and chemoattraction, cell growth and differentiation, cell cycle and apoptosis)¹⁶⁰ oncologists are interested in this molecule for its association in cancer progression^{161,162}. This molecule can be found in large amounts in the extracellular space in tumors where it effects tumor-stromal behavior and function by interacting with glycosylated molecules such as receptors, cell-cell and cell-matrix adhesion molecules¹⁶³. The inhibitory effect of galectin-3 on T-cell proliferation and function has been demonstrated in previous studies *in vivo*^{164,165}. Moreover, in yet another study *in vitro* the immunosuppressive effects mediated by human bone marrow-derived mesenchymal stem cells were overcome by knockingdown galectin-3 in these cells¹⁶⁶. However, in the present study CAFs immunosuppressive effects were not reverted by using blocking antibodies against galectin-3.

6. Discussion

Of importance, the immunosuppressive and anti-inflammatory Galectin-1 was also detected in the complete CAF secretome and could also be a potential target to revert effects mediated by CAFs. Studies in mice have shown that by blocking galectin-1 gene expression in tumor cells, the levels of T-cell mediated tumor rejection was significantly elevated¹⁶⁷. In our interest *in vitro* studies have demonstrated that galectin-1 can be blocked by a galectin-1-specific mouse monoclonal antibody¹⁶⁸.

When a tumor is being irradiated with the aim to destroy cancer cells, one might assume that stromal cells present in the tumor microenvironment follow the same fate. Previous studies however, have demonstrated that CAFs are radioresistant cells that adopt a senescent-like phenotype upon HD-RT¹⁰¹. But, how the acquired CAF-senescence-associated-secretory phenotype may impact the overall tumor fate remains elusive and poorly studied. Previous studies with chemotherapy-treated CAFs reported that chemotherapy is associated with an increased cytokine production from these cells¹⁶⁹. Here, we demonstrate by functional assays that supernatants obtained from irradiated-CAF-cultures exert the same immunosuppressive effects as the ones shown for non-irradiated CAF cell culture supernatants, effecting both, T-cells function ($P < 0.001$) and migratory capacity ($P < 0.05$). Moreover, the concentration levels of the immunosuppressive molecules, TGF- β , PGE2, IDO, IL-6, IL-10 and IL-4 measured by quantitative approaches in the irradiated CAF secretome are similar to the concentration levels detected in non-irradiated CAF secretome. Clearly, these outcomes also give a better understanding of the equal immunosuppressive effects observed by irradiated and control CAFs.

Observations in clinical trials have shown that local HD-RT may trigger a systemic immune response, triggered by the release of danger signals (DAMPs) from dying cancer cells. This damage-associated molecular patterns enhance dendritic cells phagocytosis of tumor cells which in turn prime CD8⁺ cytotoxic T-cells with the potential to eliminate tumor cells not only at the irradiated site but also remote sites. This form of cell death is called immunogenic cell death and the three danger signals that define and coordinate an ICD are (i) cell surface translocation of endoplasmic reticulum-associated calreticulin; (ii) extracellular release of DNA-binding protein HMGB1 and (iii) release of cytosolic ATP^{91,170}. Based on this premise, we hypothesized that, since HD-RT cannot overcome

6. Discussion

the immunosuppressive effects of non-irradiated CAFs the same HD-RT should not be able to trigger signals that enhance the activation of CD8⁺ T-cells. Indeed, we demonstrate here, for the first time that HD-RT does not provoke release of CAF-ICD signals (HMGB1 and ATP) at any of the measured time points.

It still remains unclear which radiotherapy regimen (dose and fractionation) is more effective to induce an optimal immunogenic cancer cell death response: to boost the patient's immune system without destroying the anti-tumorigenic immune cells at the irradiation site. To this end, some authors suggest that a high single dose of RT is more effective than a low dose^{171,172}. While other authors report that fractionated RT (i.e., smaller doses of radiation given more than once) are more effective to induce a systemic immune response than single doses^{93,173}. In any case, we demonstrate in this study that non-irradiated CAFs or CAFs treated with conventional fractionated radiotherapy (4 x 2 Gy) exert the same immunosuppressive effects as CAFs treated with single high-dose radiotherapy (*additional files C.2*).

CONCLUDING REMARKS & FUTURE DIRECTIONS

In this project we demonstrate the existence of a continual cross-talk between freshly isolated human CAFs from NSCLC and freshly isolated human T-lymphocytes from peripheral blood of healthy donors. Therefore, CAF-soluble factors may be an attractive target for anti-cancer therapy. Five main observations can be highlighted from this study: **(i)** CAF-derived soluble factors exhibit strong immunosuppressive effects over T-cells, affecting both their function and migration rates, **(ii)** the well characterized immunosuppressive factors TGF- β , IDO, PGE2, IL-6 and Galectin-3 do not seem to play a major role in the CAF-mediated effects, **(iii)** HD-RT given in a single dose of 18 Gy or in conventional fractions (4 x 2 Gy) does not overcome CAFs immunosuppressive effects, **(iv)** the secretome of irradiated CAFs contains the same levels of immunosuppressive cytokines as non-irradiated CAFs secretome **(v)** HD-RT does not trigger immunogenic cell death signals.

Much effort has been put into the development of targeted drug therapies to hinder unfavorable molecular pathways in cancer cells. However, researchers are faced with enormous challenges in trying to overcome genomic instability of tumor cells that may

6. Discussion

be responsible for acquisition of a drug-resistant phenotype. The increasing knowledge of the interactions between stromal cells and neoplastic cells and their importance in tumor initiation and cancer progression may provide us new strategies to develop novel therapies aimed at targeting the genetically more stable stromal cells or their released factors and thus increase the possibilities to overcome drug and/or radio-resistance, suppress tumor growth and gain local tumor control and overall survival in patients.

It is well documented that CAFs in the tumor microenvironment are an active participant in cancer formation and progression through the secretion of cytokines and chemokines. Thus, it is not surprising that during the last few years, CAFs have been selected as a therapeutic target against cancer progression. However, in order to generate a more effective targeted therapy against either CAFs or CAF-soluble factors, further translational research on CAF versus tumor cells and CAF versus tumor stromal cells cross-talk is needed.

It is also worth mentioning that CAFs comprise a heterogeneous population of cells and that the proportion of different CAFs subtypes can vary between organs anatomical areas, the tumor type, or the tumor stages²⁹. Therefore, considering that more than 100 types of cancer have been defined, CAF-derived soluble factors may vary significantly among tumor types. Moreover, aspects like oxygen deficiency established in fast-growing tumors may enhance the release of cytokines and chemokines not present in tumors that are highly vascularized. However, in this study we wanted to gain more knowledge on the immune-modulating properties of CAFs in general.

In the future, we could complete our study by working in different directions: **(i)** continue the search for the CAF-derived soluble factor/s responsible for the immunosuppressive effects; **(ii)** study in depth Tregs-mediated immunosuppression; **(iii)** compare the secretory phenotype of normal lung-fibroblasts obtained from non-cancer tissues with the secretory phenotype of NSCLC-associated fibroblasts showed in this study; **(iv)** study the effects of CAFs on other immune cell types such as macrophages, dendritic cells and natural killer cells; **(v)** study the role of CAFs in animal models and **(vi)** study potential association of CAF abundance with infiltration of immune cell populations (Treg, NK, Macrophages, MDSC, Th2 and Th17) in lung tissues of NSCLC patients and/or in mice. Another exciting phenomenon that could be studied in the future is the role of CAF-derived exosomes on T-cell function. It has been suggested in recent literature that one

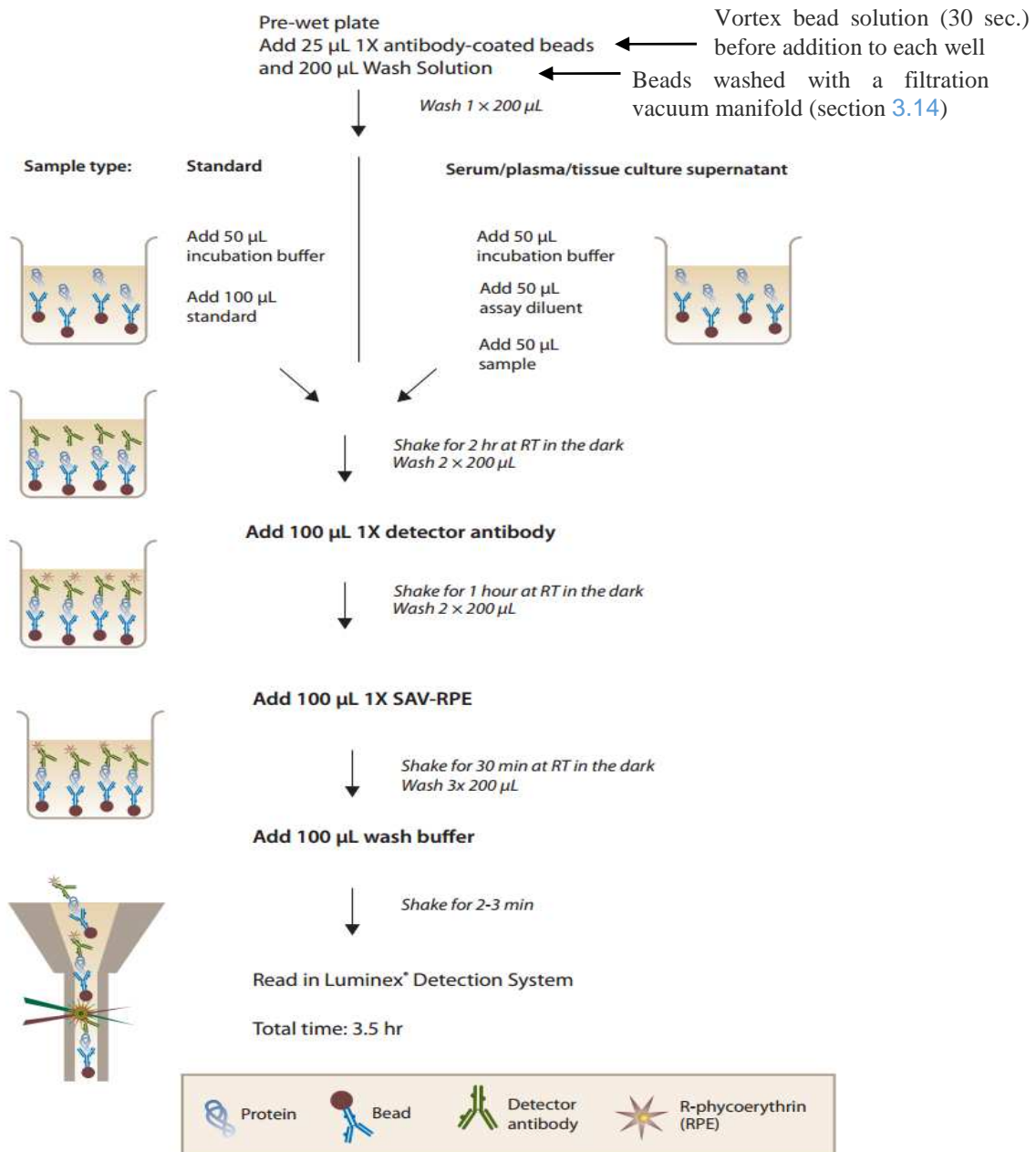
6. Discussion

form of cell-cell communication between tumor cells and the stromal cells could be through the release of extracellular vesicles or exosomes, and that these exosomes could carry a multitude of regulatory molecules involved in the regulation of the immune response^{174,175}.

Additional files

A Protocols

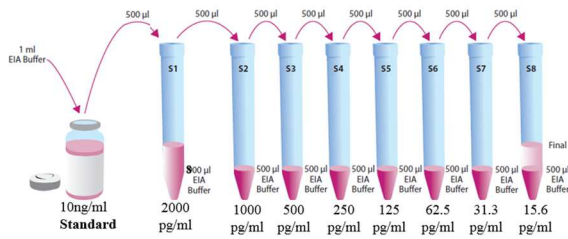
A.1 Protocol for multiplex protein array



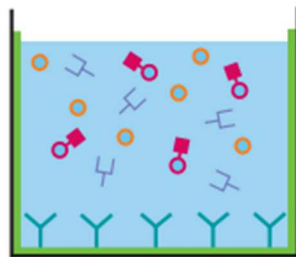
Adapted from Invitrogen protocols⁵

Additional files

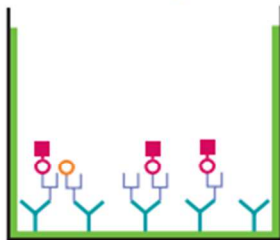
A.2 Protocol for PGE₂ Express EIA Kit (Cayman chemical)



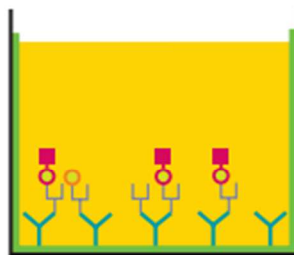
1. Prepare standard curve in complete DMEM medium
2. Prepare all the reagents and buffers according to manufacturer's instructions



3. Pre-coated plate with goat polyclonal anti-mouse IgG (Y) and blocked (—) with proprietary formulation of proteins was incubated with (1) either standard or sample (○), (2) PGE₂- AChE, (■) and (3) PGE₂ monoclonal antibodies (⌋)



4. Wash to remove all unbound agents



5. Develop the well with Ellman's Reagent

- Y = Goat polyclonal anti-mouse IgG
- = Blocking proteins
- = Acetylcholinesterase linked to PGE₂, (Tracer)
- ⌋ = Specific antibody to PGE₂
- = Free PGE₂

Add 50 µL of appropriate standard, blank and samples into wells

Immediately after

Add 50 µL of PGE₂ – AChE conjugate reconstitute with EIA Buffer

Immediately after

Add 50 µL of PGE₂ Monoclonal Antibody reconstitute with EIA Buffer

Shake for 60 min at RT in the dark

Empty the Wells and rinse 5 x with Wash buffer

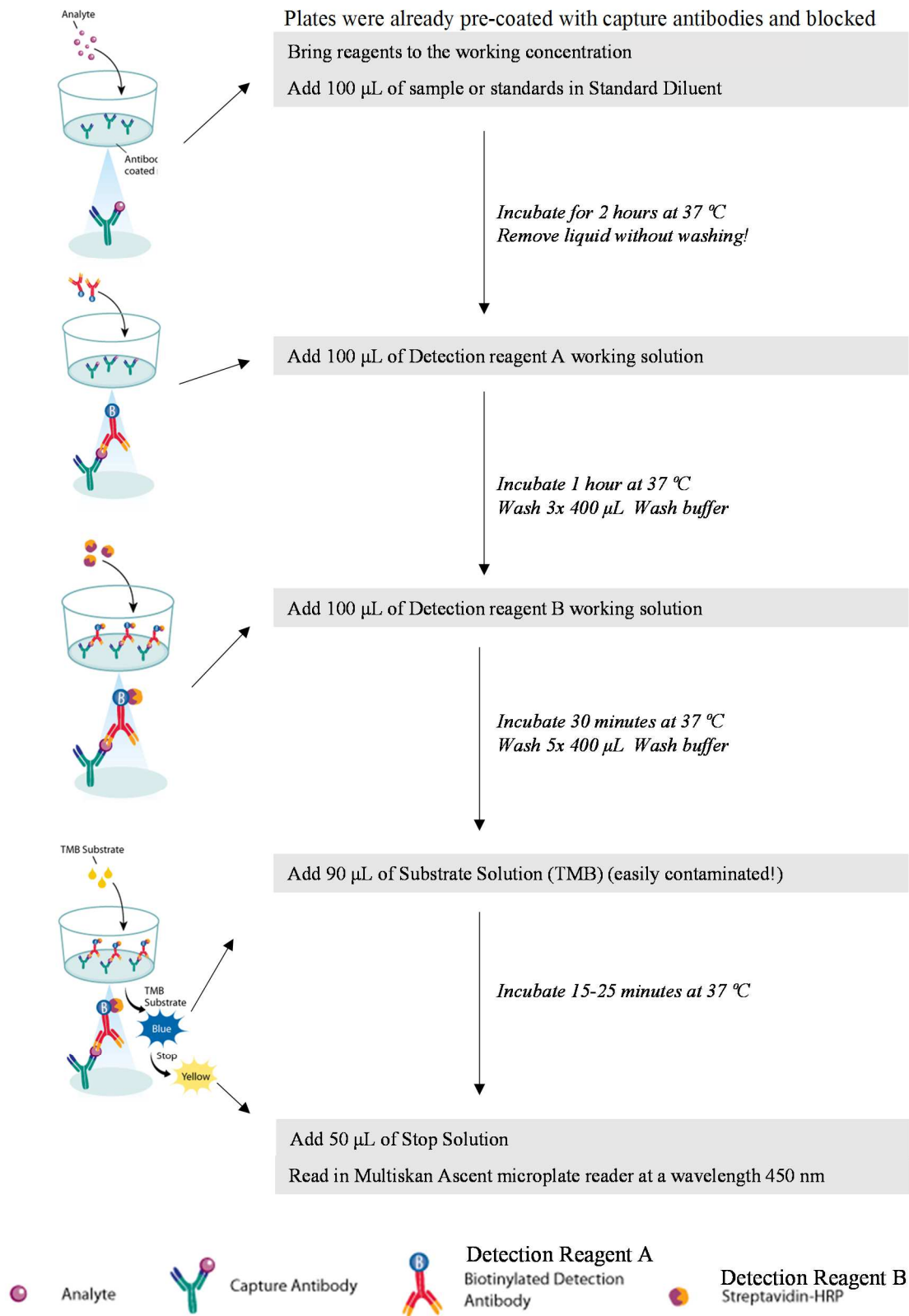
Immediately after

Add 200 µL Ellman's Reagent reconstituted with ultra pure water

Shake for 60-90 min at RT in the dark

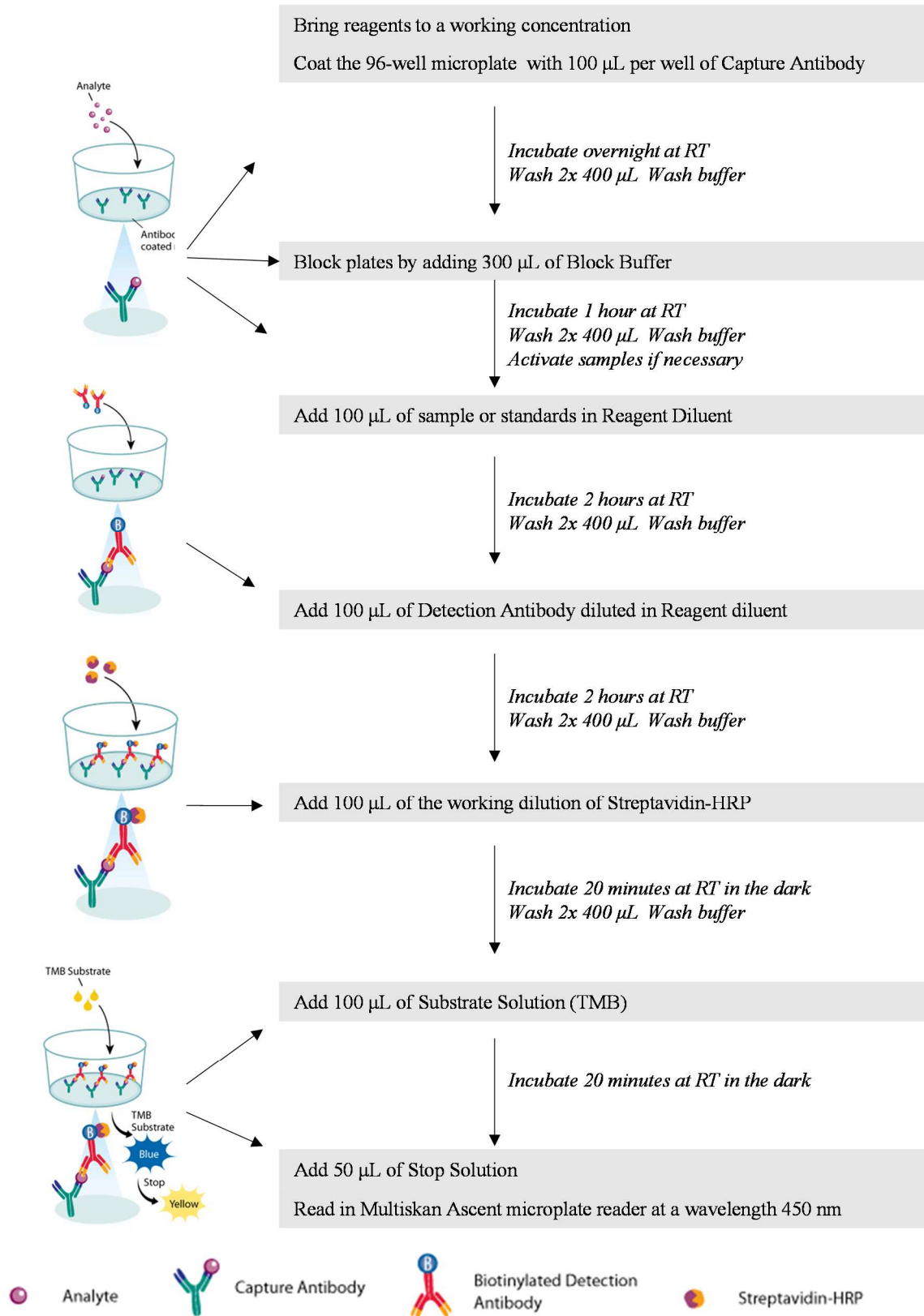
Read in EMax microplate reader at a wavelength 405-420 nm

A.3 Protocol for IDO ELISA kit (ClouD-Clone Corp.)



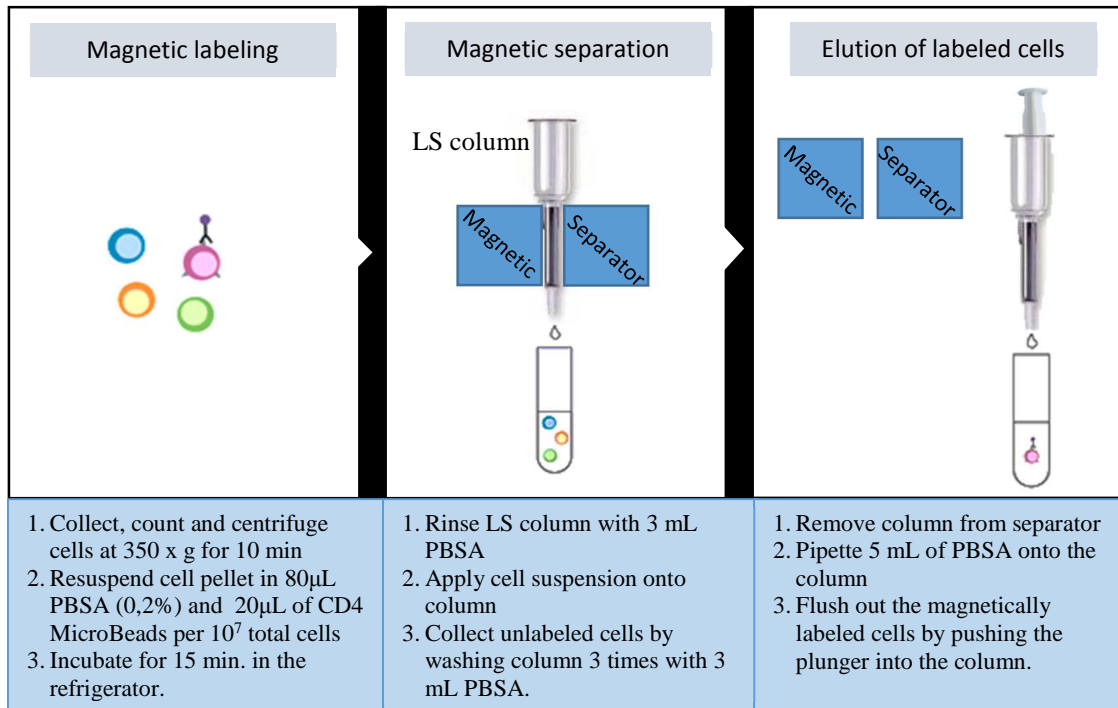
Adapted from IDO ELISA kit (ClouD-Clone Corp. section 3.8)

A.4 Protocol for DuoSet® ELISA kits (TGF-β1, IFN-γ and TNF-α) (R&D Systems)



Adapted from Human DuoSet® ELISA kits (R&D Systems section 3.8)

A.5 Protocol for positive selection of CD4⁺ T-cells from peripheral blood with a MACS[®] separation



B Solutions

B.1 Proteomics solutions

Gel-fixing Solution	
Reagent	Amount
Methanol	40 mL
Acetic Acid	10 mL
Milli-Q Water	50 mL

Work in the hood

10 mM DTT in 100 mM Ambic	
Reagent	Amount
DTT 1M	10 µl
Milli-Q water	890 µl
Ambic 1 M	100 µl

6 ng/µL Trypsin	
Reagent	Amount
Trypsin Porcine	10 µL
Digestion Buffer	160 µL

Wash Solution	
Reagent	Amount
Ambic (1M)	250 µL
Milli-Q water	4750 µL
LC-MS grade Acetonitrile (ACN)	5 mL

55 mM IAA in 100 mM Ambic	
Reagent	Amount
Iodacetamide (IAA)	10 mg
Milli-Q water	900 µL
Ambic 1M	100 µl

Digestion Buffer	
Reagent	Amount
Ambic 1M	50 µL
Milli-Q Water	900 µL

C Additional Results

C.1 Pilot experiment: minimal effective concentration of the chemo-attractant SDF-1

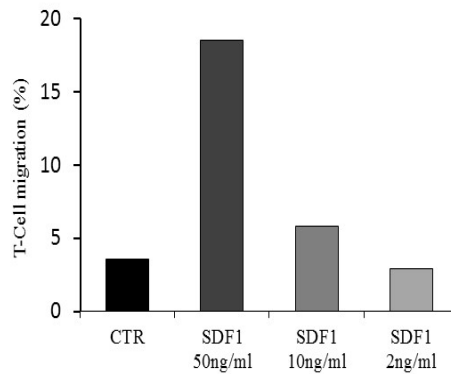


Figure C.1 Minimal effective concentration of the chemo-attractant SDF-1. Migration assays were carried out against three different concentration of SDF-1 (50, 10 and 2 ng/mL) to determine the minimal concentration of SDF-1 required for induction of T-cell migration.

C.2 T-lymphocyte proliferation assays with different radiation regimens

T-lymphocytes proliferation assays were carried with conditioned medium from CAFs cultures (n = 3) treated with fractionated radiotherapy (4 x 2 Gy), single high-dose radiotherapy (1 x 18 Gy), or left untreated (control group). Results in **Figure C.2** show that the immune-suppressive effects remained unperturbed under both radiation regimens.

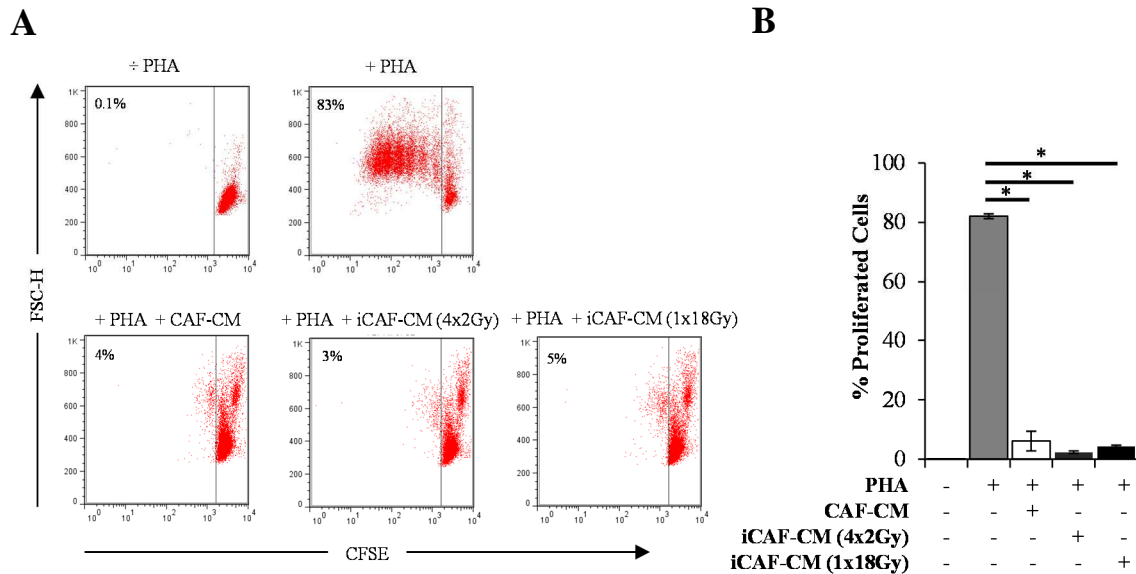


Figure C.2 T-cell proliferation assays: immune-suppressive effects elicited by irradiated and control CAF-CM. T-cell proliferation assays were performed using CellTrace CFSE-labeled human PBMCs activated with 1 μ g/ml PHA and cultured with CAF-CM at a 1:1 ratio for 5 days. Assays were performed with CM harvested three days post-IR from irradiated (iCAF-CM) or non-irradiated (CAF-CM) CAF cultures. T-cell proliferation was determined by measuring the CFSE fluorescence intensity by flow cytometry after gating the lymphocytes population by forward and side scatter. **(A)** Representative flow cytometry dot plots showing the percentage of CFSE low -labeled T-cells. One out of three representative determinations is shown. **(B)** Graph shows the rate of T-cell proliferation determined by CFSE fluorescence loss. Data points are representative for three different CAF donors with bars representing means from duplicate determinations. Student's T-test value (* $P < 0.001$).

C.3 Migration assays with non-activated T-lymphocytes

Conditioned medium from both irradiated and non-irradiated CAFs does not influence the migratory abilities of non-activated lymphocytes (**Figure C.3**).

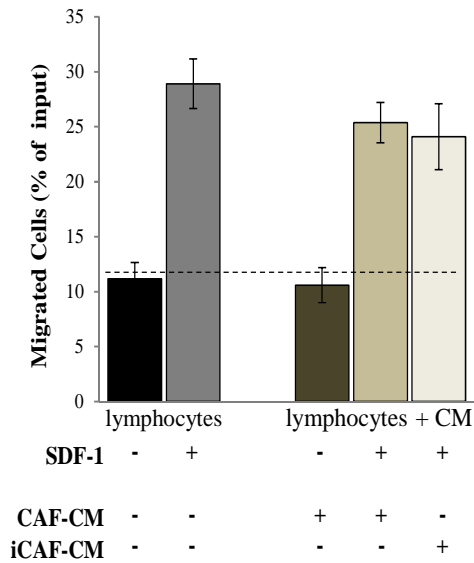


Figure C.3 Lymphocytes migration assays. Percentage of migrating lymphocytes (recovered from lower chambers). Non-activated PBMCs were added to the upper chambers. Lower chambers contained conditioned medium from irradiated (iCAF-CM) and non-irradiated (CAF-CM) cultures with or without SDF-1 (50ng/ml) as chemoattractant. Chambers were incubated for 2h at 37°C and cells migrating to the lower chambers were counted using flow cytometry. Each bar represents the mean \pm SD of two different CAFs donors measured in triplicates.

C.4 ELISA assays to check cytokine inhibition in CAF-CM

Once cytokines were blocked by appropriate drugs, ELISA tests were performed in order to confirm inhibition. Results in **Figure C.4** show that a drug concentration of 5 μ M of Diclofenac is enough to block PGE2 synthesis by COX2, we also see that DMEM with 10 % FBS gives a relatively high background. On the other hand, 500 ng/mL of α TGF- β is also enough to neutralize TGF- β , whereas serum free DMEM medium did not give any background.

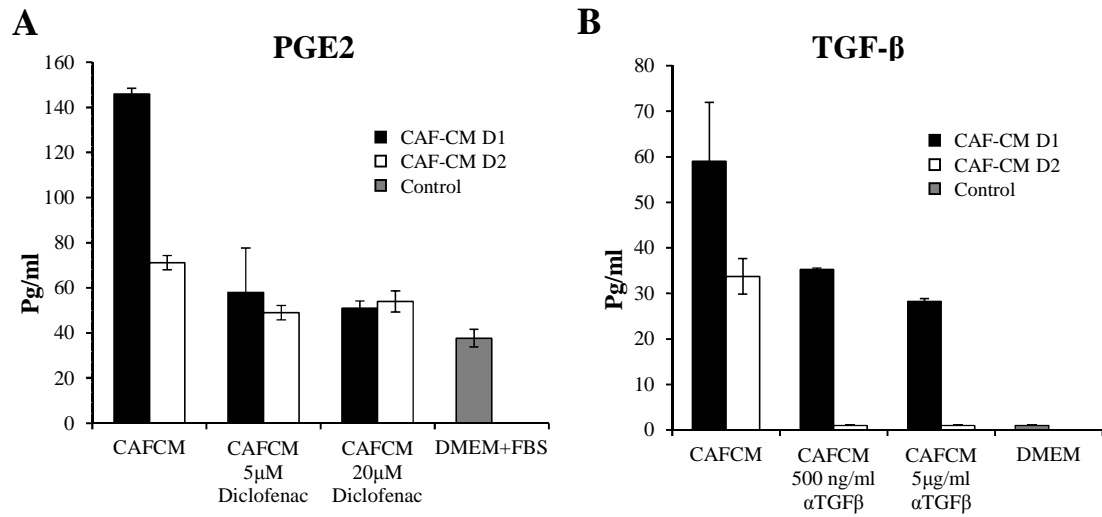


Figure C.4 ELISA test to determine the blocking of PGE2 and TGF-β. (A) PGE2 blocked with Diclofenac. (B) TGF-β blocked with anti-TGFβ monoclonal antibody. Each bar represent the mean ±SD of duplicate determinations. D1, D2: Donor 1, 2; DMEM: Dulbecco's Modified Eagle's medium

References

- 1 *Cancer Research UK*, <<http://www.cancerresearchuk.org/about-cancer/type/lung-cancer/treatment/statistics-and-outlook-for-lung-cancer>> (2014).
- 2 Chen, Y. *Lung Cancer. In PubMed Health*, <<http://www.ncbi.nlm.nih.gov/pubmedhealth/PMH0004529/>> (2011, August 24).
- 3 *National Cancer Institute*, <<http://www.cancer.gov/cancertopics/pdq/treatment/non-small-cell-lung/Patient/page1>> (April 2 2015).
- 4 Jerusalem, G., Hustinx, R., Beguin, Y. & Fillet, G. PET scan imaging in oncology. *European journal of cancer* **39**, 1525-1534 (2003).
- 5 Provencio, M., Isla, D., Sánchez, A. & Cantos, B. Inoperable stage III non-small cell lung cancer: Current treatment and role of vinorelbine. *Journal of thoracic disease* **3**, 197 (2011).
- 6 Gérard, C. & Debruyne, C. Immunotherapy in the landscape of new targeted treatments for non-small cell lung cancer. *Molecular oncology* **3**, 409-424 (2009).
- 7 Katzel, J. A., Fanucchi, M. P. & Li, Z. Recent advances of novel targeted therapy in non-small cell lung cancer. *J Hematol Oncol* **2**, E4 (2009).
- 8 Hellevik, T. & Martinez-Zubiaurre, I. Radiotherapy and the tumor stroma: the importance of dose and fractionation. *Frontiers in oncology* **4** (2014).
- 9 Palma, D. & Senan, S. Stereotactic radiation therapy: changing treatment paradigms for stage I nonsmall cell lung cancer. *Current opinion in oncology* **23**, 133-139 (2011).
- 10 Hanahan, D. & Weinberg, R. A. The hallmarks of cancer. *cell* **100**, 57-70 (2000).
- 11 Pietras, K. & Östman, A. Hallmarks of cancer: interactions with the tumor stroma. *Experimental cell research* **316**, 1324-1331 (2010).
- 12 Hanahan, D. & Weinberg, R. A. Hallmarks of cancer: the next generation. *cell* **144**, 646-674 (2011).
- 13 Quail, D. F. & Joyce, J. A. Microenvironmental regulation of tumor progression and metastasis. *Nature medicine* **19**, 1423-1437 (2013).
- 14 Donjacour, A. A. & Cunha, G. R. Stromal regulation of epithelial function. *Cancer treatment research* **53**, 335-364 (1991).
- 15 Streuli, C. Extracellular matrix remodelling and cellular differentiation. *Current opinion in cell biology* **11**, 634-640 (1999).
- 16 Mueller, M. M. & Fusenig, N. E. Friends or foes—bipolar effects of the tumour stroma in cancer. *Nature Reviews Cancer* **4**, 839-849 (2004).
- 17 De Wever, O. & Mareel, M. Role of tissue stroma in cancer cell invasion. *The Journal of pathology* **200**, 429-447 (2003).
- 18 Shimoda, M., Mellody, K. T. & Orimo, A. Carcinoma-associated fibroblasts are a rate-limiting determinant for tumour progression. *Seminars in cell & developmental biology* **21**, 19-25 (2010).
- 19 Orimo, A. & Weinberg, R. A. Stromal fibroblasts in cancer: a novel tumor-promoting cell type. *Cell cycle* **5**, 1597-1601 (2006).

References

- 20 Zeisberg, E. M., Potenta, S., Xie, L., Zeisberg, M. & Kalluri, R. Discovery of endothelial to mesenchymal transition as a source for carcinoma-associated fibroblasts. *Cancer research* **67**, 10123-10128 (2007).
- 21 Ishii, G. *et al.* Bone-marrow-derived myofibroblasts contribute to the cancer-induced stromal reaction. *Biochemical and biophysical research communications* **309**, 232-240 (2003).
- 22 Mishra, P. J. *et al.* Carcinoma-associated fibroblast-like differentiation of human mesenchymal stem cells. *Cancer research* **68**, 4331-4339 (2008).
- 23 Kalluri, R. & Neilson, E. G. Epithelial-mesenchymal transition and its implications for fibrosis. *Journal of Clinical Investigation* **112**, 1776 (2003).
- 24 Kalluri, R. & Zeisberg, M. Fibroblasts in cancer. *Nature Reviews Cancer* **6**, 392-401 (2006).
- 25 Allinen, M. *et al.* Molecular characterization of the tumor microenvironment in breast cancer. *Cancer cell* **6**, 17-32 (2004).
- 26 Östman, A. & Augsten, M. Cancer-associated fibroblasts and tumor growth-bystanders turning into key players. *Current opinion in genetics & development* **19**, 67-73 (2009).
- 27 Xing, F., Saidou, J. & Watabe, K. Cancer associated fibroblasts (CAFs) in tumor microenvironment. *Frontiers in bioscience: a journal and virtual library* **15**, 166 (2010).
- 28 Servais, C. & Erez, N. From sentinel cells to inflammatory culprits: cancer-associated fibroblasts in tumour-related inflammation. *The Journal of pathology* **229**, 198-207 (2013).
- 29 Augsten, M. Cancer-associated fibroblasts as another polarized cell type of the tumor microenvironment. *Frontiers in oncology* **4** (2014).
- 30 Zhi, K., Shen, X., Zhang, H. & Bi, J. Research Cancer-associated fibroblasts are positively correlated with metastatic potential of human gastric cancers. *J Exp Clin Cancer Res* **29**, 66-74 (2010).
- 31 Kojima, Y. *et al.* Autocrine TGF- β and stromal cell-derived factor-1 (SDF-1) signaling drives the evolution of tumor-promoting mammary stromal myofibroblasts. *Proceedings of the National Academy of Sciences* **107**, 20009-20014 (2010).
- 32 Orimo, A. *et al.* Stromal fibroblasts present in invasive human breast carcinomas promote tumor growth and angiogenesis through elevated SDF-1/CXCL12 secretion. *Cell* **121**, 335-348 (2005).
- 33 Pietras, K., Pahler, J., Bergers, G. & Hanahan, D. Functions of paracrine PDGF signaling in the proangiogenic tumor stroma revealed by pharmacological targeting. *PLoS medicine* **5**, e19 (2008).
- 34 Bhowmick, N. A., Neilson, E. G. & Moses, H. L. Stromal fibroblasts in cancer initiation and progression. *Nature* **432**, 332-337 (2004).
- 35 Bremnes, R. M. *et al.* The role of tumor stroma in cancer progression and prognosis: emphasis on carcinoma-associated fibroblasts and non-small cell lung cancer. *Journal of Thoracic Oncology* **6**, 209-217 (2011).
- 36 Silzle, T., Randolph, G. J., Kreutz, M. & Kunz-Schughart, L. A. The fibroblast: sentinel cell and local immune modulator in tumor tissue. *International journal of cancer* **108**, 173-180 (2004).
- 37 Oskarsson, T. *et al.* Breast cancer cells produce tenascin C as a metastatic niche component to colonize the lungs. *Nature medicine* **17**, 867-874 (2011).
- 38 Talts, J. F., Wirl, G., Dictor, M., Muller, W. J. & Fassler, R. Tenascin-C modulates tumor stroma and monocyte/macrophage recruitment but not tumor growth or

References

- metastasis in a mouse strain with spontaneous mammary cancer. *Journal of cell science* **112**, 1855-1864 (1999).
- 39 Gaggioli, C. *et al.* Fibroblast-led collective invasion of carcinoma cells with differing roles for RhoGTPases in leading and following cells. *Nature cell biology* **9**, 1392-1400 (2007).
- 40 Duda, D. G. *et al.* Malignant cells facilitate lung metastasis by bringing their own soil. *Proceedings of the National Academy of Sciences* **107**, 21677-21682 (2010).
- 41 Grum-Schwensen, B. *et al.* Suppression of tumor development and metastasis formation in mice lacking the S100A4 (mts1) gene. *Cancer research* **65**, 3772-3780 (2005).
- 42 Fitzpatrick, F. Inflammation, carcinogenesis and cancer. *International immunopharmacology* **1**, 1651-1667 (2001).
- 43 Maeda, H. & Akaike, T. Reviews-nitric oxide and oxygen radicals in infection, inflammation, and cancer. *Biochemistry-New York-English Translation of Biokhimiya* **63**, 854-865 (1998).
- 44 Kim, R., Emi, M. & Tanabe, K. Cancer immunoediting from immune surveillance to immune escape. *Immunology* **121**, 1-14 (2007).
- 45 Igney, F. H. & Krammer, P. H. Immune escape of tumors: apoptosis resistance and tumor counterattack. *Journal of leukocyte biology* **71**, 907-920 (2002).
- 46 Zamarron, B. F. & Chen, W. Dual roles of immune cells and their factors in cancer development and progression. *International journal of biological sciences* **7**, 651 (2011).
- 47 Barnas, J. L., Simpson-Abelson, M. R., Yokota, S. J., Kelleher Jr, R. J. & Bankert, R. B. T cells and stromal fibroblasts in human tumor microenvironments represent potential therapeutic targets. *Cancer Microenvironment* **3**, 29-47 (2010).
- 48 Shields, J. D., Kourtis, I. C., Tomei, A. A., Roberts, J. M. & Swartz, M. A. Induction of lymphoidlike stroma and immune escape by tumors that express the chemokine CCL21. *Science* **328**, 749-752 (2010).
- 49 Yang, L., Pang, Y. & Moses, H. L. TGF- β and immune cells: an important regulatory axis in the tumor microenvironment and progression. *Trends in immunology* **31**, 220-227 (2010).
- 50 Nazareth, M. R. *et al.* Characterization of human lung tumor-associated fibroblasts and their ability to modulate the activation of tumor-associated T cells. *The Journal of Immunology* **178**, 5552-5562 (2007).
- 51 Massagué, J., Blain, S. W. & Lo, R. S. TGF β signaling in growth control, cancer, and heritable disorders. *Cell* **103**, 295-309 (2000).
- 52 Massagué, J. TGF β in cancer. *Cell* **134**, 215-230 (2008).
- 53 Thomas, D. A. & Massagué, J. TGF- β directly targets cytotoxic T cell functions during tumor evasion of immune surveillance. *Cancer cell* **8**, 369-380 (2005).
- 54 Trotta, R. *et al.* TGF- β utilizes SMAD3 to inhibit CD16-mediated IFN- γ production and antibody-dependent cellular cytotoxicity in human NK cells. *The Journal of Immunology* **181**, 3784-3792 (2008).
- 55 Crane, C. A. *et al.* TGF- β downregulates the activating receptor NKG2D on NK cells and CD8+ T cells in glioma patients. *Neuro-oncology* **12**, 7-13 (2009).
- 56 Balsamo, M. *et al.* Melanoma-associated fibroblasts modulate NK cell phenotype and antitumor cytotoxicity. *Proceedings of the National Academy of Sciences* **106**, 20847-20852 (2009).
- 57 Li, T. *et al.* Hepatocellular carcinoma-associated fibroblasts trigger NK cell dysfunction via PGE2 and IDO. *Cancer letters* **318**, 154-161 (2012).

References

- 58 Deschoolmeester, V. *et al.* Tumor infiltrating lymphocytes: an intriguing player in the survival of colorectal cancer patients. *BMC immunology* **11**, 19 (2010).
- 59 Kidd, P. Th1/Th2 balance: the hypothesis, its limitations, and implications for health and disease. *Alternative Medicine Review* **8**, 223-246 (2003).
- 60 Liao, D., Luo, Y., Markowitz, D., Xiang, R. & Reisfeld, R. A. Cancer associated fibroblasts promote tumor growth and metastasis by modulating the tumor immune microenvironment in a 4T1 murine breast cancer model. *PLoS one* **4**, e7965 (2009).
- 61 Diehl, S. *et al.* Inhibition of Th1 differentiation by IL-6 is mediated by SOCS1. *Immunity* **13**, 805-815 (2000).
- 62 De Monte, L. *et al.* Intratumor T helper type 2 cell infiltrate correlates with cancer-associated fibroblast thymic stromal lymphopoietin production and reduced survival in pancreatic cancer. *The Journal of experimental medicine* **208**, 469-478 (2011).
- 63 Wang, L. *et al.* IL-17 can promote tumor growth through an IL-6–Stat3 signaling pathway. *The Journal of experimental medicine* **206**, 1457-1464 (2009).
- 64 Tosolini, M. *et al.* Clinical impact of different classes of infiltrating T cytotoxic and helper cells (Th1, th2, treg, th17) in patients with colorectal cancer. *Cancer research* **71**, 1263-1271 (2011).
- 65 Eisenstein, E. M. & Williams, C. B. The Treg/Th17 cell balance: a new paradigm for autoimmunity. *Pediatric Research* **65**, 26R-31R (2009).
- 66 Su, X. *et al.* Tumor microenvironments direct the recruitment and expansion of human Th17 cells. *The journal of immunology* **184**, 1630-1641 (2010).
- 67 Sakaguchi, S., Wing, K., Onishi, Y., Prieto-Martin, P. & Yamaguchi, T. Regulatory T cells: how do they suppress immune responses? *International immunology* **21**, 1105-1111 (2009).
- 68 Zou, W. Immunosuppressive networks in the tumour environment and their therapeutic relevance. *Nature Reviews Cancer* **5**, 263-274 (2005).
- 69 Kinoshita, T. *et al.* Forkhead box P3 regulatory T cells coexisting with cancer associated fibroblasts are correlated with a poor outcome in lung adenocarcinoma. *Cancer science* **104**, 409-415 (2013).
- 70 Colotta, F., Allavena, P., Sica, A., Garlanda, C. & Mantovani, A. Cancer-related inflammation, the seventh hallmark of cancer: links to genetic instability. *Carcinogenesis* **30**, 1073-1081 (2009).
- 71 Murdoch, C., Muthana, M., Coffelt, S. B. & Lewis, C. E. The role of myeloid cells in the promotion of tumour angiogenesis. *Nature Reviews Cancer* **8**, 618-631 (2008).
- 72 Mantovani, A., Sozzani, S., Locati, M., Allavena, P. & Sica, A. Macrophage polarization: tumor-associated macrophages as a paradigm for polarized M2 mononuclear phagocytes. *Trends in immunology* **23**, 549-555 (2002).
- 73 Augsten, M. *et al.* CXCL14 is an autocrine growth factor for fibroblasts and acts as a multi-modal stimulator of prostate tumor growth. *Proceedings of the National Academy of Sciences* **106**, 3414-3419 (2009).
- 74 Fujii, N. *et al.* Cancer-associated fibroblasts and CD163-positive macrophages in oral squamous cell carcinoma: their clinicopathological and prognostic significance. *Journal of Oral Pathology & Medicine* **41**, 444-451 (2012).
- 75 Chomarat, P., Banchereau, J., Davoust, J. & Palucka, A. K. IL-6 switches the differentiation of monocytes from dendritic cells to macrophages. *Nature immunology* **1**, 510-514 (2000).

References

- 76 Henschke, C. I. *et al.* Survival of patients with stage I lung cancer detected on CT screening. *The New England journal of medicine* **355**, 1763-1771 (2006).
- 77 Qiao, X., Tullgren, O., Lax, I., Sirzén, F. & Lewensohn, R. The role of radiotherapy in treatment of stage I non-small cell lung cancer. *Lung cancer* **41**, 1-11 (2003).
- 78 Pereira, G. C., Traughber, M. & Muzic, R. F. The role of imaging in radiation therapy planning: past, present, and future. *BioMed research international* **2014** (2014).
- 79 Verellen, D. *et al.* Innovations in image-guided radiotherapy. *Nature Reviews Cancer* **7**, 949-960 (2007).
- 80 De Ruyscher, D. *et al.* State of the art radiation therapy for lung cancer 2012: a glimpse of the future. *Clinical lung cancer* **14**, 89-95 (2013).
- 81 Timmerman, R. *et al.* Stereotactic body radiation therapy for inoperable early stage lung cancer. *Jama* **303**, 1070-1076 (2010).
- 82 Loo Jr, B. W. Stereotactic ablative radiotherapy (SABR) for lung cancer: What does the future hold? *Journal of thoracic disease* **3**, 150 (2011).
- 83 Bradley, J. D. *et al.* Stereotactic Body Radiation Therapy for Early-Stage Non-Small-Cell Lung Cancer: The Pattern of Failure Is Distant. *International Journal of Radiation Oncology* Biology* Physics* **77**, 1146-1150 (2010).
- 84 Meyer, K. K. Radiation-induced lymphocyte-immune deficiency: A factor in the increased visceral metastases and decreased hormonal responsiveness of breast cancer. *Archives of Surgery* **101**, 114-121 (1970).
- 85 Braeman, J. & Deeley, T. Radiotherapy and the immune response in cancer of the lung. *The British journal of radiology* **46**, 446-449 (1973).
- 86 Raben, M., Walach, N., Galili, U. & Schlesinger, M. The effect of radiation therapy on lymphocyte subpopulations in cancer patients. *Cancer* **37**, 1417-1421 (1976).
- 87 Wara, W. M., PHILLIPS, T. L., WARA, D. W., AMMANN, A. J. & SMITH, V. Immunosuppression following radiation therapy for carcinoma of the nasopharynx. *American Journal of Roentgenology* **123**, 482-485 (1975).
- 88 Ehlers, G. & Fridman, M. Abscopal effect of radiation in papillary adenocarcinoma. *The British journal of radiology* **46**, 220-222 (1973).
- 89 Rees, G. & Ross, C. Abscopal regression following radiotherapy for adenocarcinoma. *The British journal of radiology* **56**, 63-66 (1983).
- 90 Demaria, S. *et al.* Ionizing radiation inhibition of distant untreated tumors (abscopal effect) is immune mediated. *International Journal of Radiation Oncology* Biology* Physics* **58**, 862-870 (2004).
- 91 Golden, E. B., Pellicciotta, I., Demaria, S., Barcellos-Hoff, M. H. & Formenti, S. C. The convergence of radiation and immunogenic cell death signaling pathways. *Frontiers in oncology* **2** (2012).
- 92 Formenti, S. C. & Demaria, S. Systemic effects of local radiotherapy. *The lancet oncology* **10**, 718-726 (2009).
- 93 Dewan, M. Z. *et al.* Fractionated but not single-dose radiotherapy induces an immune-mediated abscopal effect when combined with anti-CTLA-4 antibody. *Clinical Cancer Research* **15**, 5379-5388 (2009).
- 94 Handschel, J. *et al.* Irradiation induces increase of adhesion molecules and accumulation of β 2-integrin-expressing cells in humans. *International Journal of Radiation Oncology* Biology* Physics* **45**, 475-481 (1999).
- 95 Matsumura, S. *et al.* Radiation-induced CXCL16 release by breast cancer cells attracts effector T cells. *The Journal of Immunology* **181**, 3099-3107 (2008).

References

- 96 Reits, E. A. *et al.* Radiation modulates the peptide repertoire, enhances MHC class I expression, and induces successful antitumor immunotherapy. *The Journal of experimental medicine* **203**, 1259-1271 (2006).
- 97 Gasser, S., Orsulic, S., Brown, E. J. & Raulet, D. H. The DNA damage pathway regulates innate immune system ligands of the NKG2D receptor. *Nature* **436**, 1186-1190 (2005).
- 98 Klug, F. *et al.* Low-dose irradiation programs macrophage differentiation to an iNOS⁺/M1 phenotype that orchestrates effective T cell immunotherapy. *Cancer cell* **24**, 589-602 (2013).
- 99 Chakraborty, M. *et al.* External beam radiation of tumors alters phenotype of tumor cells to render them susceptible to vaccine-mediated T-cell killing. *Cancer research* **64**, 4328-4337 (2004).
- 100 Lugade AA, S. E., Gerber SA, Moran JP, Frelinger JG, Lord EM. Radiation-induced IFN-gamma production within the tumor microenvironment influences antitumor immunity. *J Immunol.* **5**, 3132-3139 (2008).
- 101 Martinez-Zubiaurre, I. *et al.* Tumorigenic responses of cancer-associated stromal fibroblasts after ablative radiotherapy: a transcriptome-profiling study. *Journal of Cancer Therapy* **4**, 208 (2013).
- 102 Rodier, F. *et al.* Persistent DNA damage signalling triggers senescence-associated inflammatory cytokine secretion. *Nature cell biology* **11**, 973-979 (2009).
- 103 Hellevik, T. *et al.* Changes in the secretory profile of NSCLC-associated fibroblasts after ablative radiotherapy: potential impact on angiogenesis and tumor growth. *Translational oncology* **6**, 66-74 (2013).
- 104 Papadopoulou, A. & Kleitas, D. Human lung fibroblasts prematurely senescent after exposure to ionizing radiation enhance the growth of malignant lung epithelial cells in vitro and in vivo. *International journal of oncology* **39**, 989-999 (2011).
- 105 Krtolica, A., Parrinello, S., Lockett, S., Desprez, P.-Y. & Campisi, J. Senescent fibroblasts promote epithelial cell growth and tumorigenesis: a link between cancer and aging. *Proceedings of the National Academy of Sciences* **98**, 12072-12077 (2001).
- 106 Davalos, A. R., Coppe, J.-P., Campisi, J. & Desprez, P.-Y. Senescent cells as a source of inflammatory factors for tumor progression. *Cancer and Metastasis Reviews* **29**, 273-283 (2010).
- 107 Wu, G. *Assay development: fundamentals and practices*. (John Wiley & Sons, 2010).
- 108 Oh, H.-Y. *et al.* Characteristics of primary and immortalized fibroblast cells derived from the miniature and domestic pigs. *BMC cell biology* **8**, 20 (2007).
- 109 Bakke, A. C. The principles of flow cytometry. *Lab Medicine* **32**, 207-211 (2001).
- 110 Chen, H.-C. in *Cell Migration* 15-22 (Springer, 2005).
- 111 *Human Cytokine 10-Plex Panel*, <https://tools.lifetechnologies.com/content/sfs/manuals/LHC0001_Protocol_Rev2.pdf> (2010).
- 112 Aebersold, R. & Mann, M. Mass spectrometry-based proteomics. *Nature* **422**, 198-207 (2003).
- 113 Ho, C. *et al.* Electrospray ionisation mass spectrometry: principles and clinical applications. *The Clinical Biochemist Reviews* **24**, 3 (2003).
- 114 Yamazaki, T. *et al.* Defective immunogenic cell death of HMGB1-deficient tumors: compensatory therapy with TLR4 agonists. *Cell Death & Differentiation* **21**, 69-78 (2014).

References

- 115 Hellevik, T. *et al.* Cancer-associated fibroblasts from human NSCLC survive ablative doses of radiation but their invasive capacity is reduced. *Radiation Oncology* **7**, 59 (2012).
- 116 Ohshio, Y. *et al.* Cancer-associated fibroblast-targeted strategy enhances antitumor immune responses in dendritic cell-based vaccine. *Cancer science* **2**, 134-142 (2015).
- 117 Kraman, M. *et al.* Suppression of antitumor immunity by stromal cells expressing fibroblast activation protein- α . *Science* **330**, 827-830 (2010).
- 118 Loeffler, M., Krüger, J. A., Niethammer, A. G. & Reisfeld, R. A. Targeting tumor-associated fibroblasts improves cancer chemotherapy by increasing intratumoral drug uptake. *Journal of Clinical Investigation* **116**, 1955 (2006).
- 119 Levings, M. K., Sangregorio, R. & Roncarolo, M.-G. Human CD25+ CD4+ T regulatory cells suppress naive and memory T cell proliferation and can be expanded in vitro without loss of function. *The Journal of experimental medicine* **193**, 1295-1302 (2001).
- 120 Longhi, M. S. *et al.* Functional study of CD4+ CD25+ regulatory T cells in health and autoimmune hepatitis. *The Journal of Immunology* **176**, 4484-4491 (2006).
- 121 Wichers, M. C. & Maes, M. The role of indoleamine 2, 3-dioxygenase (IDO) in the pathophysiology of interferon- α -induced depression. *Journal of Psychiatry and Neuroscience* **29**, 11 (2004).
- 122 Formenti, S. C. & Demaria, S. Combining radiotherapy and cancer immunotherapy: a paradigm shift. *Journal of the National Cancer Institute* **4**, 256-265 (2013).
- 123 Özdemir, B. C. *et al.* Depletion of carcinoma-associated fibroblasts and fibrosis induces immunosuppression and accelerates pancreas cancer with reduced survival. *Cancer Cell* **25**, 719-734 (2014).
- 124 Pinchuk, I. V. *et al.* PD-1 ligand expression by human colonic myofibroblasts/fibroblasts regulates CD4+ T-cell activity. *Gastroenterology* **135**, 1228-1237. e1222 (2008).
- 125 Kusmartsev, S., Nefedova, Y., Yoder, D. & Gabrilovich, D. I. Antigen-specific inhibition of CD8+ T cell response by immature myeloid cells in cancer is mediated by reactive oxygen species. *The Journal of Immunology* **172**, 989-999 (2004).
- 126 Gabrilovich, D. I., Velders, M. P., Sotomayor, E. M. & Kast, W. M. Mechanism of immune dysfunction in cancer mediated by immature Gr-1+ myeloid cells. *The Journal of Immunology* **166**, 5398-5406 (2001).
- 127 Nagaraj, S. *et al.* Antigen-specific CD4+ T cells regulate function of myeloid-derived suppressor cells in cancer via retrograde MHC class II signaling. *Cancer research* **72**, 928-938 (2012).
- 128 Brooks, D. G., Walsh, K. B., Elsaesser, H. & Oldstone, M. B. IL-10 directly suppresses CD4 but not CD8 T cell effector and memory responses following acute viral infection. *Proceedings of the National Academy of Sciences* **107**, 3018-3023 (2010).
- 129 Dieckmann, D., Plöttner, H., Dotterweich, S. & Schuler, G. Activated CD4+ CD25+ T cells suppress antigen-specific CD4+ and CD8+ T cells but induce a suppressive phenotype only in CD4+ T cells. *Immunology* **115**, 305-314 (2005).
- 130 Springer, T. A. Traffic signals for lymphocyte recirculation and leukocyte emigration: the multistep paradigm. *Cell* **76**, 301-314 (1994).

References

- 131 Bleul, C. C., Fuhlbrigge, R. C., Casasnovas, J. M., Aiuti, A. & Springer, T. A. A highly efficacious lymphocyte chemoattractant, stromal cell-derived factor 1 (SDF-1). *The Journal of experimental medicine* **184**, 1101-1109 (1996).
- 132 Siveke, J. T. & Hamann, A. Cutting edge: T helper 1 and T helper 2 cells respond differentially to chemokines. *The Journal of Immunology* **160**, 550-554 (1998).
- 133 Dighe, A. S., Richards, E., Old, L. J. & Schreiber, R. D. Enhanced in vivo growth and resistance to rejection of tumor cells expressing dominant negative IFN γ receptors. *Immunity* **1**, 447-456 (1994).
- 134 Calzascia, T. *et al.* TNF- α is critical for antitumor but not antiviral T cell immunity in mice. *The Journal of clinical investigation* **117**, 3833 (2007).
- 135 Vila-del Sol, V., Punzón, C. & Fresno, M. IFN- γ -induced TNF- α expression is regulated by interferon regulatory factors 1 and 8 in mouse macrophages. *The Journal of Immunology* **181**, 4461-4470 (2008).
- 136 Moore, K. W., de Waal Malefyt, R., Coffman, R. L. & O'Garra, A. Interleukin-10 and the interleukin-10 receptor. *Annual review of immunology* **19**, 683-765 (2001).
- 137 Croci, D. O. *et al.* Dynamic cross-talk between tumor and immune cells in orchestrating the immunosuppressive network at the tumor microenvironment. *Cancer Immunology, Immunotherapy* **56**, 1687-1700 (2007).
- 138 Sica, A. *et al.* Autocrine production of IL-10 mediates defective IL-12 production and NF- κ B activation in tumor-associated macrophages. *The Journal of Immunology* **164**, 762-767 (2000).
- 139 Dieckmann, D., Plottner, H., Berchtold, S., Berger, T. & Schuler, G. Ex vivo isolation and characterization of CD4⁺ CD25⁺ T cells with regulatory properties from human blood. *The Journal of experimental medicine* **193**, 1303-1310 (2001).
- 140 Shi, Y. *et al.* Granulocyte-macrophage colony-stimulating factor (GM-CSF) and T-cell responses: what we do and don't know. *Cell research* **16**, 126-133 (2006).
- 141 Hamilton, J. A. GM-CSF in inflammation and autoimmunity. *Trends in immunology* **23**, 403-408 (2002).
- 142 Hamilton, J., Stanley, E., Burgess, A. & Shadduck, R. Stimulation of macrophage plasminogen activator activity by colony-stimulating factors. *Journal of cellular physiology* **103**, 435-445 (1980).
- 143 Bayne, L. J. *et al.* Tumor-derived granulocyte-macrophage colony-stimulating factor regulates myeloid inflammation and T cell immunity in pancreatic cancer. *Cancer cell* **21**, 822-835 (2012).
- 144 Bronte, V. *et al.* Unopposed production of granulocyte-macrophage colony-stimulating factor by tumors inhibits CD8⁺ T cell responses by dysregulating antigen-presenting cell maturation. *The Journal of Immunology* **162**, 5728-5737 (1999).
- 145 Dranoff, G. Cytokines in cancer pathogenesis and cancer therapy. *Nature Reviews Cancer* **4**, 11-22 (2004).
- 146 Ozaki, K. & Leonard, W. J. Cytokine and cytokine receptor pleiotropy and redundancy. *Journal of Biological Chemistry* **277**, 29355-29358 (2002).
- 147 Okada, H. & Kuwashima, N. Gene therapy and biologic therapy with interleukin-4. *Current gene therapy* **2**, 437-450 (2002).
- 148 Jakowlew, S. B. Transforming growth factor- β in cancer and metastasis. *Cancer and Metastasis Reviews* **25**, 435-457 (2006).
- 149 Naugler, W. E. & Karin, M. The wolf in sheep's clothing: the role of interleukin-6 in immunity, inflammation and cancer. *Trends in molecular medicine* **14**, 109-119 (2008).

References

- 150 Krelin, Y. *et al.* Interleukin-1 β -Driven Inflammation Promotes the Development and Invasiveness of Chemical Carcinogen-Induced Tumors. *Cancer research* **67**, 1062-1071 (2007).
- 151 Tu, S. *et al.* Overexpression of interleukin-1 β induces gastric inflammation and cancer and mobilizes myeloid-derived suppressor cells in mice. *Cancer cell* **14**, 408-419 (2008).
- 152 Mellor, A. L. & Munn, D. H. IDO expression by dendritic cells: tolerance and tryptophan catabolism. *Nature Reviews Immunology* **4**, 762-774 (2004).
- 153 Mellor, A. L., Keskin, D. B., Johnson, T., Chandler, P. & Munn, D. H. Cells expressing indoleamine 2, 3-dioxygenase inhibit T cell responses. *The Journal of Immunology* **168**, 3771-3776 (2002).
- 154 Ling, W. *et al.* Mesenchymal stem cells use IDO to regulate immunity in tumor microenvironment. *Cancer research* **74**, 1576-1587 (2014).
- 155 Chen, J.-Y. *et al.* Cancer/stroma interplay via cyclooxygenase-2 and indoleamine 2, 3-dioxygenase promotes breast cancer progression. *Breast Cancer Res* **16**, 410 (2014).
- 156 Kehrl, J. H. *et al.* Production of transforming growth factor beta by human T lymphocytes and its potential role in the regulation of T cell growth. *The Journal of experimental medicine* **163**, 1037-1050 (1986).
- 157 Letterio, J. J. & Roberts, A. B. Regulation of immune responses by TGF- β *. *Annual review of immunology* **16**, 137-161 (1998).
- 158 Broderick L, B. R. Membrane-associated TGF-beta1 inhibits human memory T cell signaling in malignant and nonmalignant inflammatory microenvironments. *J Immunol.* **177**, 3082-3088 (2006).
- 159 Hughes, R. C. Galectins as modulators of cell adhesion. *Biochimie* **83**, 667-676 (2001).
- 160 Dunic, J., Dabelic, S. & Flögel, M. Galectin-3: an open-ended story. *Biochimica et Biophysica Acta (BBA)-General Subjects* **1760**, 616-635 (2006).
- 161 Nakamura, M. *et al.* Involvement of galectin-3 expression in colorectal cancer progression and metastasis. *International journal of oncology* **15**, 143-151 (1999).
- 162 Berberat, P. O. *et al.* Comparative analysis of galectins in primary tumors and tumor metastasis in human pancreatic cancer. *Journal of Histochemistry & Cytochemistry* **49**, 539-549 (2001).
- 163 Fortuna-Costa, A., Gomes, A. M., Kozłowski, E. O., Stelling, M. P. & Pavão, M. S. Extracellular galectin-3 in tumor progression and metastasis. *Frontiers in oncology* **4** (2014).
- 164 Demetriou, M., Granovsky, M., Quaggin, S. & Dennis, J. W. Negative regulation of T-cell activation and autoimmunity by Mgat5 N-glycosylation. *Nature* **409**, 733-739 (2001).
- 165 Peng, W., Wang, H. Y., Miyahara, Y., Peng, G. & Wang, R.-F. Tumor-associated galectin-3 modulates the function of tumor-reactive T cells. *Cancer research* **68**, 7228-7236 (2008).
- 166 Sioud, M., Mobergslien, A., Boudabous, A. & Fløisand, Y. Evidence for the Involvement of Galectin-3 in Mesenchymal Stem Cell Suppression of Allogeneic T-Cell Proliferation. *Scandinavian journal of immunology* **71**, 267-274 (2010).
- 167 Rubinstein, N. *et al.* Targeted inhibition of galectin-1 gene expression in tumor cells results in heightened T cell-mediated rejection: a potential mechanism of tumor-immune privilege. *Cancer cell* **5**, 241-251 (2004).
- 168 Garín, M. I. *et al.* Galectin-1: a key effector of regulation mediated by CD4+ CD25+ T cells. *Blood* **109**, 2058-2065 (2007).

References

- 169 Lotti, F. *et al.* Chemotherapy activates cancer-associated fibroblasts to maintain colorectal cancer-initiating cells by IL-17A. *The Journal of experimental medicine* **210**, 2851-2872 (2013).
- 170 Golden, E. B. & Apetoh, L. Radiotherapy and Immunogenic Cell Death. *Seminars in radiation oncology* **25**, 11-17 (2015).
- 171 Apetoh, L. *et al.* Toll-like receptor 4–dependent contribution of the immune system to anticancer chemotherapy and radiotherapy. *Nature medicine* **13**, 1050-1059 (2007).
- 172 Gupta, A. *et al.* Radiotherapy promotes tumor-specific effector CD8+ T cells via dendritic cell activation. *The Journal of Immunology* **189**, 558-566 (2012).
- 173 Schaeue, D., Ratikan, J. A., Iwamoto, K. S. & McBride, W. H. Maximizing tumor immunity with fractionated radiation. *International Journal of Radiation Oncology* Biology* Physics* **83**, 1306-1310 (2012).
- 174 Penfornis, P., Vallabhaneni, K. C., Whitt, J. & Pochampally, R. Extracellular vesicles as carriers of microRNA, proteins and lipids in tumor microenvironment. *International Journal of Cancer* (2015).
- 175 Dayan, D. *et al.* Molecular crosstalk between cancer cells and tumor microenvironment components suggests potential targets for new therapeutic approaches in mobile tongue cancer. *Cancer medicine* **1**, 128-140 (2012).